Final Technical Report

Project Title: Stabilization of Bio-Oil Fractions for Insertion into Petroleum Refineries

Award Number: DE-EE0006066

Recipient: Iowa State University of Science and Technology

Project Location(s): Ames (Story County), Iowa;
Richland (Benton County), Washington;
Norman (Cleveland County), Oklahoma

Project Period: January 1, 2013 – June 30, 2014
Date of Report: September 28, 214
Written by: Robert Brown, Ryan Smith, Mark Wright (ISU), Douglas Elliott (PNNL), Daniel Resasco, Steven Crossley (OU)
Program Manager: Robert Brown
Principal Investigators: Robert Brown, Mark Wright, Ryan Smith (ISU); Douglas Elliott (PNNL); Daniel Resasco, Steven Crossley (OU)

Subcontractors: Pacific Northwest National Laboratory, University of Oklahoma

Cost-Sharing Partners: Iowa State University, University of Oklahoma

DOE Project Team
DOE-HQ contact: Brenda Dias
DOE Field Project Officer: Prasad Gupte
DOE Contract Specialist: Trevor Smith
DOE Project Engineer:

Acknowledgment: This material is based upon work supported by the Department of Energy under Award Number DE-EE0006066.

Final Scientific/Technical Report Content

1. Identify the DOE award number; name of recipient; project title; name of project director/principal investigator; and consortium/teaming members.

DOE award number: DE-EE0006066
Name of recipient: Iowa State University
Project title: Stabilization of Bio-Oil Fractions for Insertion into Petroleum Refineries

Name of project director/principal investigator:
Robert Brown, Iowa State University (ISU), Ames, IA

Consortium/teaming members:
Mark Wright, Ryan Smith (ISU)
Doug Elliott, Pacific Northwest National Laboratory (PNNL), Richland, WA
Daniel Resasco, Steven Crossley, University of Oklahoma (OU), Norman, OK

2. Display prominently on the cover of the report any authorized distribution limitation notices, such as patentable material or protected data. Reports delivered without such notices may be deemed to have been furnished with unlimited rights, and the Government assumes no liability for the disclosure, use or reproduction of such reports.

3. Provide an executive summary, which includes a discussion of 1) how the research adds to the understanding of the area investigated; 2) the technical effectiveness and economic feasibility of the methods or techniques investigated or demonstrated; or 3) how the project is otherwise of benefit to the public. The discussion should be a minimum of one paragraph and written in terms understandable by an educated layman.

Executive Summary

This project is part of a collaboration effort between Iowa State University (ISU), University of Oklahoma (OK) and Pacific Northwest National Laboratory (PNNL). The purpose of this project is to stabilize bio-oil fractions and improve their suitability for insertion into petroleum refineries.

Bio-oil from fast pyrolysis of biomass is a complex mixture of unstable organic compounds. These organic compounds react under standard room conditions resulting in increases in bio-oil viscosity and water content – both detrimental for bio-oil storage and transportation. This study employed fractionation and upgrading systems to improve the stability of bio-oil. The fractionation system consists of a series of condensers, and electrostatic precipitators designed to separate bio-oil into five fractions: soluble carbohydrates (SF1&2), clean phenolic oligomers (CPO) and middle fraction (SF3&4), light oxygenates (SF5). A two-stage upgrading process was designed to process bio-oil stage fractions into stable products that can be inserted into a refinery. In the upgrading system, heavy and middle bio-oil fractions were upgraded into stable oil via cracking and subsequent hydrodeoxygenation. The light oxygenate fraction was steam reformed to provide a portion of requisite hydrogen for hydroprocessing. Hydrotreating and hydrocracking employed hydrogen from natural gas, fuel gas and light oxygenates reforming. The finished products from this study consist of gasoline- and diesel-blend stock fuels.

Clean Phenolic Oligomers (CPO) were evaluated in hydroprocessing tests for production of liquid hydrocarbon products. These hydroprocessing tests showed good results using catalytic hydroprocessing strategies developed for unfractionated bio-oil. Both sulfided base metal catalyst and unsulfided precious metal catalysts were evaluated. Equal-sized catalyst beds of Ru on C catalyst operated at 140 °C and Pd on C catalyst operated at 370 °C were tested. A single bed of sulfided CoMo on Al2O3 catalyst operated at 400 °C was also tested. The continuous-flow reactor was operated at a pressure of 12.4 MPa with flowing hydrogen. The condensed liquid products were analyzed and found that the hydrocarbon liquid was significantly hydrotreated so that nitrogen and sulfur were below the level of detection, while the residual oxygen ranged from 0.4 to 5.0%. The density of the products varied from 0.81 g/mL up to 0.88 g/mL with a correlated change of the hydrogen to carbon atomic ratio from 1.79 down to 1.57. In the extended tests the product quality decreased over time suggesting some loss of catalyst activity through the test. These tests provided the data needed to assess the suite of liquid fuel products from the process and the activity of the catalyst in relationship to the existing catalyst lifetime barrier for the technology. The data were used in process modeling to estimate processing costs and evaluated by refinery partners to assess the ability for use as petroleum refinery feedstock.

The stabilized intermediates were assessed for suitability into specific processes within a refinery based on chemical and physical characteristics. Appropriate targeted refinery insertion points were identified for each stabilized fraction. A techno-economic model was developed to analyze the cost-benefit tradeoffs of bio-oil stabilization for the production of renewable transportation fuels. Economic production of stable bio-oils could reduce the carbon footprint of transportation vehicles by replacing fossil fuel inputs in petroleum refineries. This study employed 2000 metric tons per day (MT/day) of red oak biomass with 30 wt. % moisture, 0.3 wt% ash and nominal size of 1 mm. The biomass conversion process is based on an N^{th} plant design. This design assumes that all the necessary engineering breakthroughs have been achieved and technical bottlenecks have been resolved. The commercial viability of the process is based on projections of the Minimum Fuel Selling Prices (MFSP). A Discounted Cash Flow Rate of Return (DCFROR) analysis was developed under assumptions of a 30-year plant life, 40% equity and a 10% internal rate of return. The fixed capital investment and the total project investment for stabilization process were estimated at $ 561 and $ 667 million respectively based on a gasoline and diesel yield of 54.3 million gallons/year (MM/year). The MSFP was assessed as $3.77/gal based on the current facility configuration. Improving the utilization of process off-gas, increasing diesel yields, and generating revenue from chemical by-products could decrease the MSFP.

4. Provide a comparison of the actual accomplishments with the goals and objectives of the project. Where applicable, address any comparisons of actual results to programmatic technical barriers and milestones.

The results of these hydroprocessing tests provided the needed data on a component of the overall process in order to evaluate the conceptual process and determine potential economics.

The techno-economic analysis (TEA) designed and assessed a commercial-scale facility that could convert biomass into stable bio-oil fractions that could be inserted into existing petroleum refineries. Specifically, the TEA estimated the minimum fuel-selling price (MFSP) required for the facility to achieve profitability (based on 10% internal rate of return over a 30-year period). Furthermore, the study investigates the sensitivity of the MFSP to variations in key process and financial parameters. These project results address several technical barriers and key process milestones.

This project sought to establish a baseline chemical process design for a commercial-scale bio-oil stabilization biorefinery. This study provides the process design of a 2000 metric tonne per day facility for the conversion of biomass (red oak) into stable bio-oil fractions and their subsequent upgrading to gasoline- and diesel-blend stock. The facility is designed as the N^{th} plant of its kind, which assumes that major engineering breakthroughs have been accomplished and technical barriers have been resolved. Process operating conditions are based on experimental data gathered from this project. Specifically, biomass fast pyrolysis operating conditions and process yields are based on experiments conducted at Iowa State University. Bio-oil stage fraction yields are compositions are modeled based on ISU data. Bio-oil upgrading reactor operating conditions are based on guidelines provided by PNNL and OK.

This design achieves a total biofuel yield of 82.6 gallons per ton of dry biomass input. The annual biofuel output is 54.3 million gallons/year. The fixed capital investment and the total project investment for the process are estimated at $561 and $667 million respectively. The biomass conversion (pretreatment and pyrolysis) and stabilization sections contribute a significant portion of the capital cost. The MSFP was estimated as $3.77/gal based on the current facility configuration. Improving the utilization of process off-gas, increasing diesel yields, and generating revenue from chemical by-products could decrease the MSFP.

5. Summarize project activities for the entire period of funding, including original hypotheses, approaches used, problems encountered and departure from planned methodology, and an assessment of their impact on the project results. Include, if applicable, facts, figures, analyses, and assumptions used during the life of the project to support the conclusions.

Task 1: Production and analysis of bio-oil fractions (ISU)

Bio-oil fractions with like physical and chemical characteristics were produced from both red oak and corn stover using Iowa State University's 8 kg/h fluidized bed fast pyrolysis process development unit. Fractionation is achieved by replacing the chilled water traditionally used in bio-oil condensers with coolants operated at temperatures carefully prescribed to encourage selective condensation of classes of molecules according to their dew points in the pyrolysis vapor stream. Each condenser stage is followed by an electrostatic separator (ESP) stage designed to collect the aerosols that are inevitably produced in the cooled gas flow (Fig. 1 and 2).

One of the distinguishing features of this approach to bio-oil recovery is that water normally found in bio-oil is concentrated in a single fraction with the other fractions containing relatively little water. This has distinct advantages in catalytic upgrading since many catalyst supports are unstable in the presence of water. Two of the heaviest fractions of bio-oil contain both water-soluble carbohydrate (mostly anhydrosugars and monosaccharides) and water-insoluble phenolic oligomers derived from lignin. Unlike conventional bio-oil, where the sugars are dissolved in the aqueous phase, it is possible to recover the sugars as a concentrated solution (20% or more) by simply washing the heavy fraction with water. The bio-oil recovery process developed at ISU results in four distinctive fractions of bio-oil:

- Soluble carbohydrate: A concentrated solution of anhydrosugars (mostly levoglucosan), monosaccharides, and a smaller amount of aldehydes and ketones derived from plant polysaccharides;
- Clean phenolic oligomers (CPO): A low-moisture fraction consisting of relatively low molecular weight (200-400 Daltons) oligomers derived from the depolymerization of lignin during pyrolysis;
- Middle fraction: A low-moisture fraction containing mostly phenolic monomers and furans;
- Light oxygenates: An aqueous phase containing mostly aldehydes and carboxylic acids.

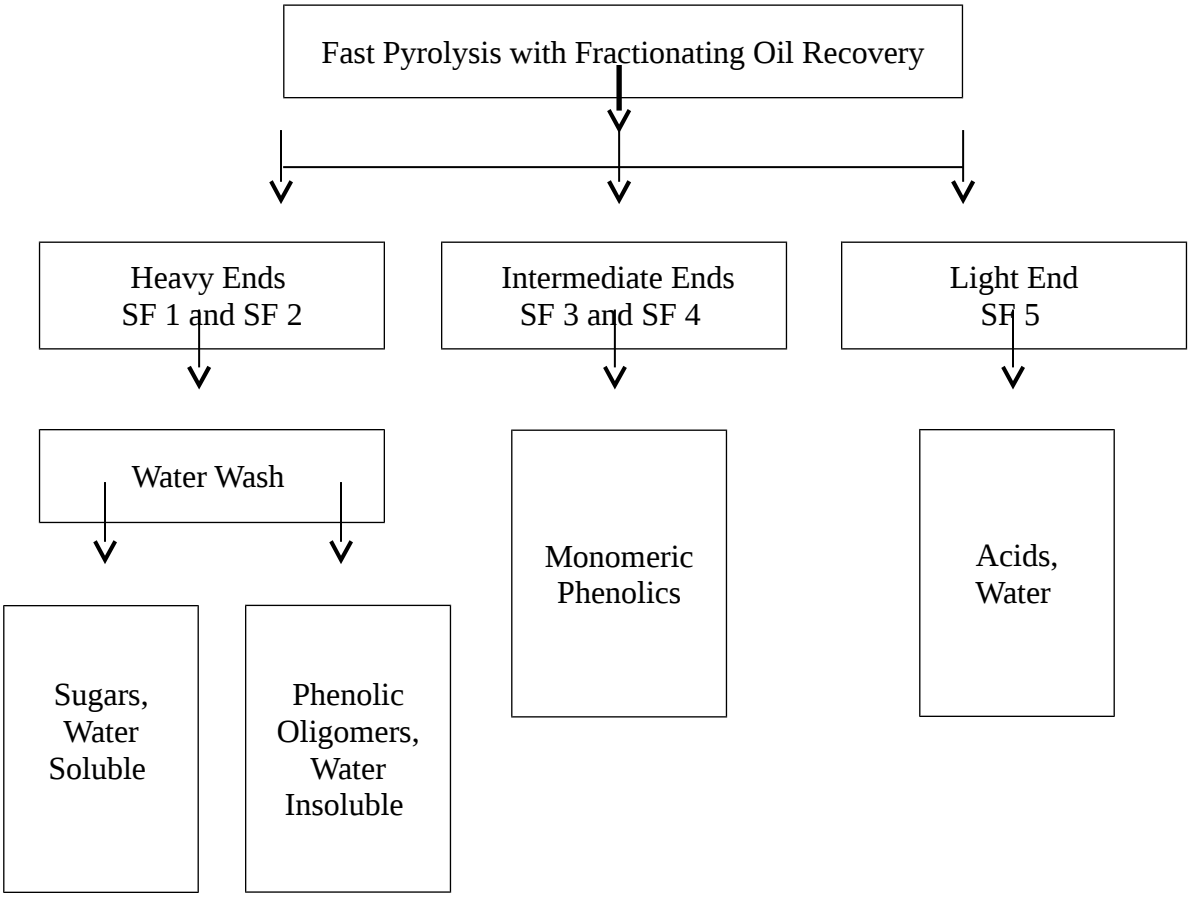

Figure 1. Fast Pyrolysis and bio-oil fraction recovery process flow

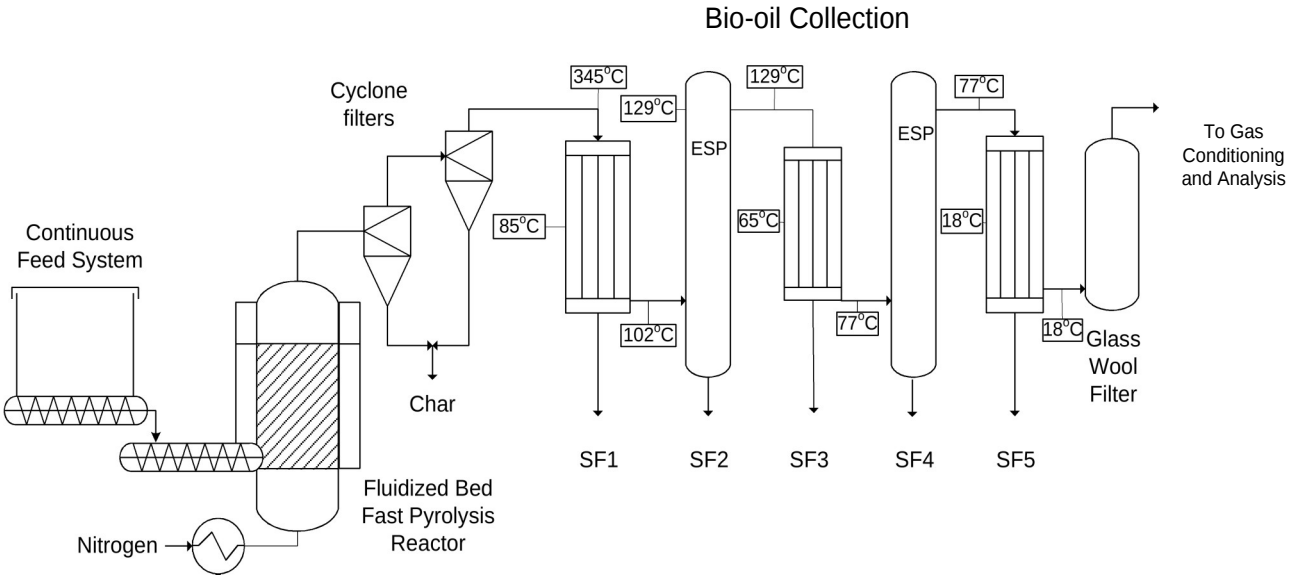

Figure 2. Fast Pyrolysis and bio-oil fraction recovery system schematic

As shown in Table 1 and Table 2, the total liquid yield was significantly lower when pyrolyzing corn stover, with most of the difference being in the heavy end (soluble carbohydrate and clean phenolic oligomer) fractions. As shown in Tables 1 and 2 and Figure 1 below, overall moisture content is higher for pyrolysis of corn stover. Not only is the moisture content for the light oxygenate fraction from corn stover higher than that from red oak (Figure 1), the yield of the light oxygenate fraction is also higher when pyrolyzing corn stover (Tables 1 and 2). Overall carbon, hydrogen, and nitrogen content for the fractions remained relatively consistent with one exception. As Figure 2 shows, there is a significant difference in carbon content in the middle fraction between the two corn stover runs. To investigate further, sulfur and oxygen contents will be measured for these fractions. This coincides with a difference in moisture contents in the middle fraction between the corn stover runs.

Table 1. Product Distribution of red oak fast pyrolysis

Fraction	**Yield (biomass basis)**
Soluble carbohydrate	16.19%
Clean phenolic oligomer	12.56%
Middle	5.36%
Light Oxygenates	28.99%
Total liquid yield	*63.10%*
Char	15.23%
Non-condensable Gases	25.47%
Total Mass Balance	**103.80%**

Table 2. Product Distribution of corn stover fast pyrolysis

Fraction	**Yield (biomass basis)**
Heavy Ends*	18.76%
Middle	4.88%
Light Oxygenates	29.36%
Total liquid yield	*53.00%*
Char	19.83%
Non-condensable Gases	29.42%
Total Mass Balance	**102.25%**

*CPO and Soluble Carbohydrate fraction yields still to be determined

Table 3. Carbon balance of bio-oil fractions from red oak

Red oak pyrolysis bio-oil fraction	Normalized Yield (wet bio-oil basis)	Carbon content of fraction	Carbon yield (wet bio-oil basis)
CPO	24.4%	54.3%	37.4%
Sugar	22.6%	47.5%	30.5%
Middle	9.0%	47.6%	12.1%
Light Oxygenates	44.0%	16.1%	20.0%
Total	**100.00%**		**100.00%**

Table 4. Carbon balance of bio-oil fractions from corn stover

Corn stover pyrolysis bio-oil fraction	Normalized Yield (wet bio-oil basis)	Carbon content of fraction	Carbon yield (wet bio-oil basis)
CPO	25.3%	55.6%	50.5%
Sugar	3.3%	48.7%	5.8%
Middle	9.4%	54.4%	18.3%
Light Oxygenates	62.0%	11.4%	25.3%
Total	**100.00%**		**100.00%**

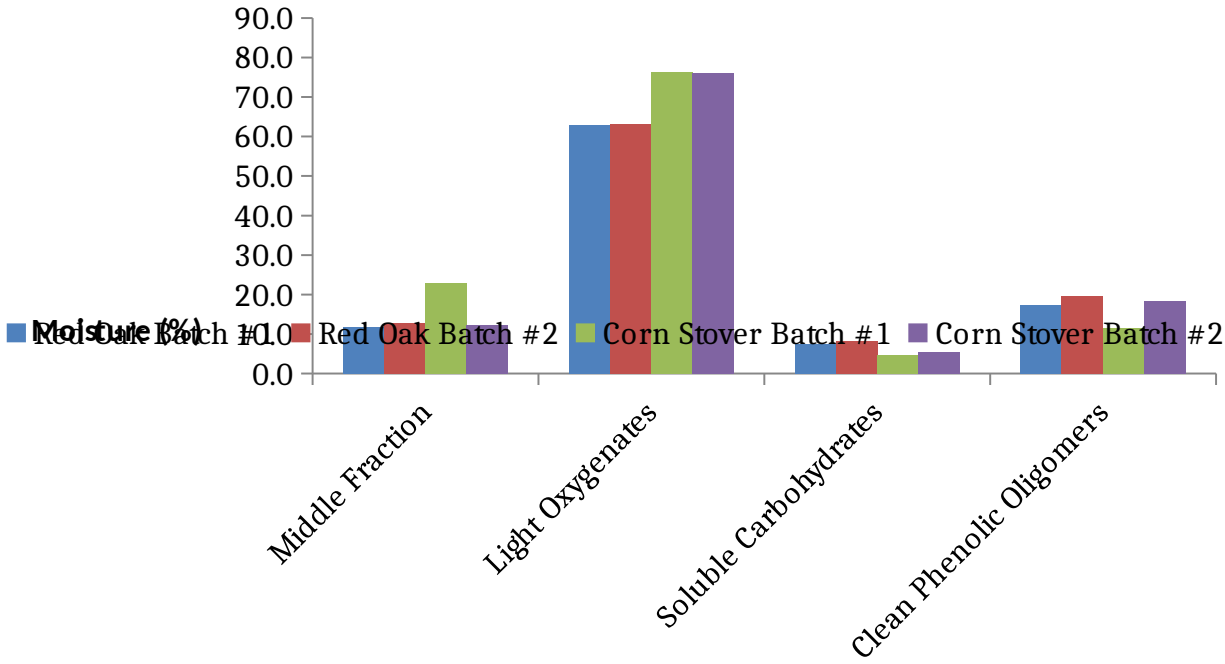

Figure 3. Moisture content of red oak and corn stover pyrolysis fractions

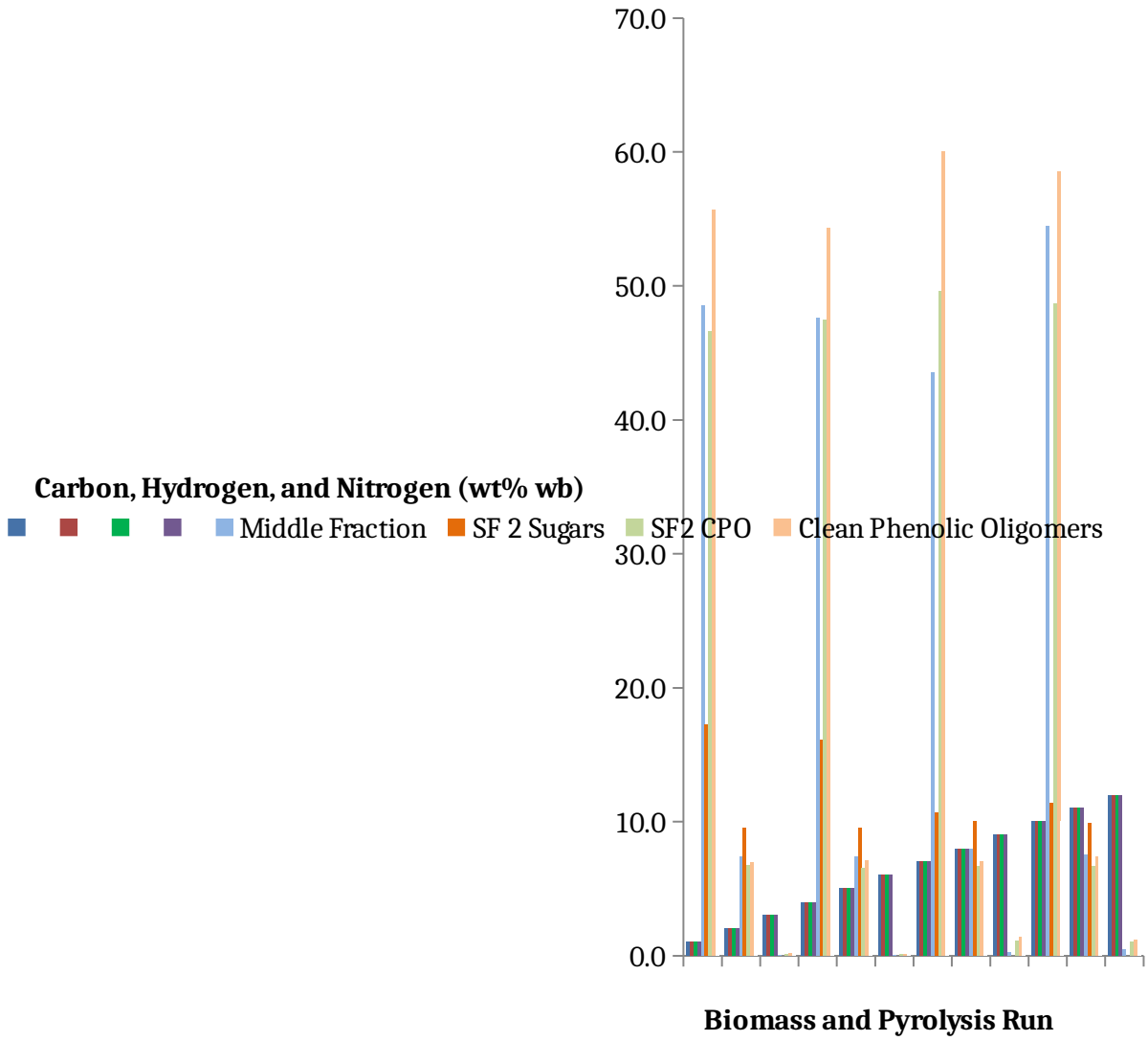

Figure 4. Carbon, hydrogen, and nitrogen content of red oak and corn stover pyrolysis fractions

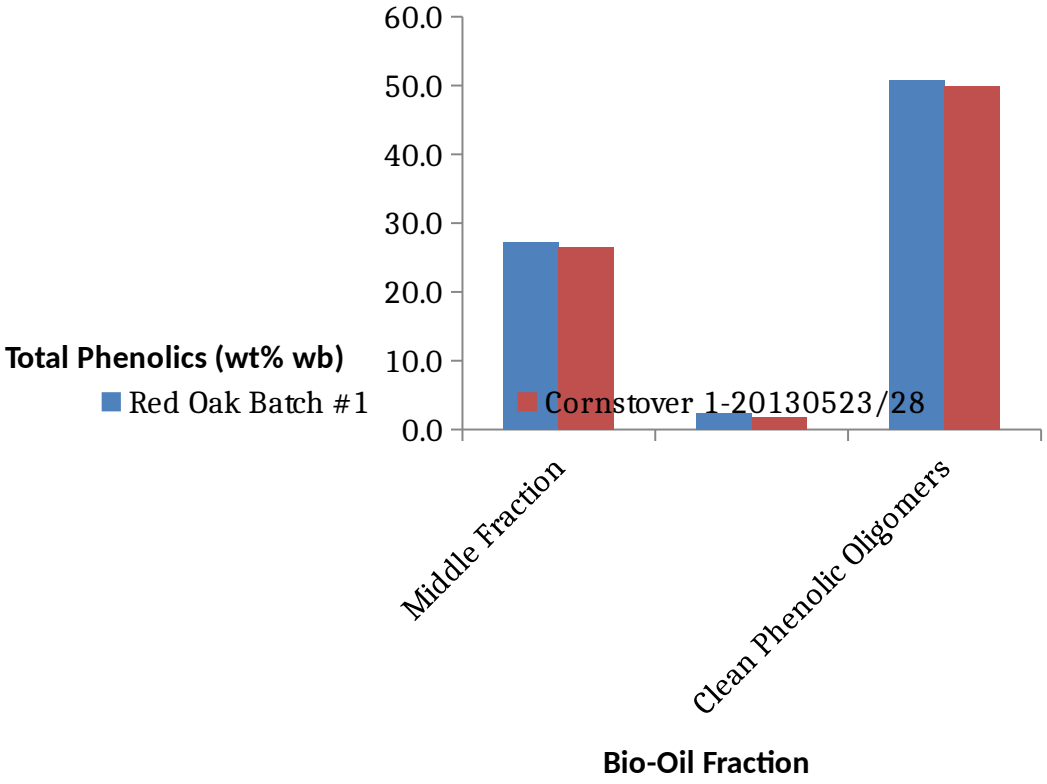

Figure 5. Total phenolic content of red oak and corn stover pyrolysis fractions

Additional analysis was done of the soluble carbohydrate, phenolic oligomer, middle, and light oxygenate fractions. Additionally, analyses of the individual stage fractions as collected from the current pyrolysis condensation system was conducted to highlight differences within the major groups being upgraded.

For reference in Task 1, the stage fractions (SF) are as follows:

- SF1 = Heavy end product collected in a condenser, prior to separation of soluble carbohydrates and lignin oligomers
- SF2 = Heavy end product collected in an electrostatic precipitator (ESP), prior to separation of soluble carbohydrates and lignin oligomers
- SF3 = Middle fraction product collected in a condenser
- SF4 = Middle fraction product collected in an ESP
- SF5 = Light oxygenate product
- SF1 Sugars = soluble carbohydrates collected from SF1
- SF1 CPO = lignin oligomers collected from SF1
- SF2 Sugars = soluble carbohydrates collected from SF2
- SF2 CPO = lignin oligomers collected from SF2

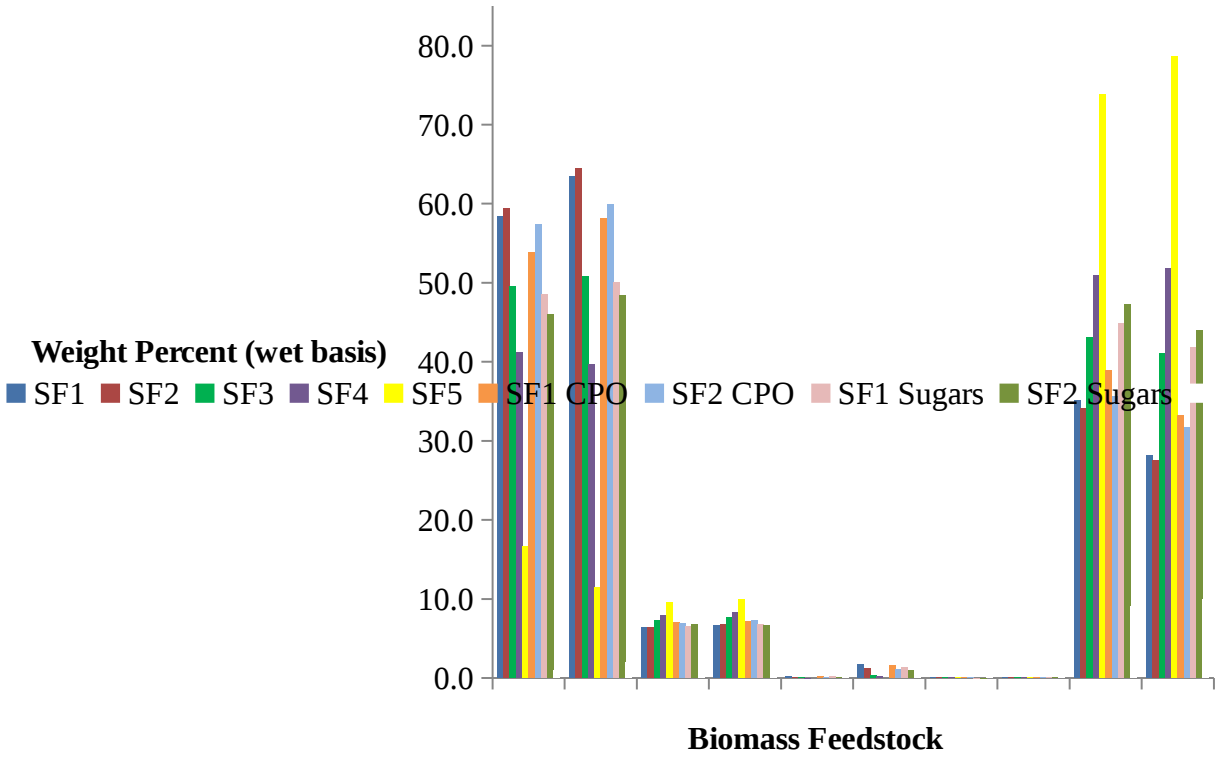

Figure 6. Ultimate analysis comparison of bio-oils produced by fast pyrolysis using red oak and cornstover biomass.

As shown in figure 6, the carbon, hydrogen, nitrogen, sulfur, and oxygen content was very similar for both the red oak and corn stover bio-oils. However, there was a difference in the nitrogen content. The corn stover showed higher values versus the red oak. This was not unexpected due to the extra nitrogen added to soil for optimum corn production.
As shown in figure 7, the major differences in the red oak and the corn stover bio-oils proximate analyses were the fixed carbon and the ash content. The corn stover bio-oil ash content was higher. This may influence stability of corn stover bio-oil, negatively. Ash content can catalyze unwanted reactions in bio-oil during production and storage.

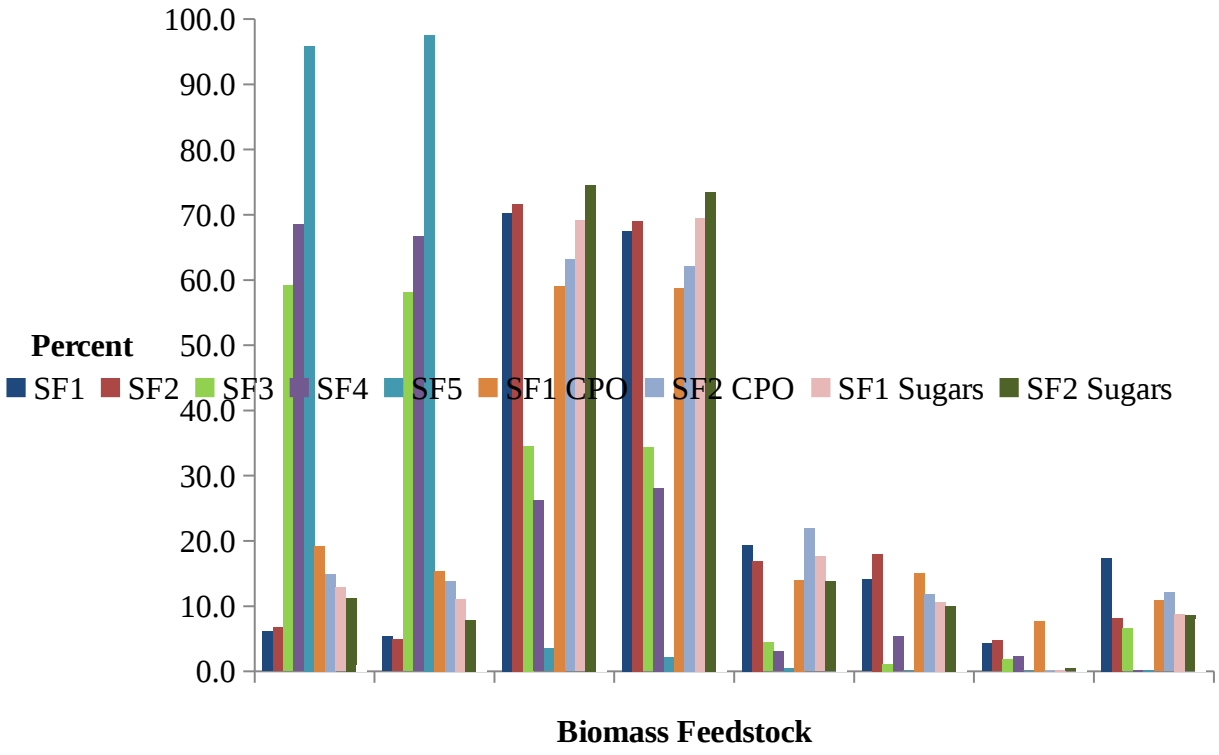

Figure 7. Proximate analysis comparison of bio-oils produced by fast pyrolysis using red oak and corn stover biomass.

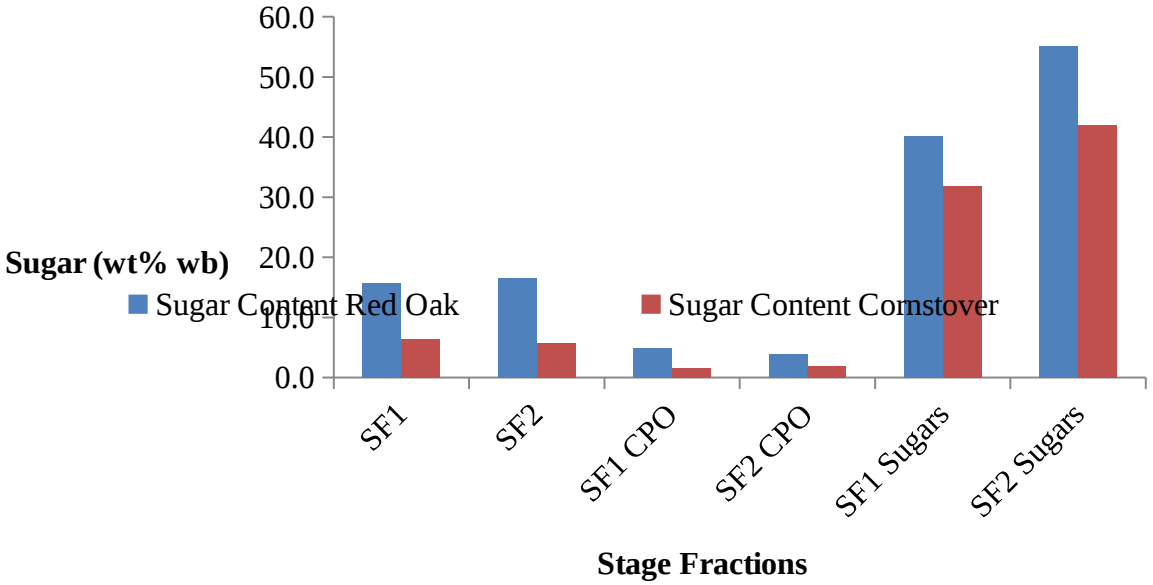

Figure 8. Comparison of total soluble sugar content in stage fractions (SF) 1 and SF2.

The soluble sugar content remaining in the clean phenolic oligomers (CPO) fraction after the washing procedure used to remove the sugars from the bio-oil is also compared.

The amount of sugar in the bio-oil was higher in the bio-oil produced from red oak (Figure 8). There are soluble sugars remaining in the water insoluble fraction. An in-line washing system may improve the removal of the sugars from the phenolic oligomers.

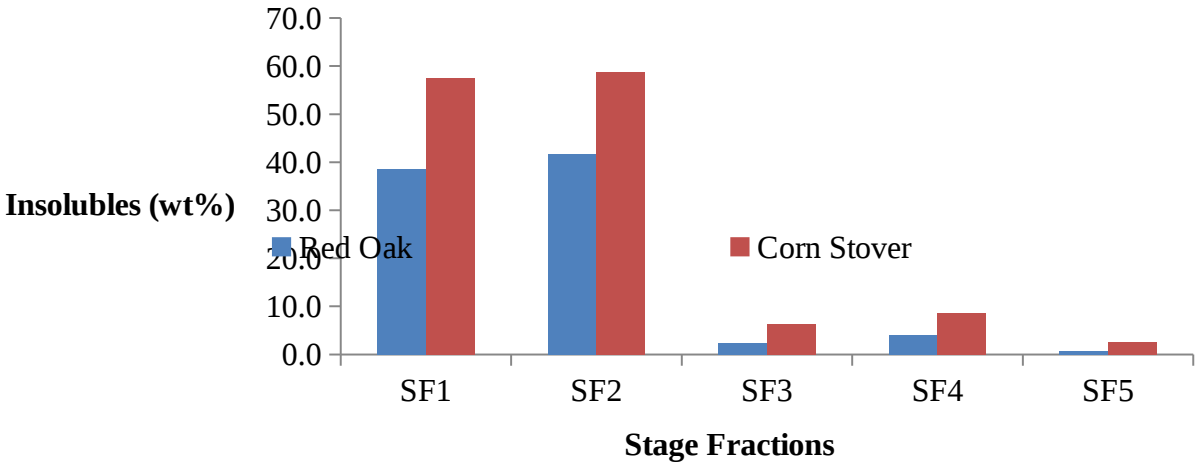

Figure 9. Comparison of the water insoluble content in each stage fraction (SF) for bio-oils produced from red oak and corn stover biomass.

The majority of the insoluble content (phenolic oligomers) is collected in SF1 and SF2 (Figure 9). This is due to the fractionated condenser system and thus has potential to improve the prospective of upgrading each SF for increased value end use products.

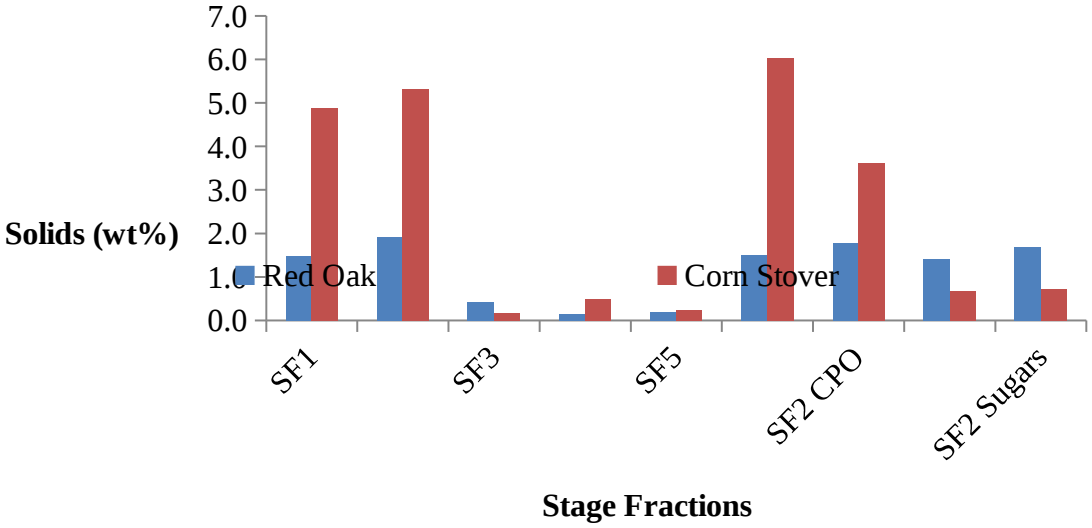

Figure 10. Comparison of solids content in bio-oil produced from red oak and corn stover biomass.

As shown in figure 10, the solids content in the corn stover bio-oil is much higher versus the bio-oil produced from red oak. Solids are anything that does not dissolve in methanol. This would include larger molecular weight species. The higher solids content in the corn stover bio-oil may indicate polymerization due to the higher percentages of ash content seen in this same oil. Ash content may promote polymerization of the phenolic species.

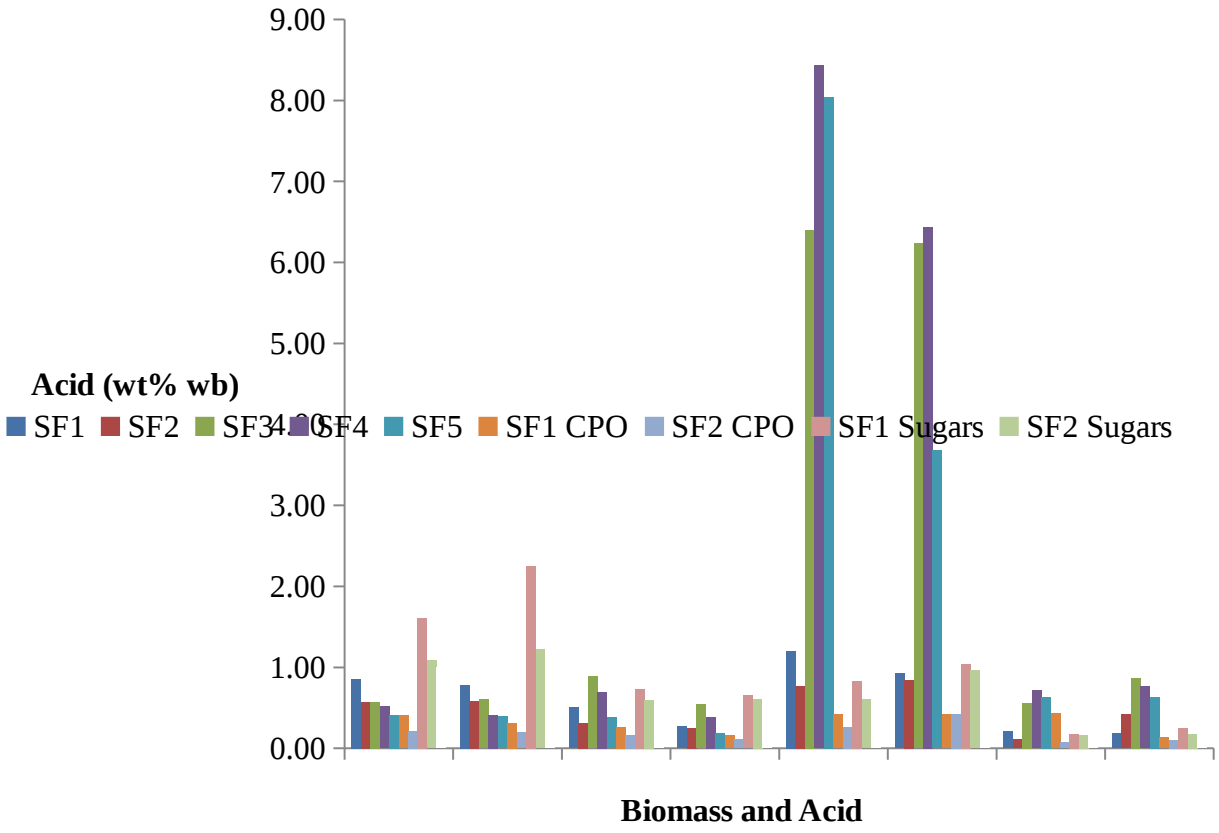

Figure 11. Comparison of acid content in red oak and corn stover bio-oils.

The acids content in both the red oak and corn stover bio-oils was very similar (Figure 11). More acetic acid was produced and collected in SF3-5 for the red oak bio-oil.

Task 2. Stabilization of the light oxygenate fraction (SF5) at OU

Product Analysis

Light oxygenate fraction samples were analyzed at OU upon receipt from ISU. The most abundant species in the samples are shown in Table 5.

Table 5. Relative concentrations of major species in light oxygenate fraction

Compound	GC Peak Area %
Acetic acid	24.01
Acetone	22.10
2H-Pyran-2-one	12.06
2,3-Pentanedione	2.52
Mequinol	2.47
1-Hydroxy-2-butanone	2.25
Propanoic acid	2.21
2(5H)-Furanone	1.72
Acetaldehyde	1.61
6-Oxa-bicyclo[3.1.0] hexan-3-one	1.47

The as-received light oxygenate fraction from red oak was first filtered through a bed of silica gel to remove all char residues. The pre-filtered sample was then analyzed by GC-MS and GC-FID. The chromatograms are shown in Figure. As shown, the fraction contains light oxygenates including acetaldehyde, acetone, acetic and acetol as expected. However, a significant amount of furanic compounds (primarily furfural) and phenolics were also detected. As discussed below, the presence of furanics has a strong deactivating effect on the catalyst.

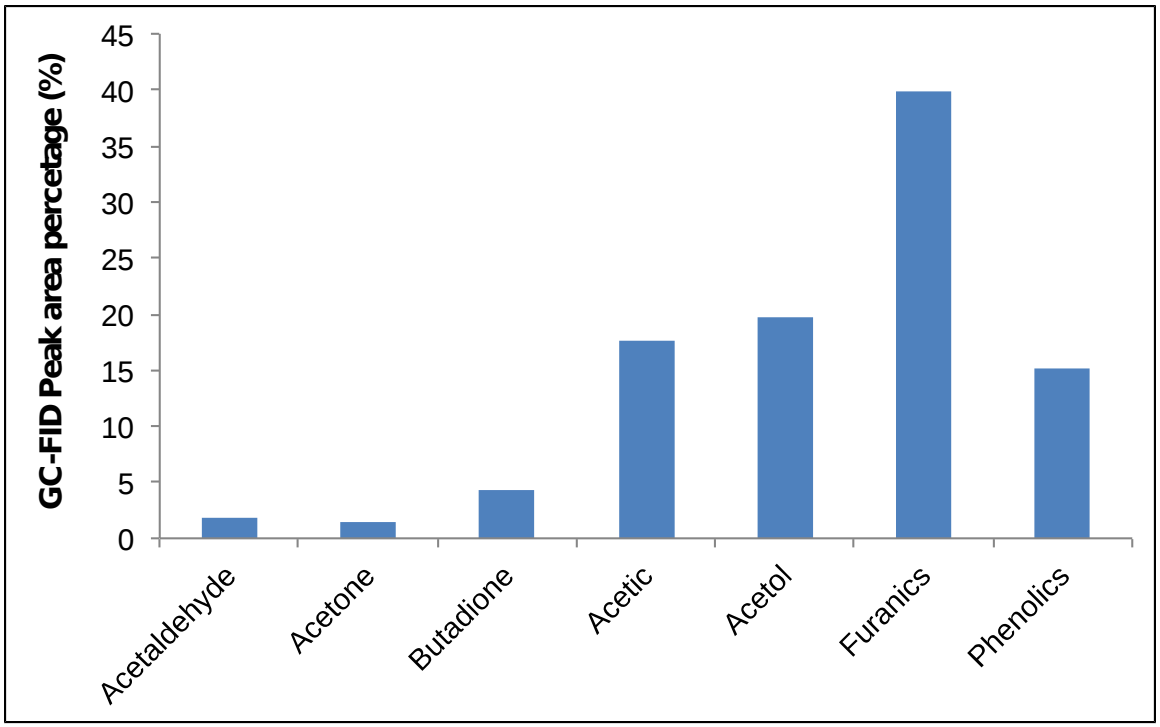

Figure 12. Relative concentrations of major species by GC-FID

Vapor Phase Condensation

An existing Plug Flow Reaction (PFR) system was modified to handle the complex light oxygenate fraction. Catalyst selections of Ru/TiO_2 , Ru/TiO_2 /carbon , and $Ni/CeZrO_2$ were based on model compound mixtures. Reaction temperatures, pressures, hydrogen levels and catalyst pretreatments were optimized.

The vapor-phase conversion of pre-filtered SF5 over Ru/TiO_2 was measured in an isothermal tubular reactor equipped with high-precision flow and temperature controllers. The catalyst was held at the center of a vertical tubular quartz reactor (6 mm I.D.) between two layers of quartz wool. Before reaction, the catalyst was reduced in situ for 1 h at 400ºC under a 50 ml/min flow of H_2. After reduction, the reactor was cooled down to the selected reaction temperature (285 ºC) under a He flow of 20ml/min. Pre-filtered SF5 (no dilution) was fed from a syringe pump and continuously vaporized into the He carrier gas stream. The reaction products were analyzed online by gas chromatography.

The results are shown in Figure 13. Similar to the case of the reaction in the liquid phase, we observed a large decrease in acetic acid, acetol, furanics, and phenolics together with the increase of acetaldehyde, acetone and condensation products. Deactivation of catalyst was also observed.

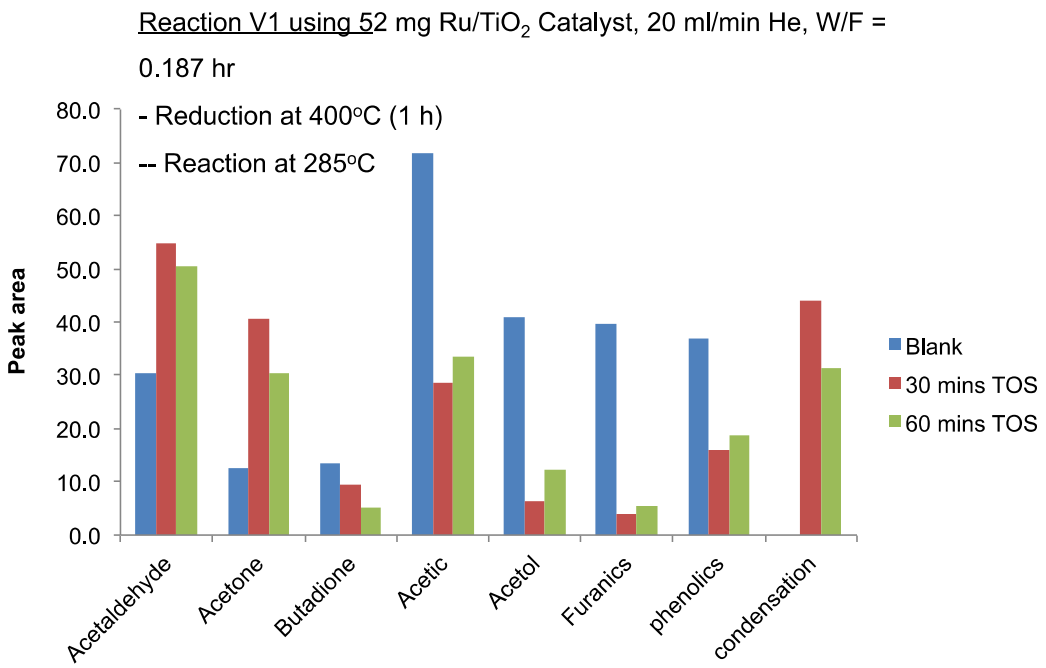

Figure 13. Relative concentrations of major species resulting from vapor phase condensation reaction

It is worth mentioning that after 60 min time on stream, small solid formed at high temperature at the needle tip of syringe pump caused the blockage of the reactor system in spite of our pre-filtration efforts.

Liquid Phase Condensation

An existing Parr reactor was modified to handle the complex light oxygenate fraction. Ru/TiO_2, Ru/TiO_2/carbon, and $Ni/CeZrO_2$ catalysts were selected based on model compound mixtures. Reaction temperatures, pressures, hydrogen levels and catalyst pretreatments were optimized.

An important step in the upgrading of SF 5 is acetic acid removal via ketonization. This upgrading strategy offers a great advantage since it not only removes the highly reactive acidic carboxylic groups and reduces oxygen content in SF5, but also increase the carbon chain length of small acids. This quarter we performed ketonization of the SF5 fraction in the vapor phase over a Ru/TiO_2 catalyst supported on carbon, which has been previously proven to be highly active and selective with clean acetic acid model feeds.[Pha12]

As mentioned above, the as-received SF5 samples were pre-filtered through a bed of silica gel in order to remove char residues and avoid reactor blockage during the reaction. When the fraction was injected as received, severe plugging of reactor and lines was observed.

We carried out the upgrading reaction in the aqueous phase using a 50 mL batch stainless steel autoclave reactor (Parr Corporation), equipped with impeller, temperature and pressure controllers. Activated carbon supported Ru/TiO_2 was used as the catalyst. After loading catalyst in the reactor vessel, we purged the reactor system with N2 to displace all air, then

pressurized with H_2 to 400 psi, and heated up to 250 °C for 4 h in order to reduce the catalyst. After completing the reduction period, the reactor was cooled down to room temperature, the pressure was released, and H_2 was purged out with N_2 at atmospheric pressure. The reactant feed, which was pre-filtered SF-5 sample diluted with deionized water at 2:1 volume ratio, was introduced to the reactor. Reaction temperature was at 250 °C, and pressure was 400 psi in Nitrogen. After reaction, the sample was filtered and analyzed using GC-MS and FID.

Figure 14 illustrates the change in sample color before and after reaction. As clearly indicated, after reaction, the samples become significantly more clear and clean.

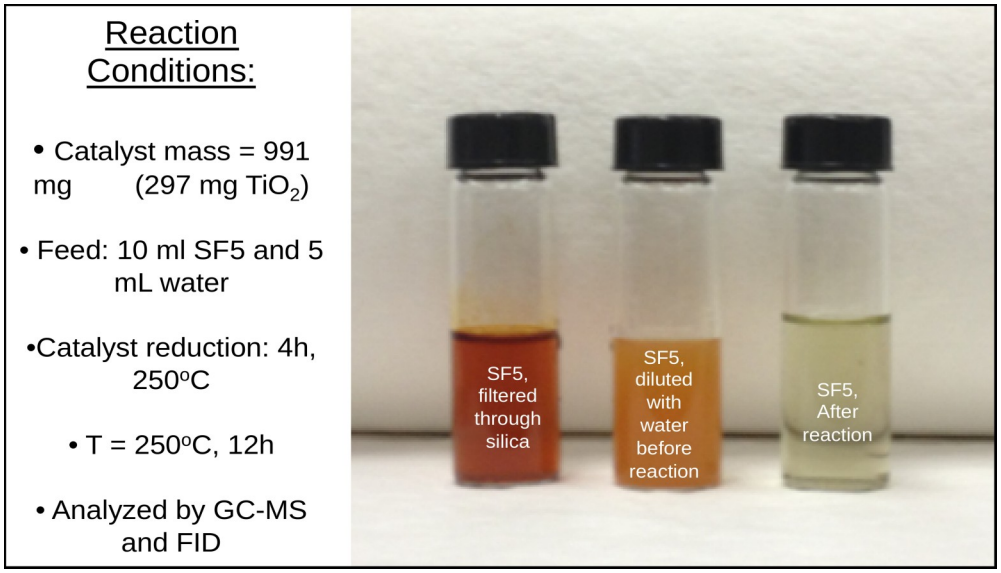

Figure 14. Sample color changes before and after liquid phase condensation reaction

Changes in the light oxygenate fraction before and after reaction are shown in Figures 15 and 16. Three major changes are observed after reaction

- Acetic and acetol significantly decreased along with the great increase in acetone amount
- Furanics and phenolics compounds suppressed
- Formation of some new condensation compounds: 2, 5-hexanedione, 2-cyclopentene-1-one-2methyl, 2-cyclopentene-1-one-2,3-dimethyl

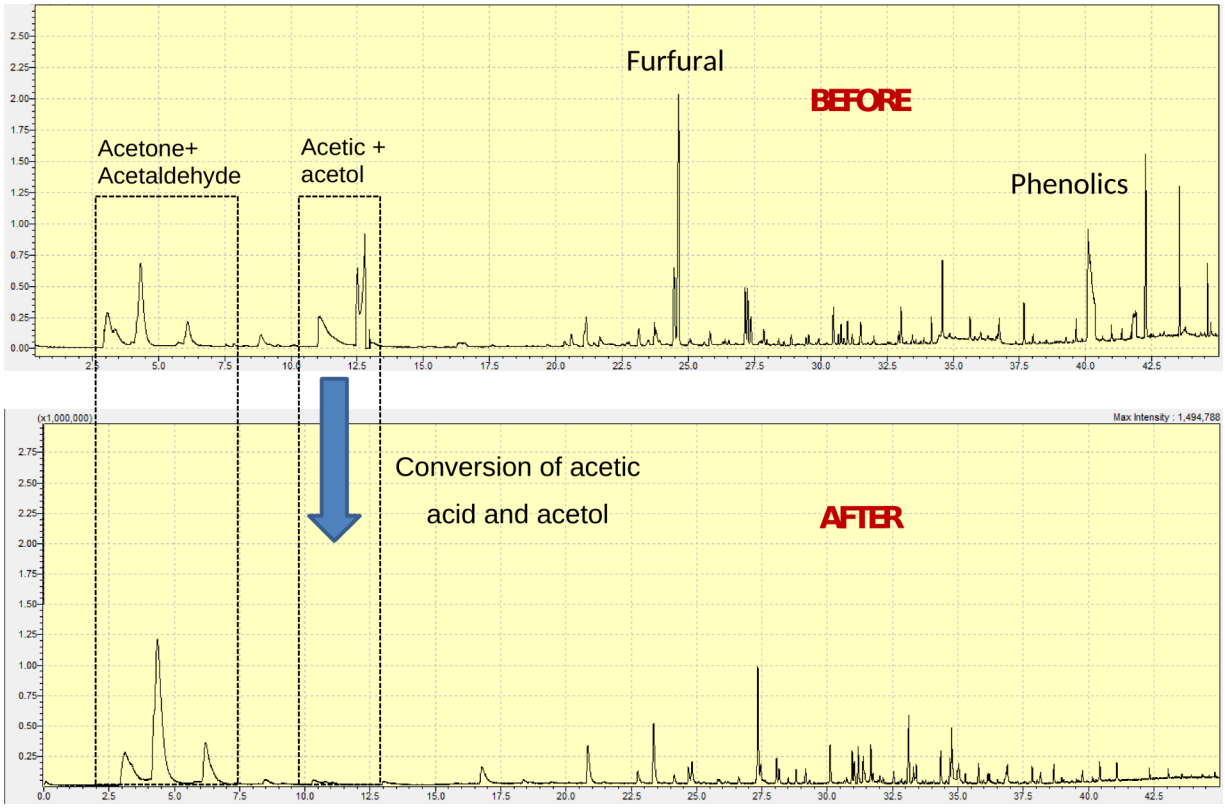

Figure 15. GC-MS analysis of light oxygenate samples before and after reaction

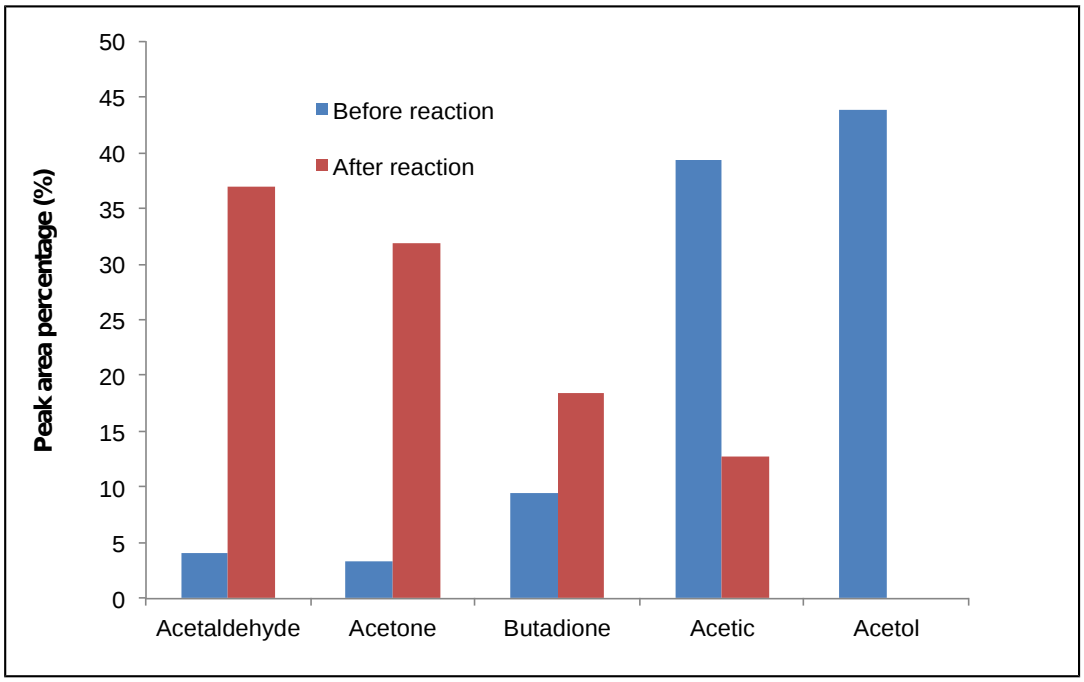

Figure 16. Comparison in changes in major species before and after reaction

The drastic reduction in acetic acid and production of ketones is a highly desirable feature. As described before, a subsequent hydrogenation of ketones produces alcohols, which can be used for alkylation and direct incorporation in the fuel pool.

A less desirable outcome is the carbon balance. Based on the total GC-peak area approximately 50% of the total carbon entering the ketonization reactor is lost from the product, which is unacceptably high. Our hypothesis is that the furanics and phenolics present in this fraction may undergo some polymerization to humins and coke deposits over the catalyst. Under identical conditions, using only acetic acid as a feed results in > 90% carbon balance.

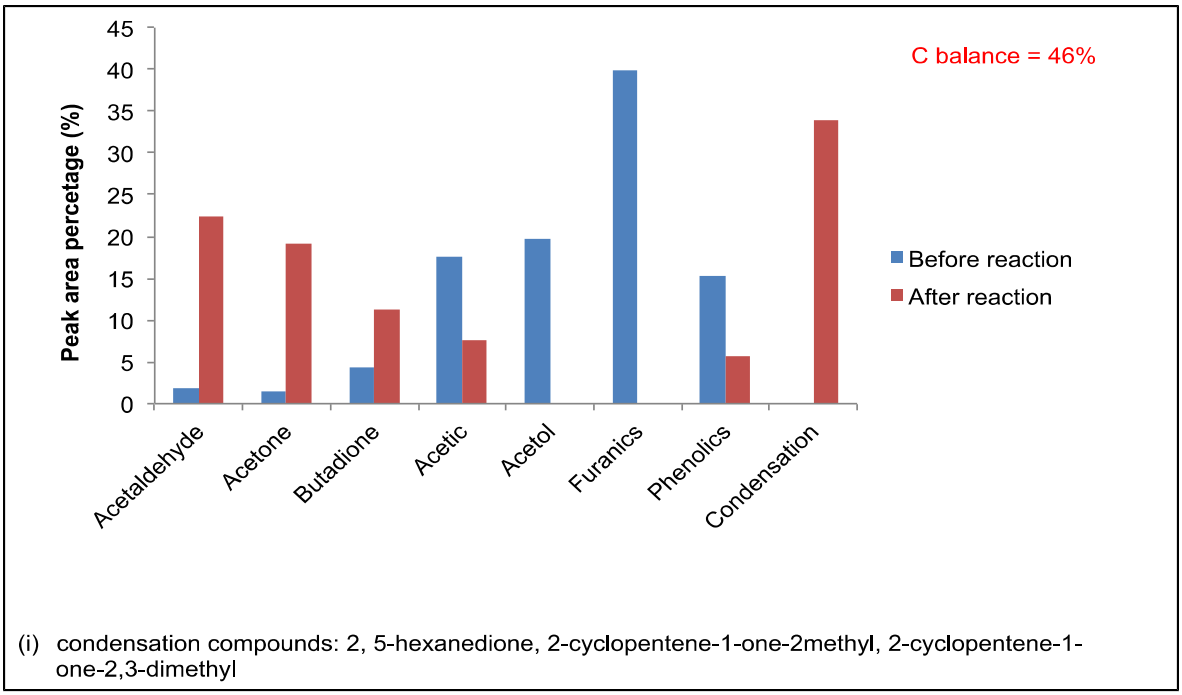

Figure 17. Comparison in changes in major species before and after reaction

Since acetol was completely converted after the reaction period, understanding of acetol reaction pathway during the upgrading process is necessary. Therefore, we performed the reaction of acetol in the liquid phase using the same catalyst ($Ru/TiO_2/C$) and reaction conditions as in SF5 upgrading reaction.

GC-MS data shows the formation of acetone, and some condensation products after the reaction which is mainly 2,5-hexadione. It is hypothesized that:

- Acetone is produced from acetol possibly via acetic acid
- Acetaldehyde might be formed but quickly undergo condensation to heavier compounds

As described in the report for Task 3, the upgrading of the soluble carbohydrate fraction results in a clean stream of glucose that can be readily converted into gluconic acid. One of the goals of that task is to convert gluconic acid into hexanoic acid. Tests were conducted with a

combined run of acetic acid (from the light oxygenate fraction) with hexanoic acid (from the soluble carbohydrate fraction).

The goal is to simultaneously upgrade different stage fractions of bio-oil. Hexanoic acid with the long hydrocarbon chain and light oxygenates in the light oxygenate fraction will spontaneously partition in the decalin and water phases, respectively. The catalyst located at the interface will be enable to catalyze the ketonization of acetic acid in the light oxygenate fraction as well as hexanoic acid from the soluble carbohydrate fraction. Together with self coupling, cross coupling between two acids is expected to occur, generating C7 ketone. All ketone products can further undergo condensation with each other to elongate the C chain length

More interestingly, the rate of cross ketonization between acetic acid and hexanoic acid is believed to be much faster than self ketonization rate of hexanoic acids, which will enhance the conversion of hexanoic acid.

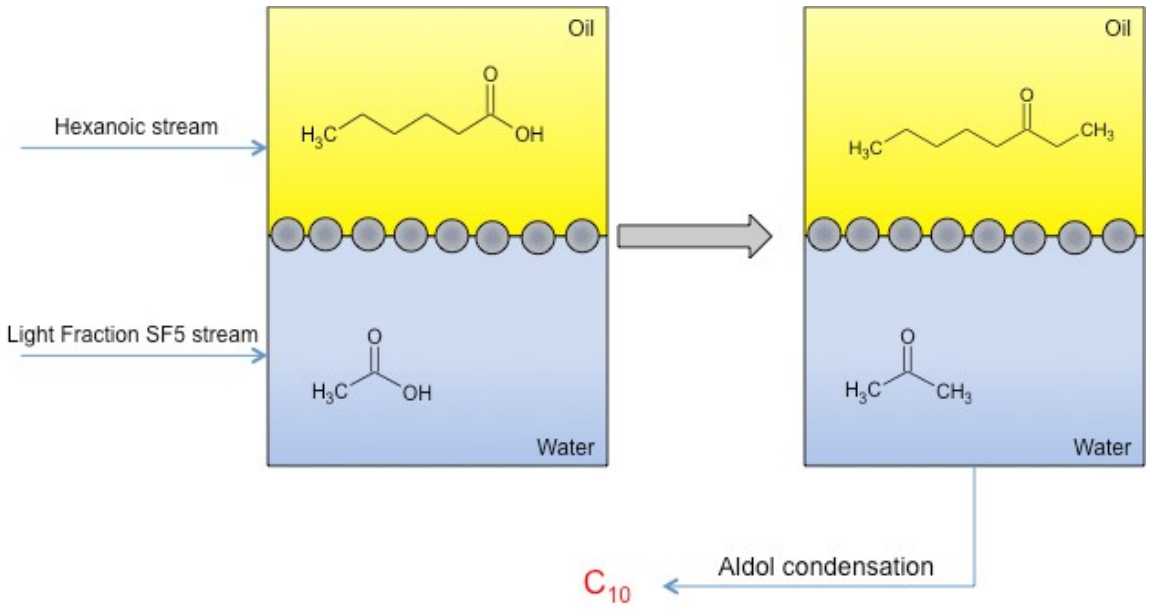

Figure 18. Biphasic reaction using products from the light oxygenate and soluble carbohydrate fractions

Figure 19 compares the ketone yield and C balance obtained at 300°C, 280°C, and 300°C with ethanol as cofeeder over $Ru/TiO_2/C$ catalyst. Three ketones are observed as major products: acetone, amylmethylketone and undecanone. As can be seen, ketonization rate decreases in the order : self ketonization of acetic acid > cross ketonization of acetic-hexanoic acid > self ketonization of hexanoic acid. It is important to note that by cofeeding acetic acid in the biphasic system, the total yield of ketones produced from hexanoic significantly increased in comparison with the run in single decalin phase using single hexanoic acid feed.

At 300ºC without ethanol as cofeeder, the Carbon balance of hexanoic acid is quite low. However, by lowering the temperature or cofeeding with ethanol, we can significantly improve the Carbon balance for this acid.

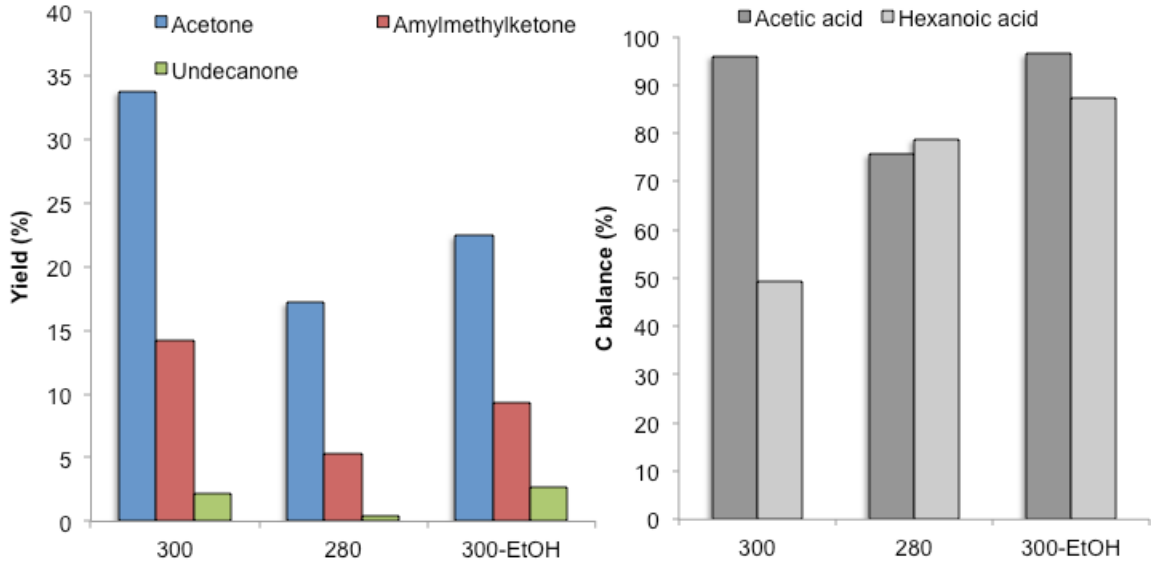

Figure 19. Ketone yield and carbon balance of different reactions

In summary,

- $Ru/TiO_2/C$ shows some loss in activity after regeneration, which might be due to the strong adsorption of furanics compounds present in the light oxygenate fraction.
- $Ru/TiO_2/C$ can be used to upgrade hexanoic stream from the soluble carbohydrate fraction to desirable C11 ketones. Co feeding hexanoic with alcohol can help to improve the Carbon balance of the process.
- Combined upgrading of the light oxygenate fraction and hexanoic stream from soluble carbohydrate fraction in a biphasic liquid system are proved to be effective and advantageous

Task 3. Stabilization of Soluble Carbohydrate Fraction (OU)

Analysis and Filtration of Soluble Carbohydrate Fraction

The HPLC analysis indicates that the most abundant *observable* compound in this fraction is ***levoglucosan*** (> 70 %) particles included in this fraction as well. See HPLC chromatogram in Figure 20.

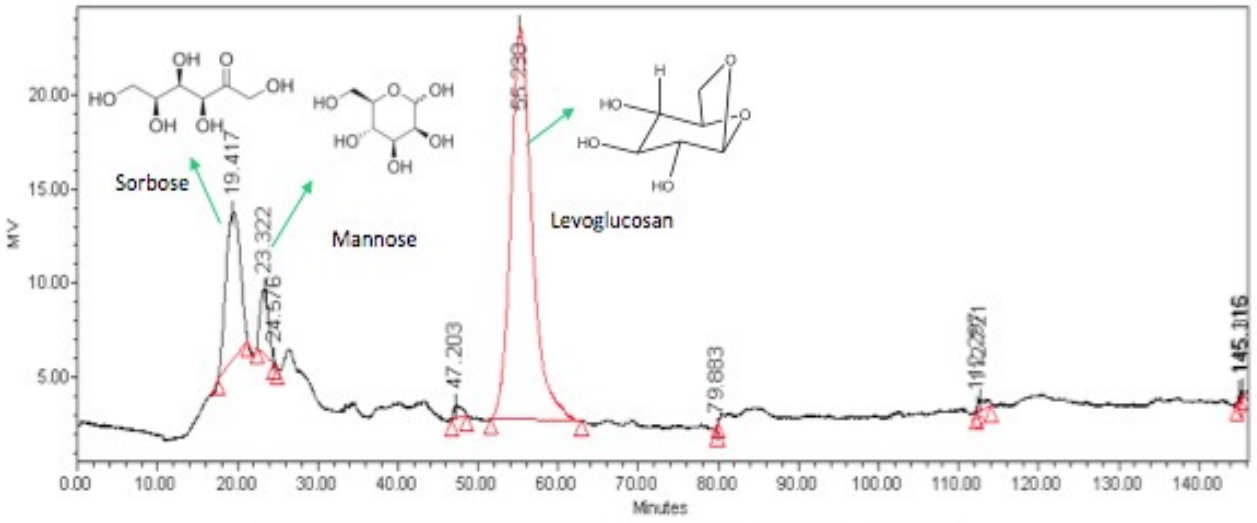

	Name	Retention Time (min)	Area (µV*sec)	% Area	Height (µV)
1		19.417	972620	18.67	7840
2		23.322	259347	4.98	3464
3		24.576	3167	0.06	338
4		47.203	47707	0.92	768
5	Levoglucosan	55.238	3860107	74.10	20816
6		79.883	585	0.01	0
7		112.297	3870	0.07	371
8		112.721	42868	0.82	670
9		145.115	7672	0.15	504
10		145.316	11107	0.21	499

Figure 20. HPLC analysis of soluble carbohydrate fraction using Aminex HPX-87P column

We discovered, however, there are suspended solid particles included in this fraction as well. This leads to significant problems associated with the conversion and subsequent upgrading of these fractions. Because of this, the bio oil fraction was purified by mixing with activated carbon, and then filtering as shown in Figure 21. The concentration of detected levoglusosan and sugars remained similar after filtration, indicating that the only species adsorbed on the activated carbon were suspended solid char particles and humins.

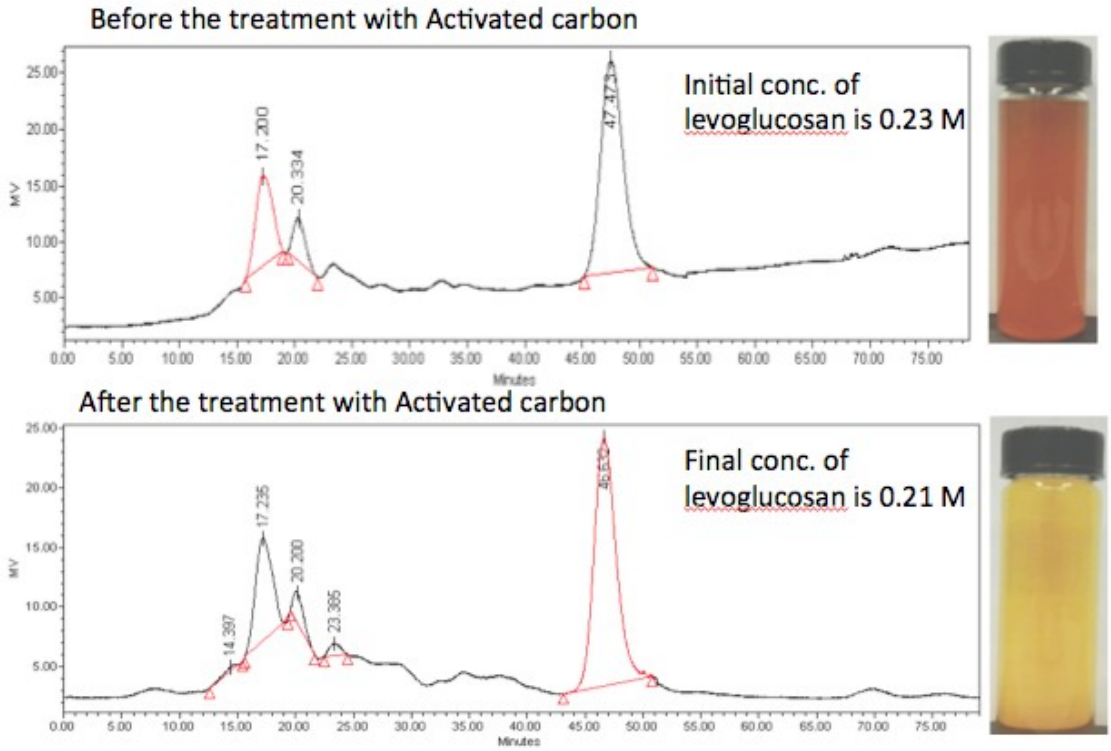

Figure 21. HPLC chromatograms and sample images of soluble carbohydrate fractions before and after activated carbon treatment

Separation of the glucose from gluconic acid was conducted by changing the column to at Aminex HPX-87H column, and using two detectors. The RI detector was found to show signals for glucose, levoglucosan, as well as the gluconic acid, while the UV detector is sensitive only for the sodium gluconate. This is important for the determination of gluconanic acid in the presence of unreacted glucose. These are demonstrated by the use of standard solutions in Figure 22.

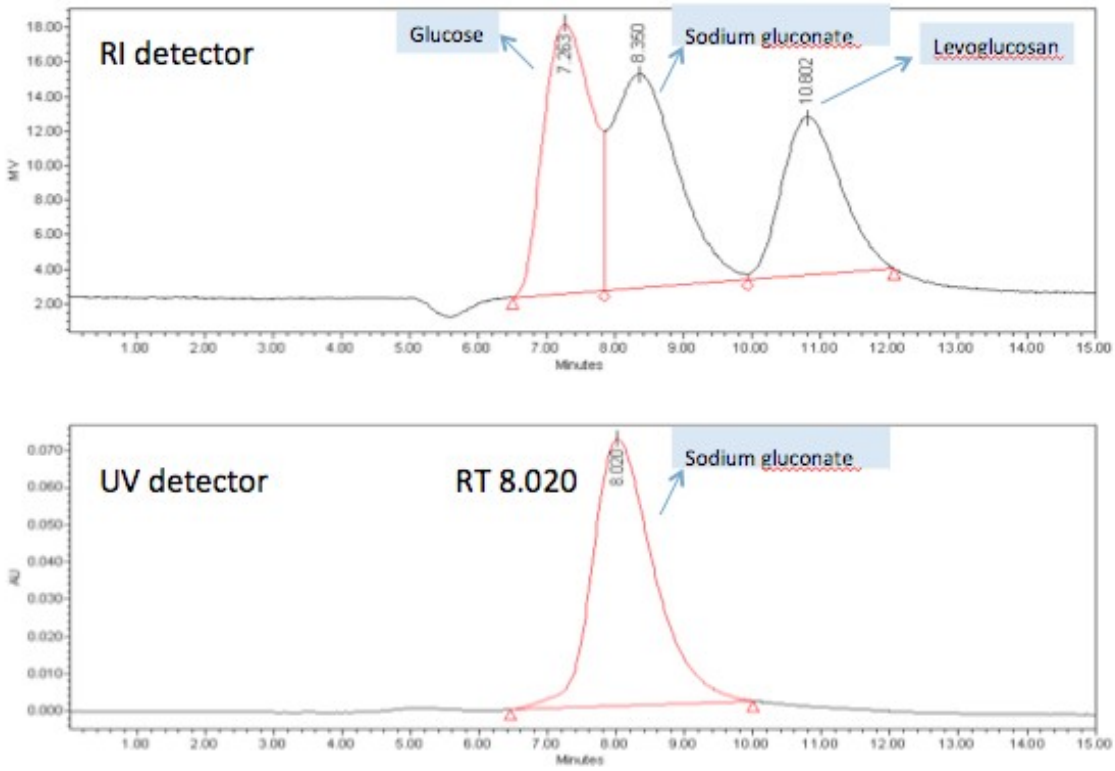

Figure 22. HPLC chromatogram of standard compounds using Aminex HPX-87H column and RI and UV detectors

Hydrolysis of Model Compounds

Based on our product analysis, levoglucosan was chosen as the model compound for hydrolysis. This hydrolysis step is necessary to expose the levoglucosan for selective attack to the acid. Without the hydrolysis step, oxidation conditions must be more severe and product selectivity to monofunctional acids decreases. Amberlyst-15 was chosen as a strong acid capable of hydrolyzing levoglucosan to glucose, as will be discussed below. It is important to note that as the project progresses, attempts will be made to combine the hydrolysis and oxidation steps in a single reaction step.

Levoglucosan can be converted over Amberlyst-15 under relatively mild conditions, as shown Table 6. These relatively mild conditions are capable of producing the desired product, glucose, in high abundance. These conditions produced 94% conversion of levoglucosan to glucose with 100% selectivity. The chromatographs are shown in Figure 23.

Table 6. Levoglucosan conversion conditions

Reactor	Glass reactor
Reactant	Levoglucosan
Concentration	0.25 M
Catalyst	Amberlyst-15
Temperature	110 °C
Pressure	Atmospheric pressure
Reaction time	24 hrs
Volume of reactant	25 ml
Amount of catalyst	160 mg

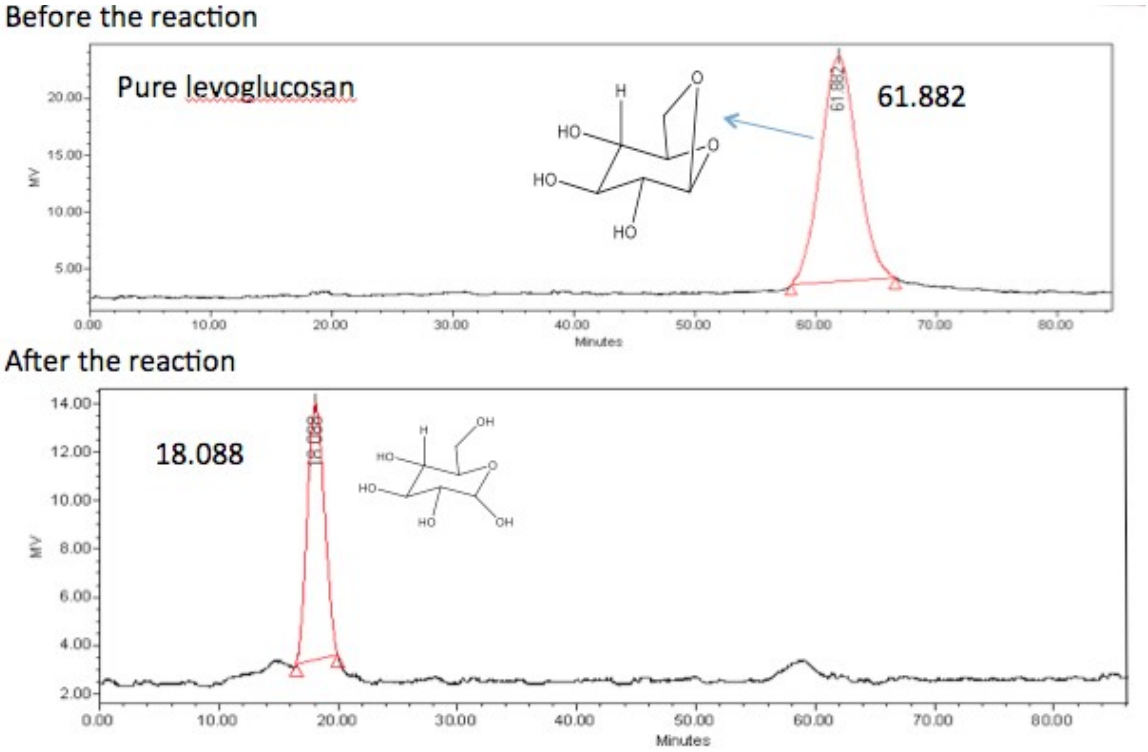

Figure 23. HPLC chromatogram after the hydrolysis of model compound levoglucosan to glucose over Amberlyst-15

Hydrolysis of Soluble Carbohydrate Fraction to Obtain Sugars

Several catalysts were tested for the hydrolysis of the SF1 and SF4 fraction to glucose. These include aqueous sulfuric acid (2M), HY zeolite, sulfonated multiwalled carbon nanotubes (SO_3-H/MWNT), and the previously discussed Amberlyst 15. Of the heterogeneous catalysts employed, Amberlyst-15 exhibited the greatest activity.

Reaction conditions were chosen based on those determined promising from the model compound studies. The same conditions were utilized. Products were analyzed using the same techniques discussed above. Reaction results are shown in Table 7.

Table 7. Soluble carbohydrate hydrolysis products

Catalyst	Conversion (%) Levoglucosan	Selectivity (%) Glucose
Sulphuric acid	88	100
Zeolite (Si/Al = 2.6)	No conversion	---
SO_3H-MWNT	2	100
Amberlyst-15	83	100

Amberlyst-15 showed promising conversion, comparable to the 2M sulfuric acid solution. Similar weights of protonated zeolite, or sulfonated nanotubed did not show comparable activity. The disappearance of levoglucosan yielded glucose in all cases, although these samples still contain mannose and sorbose impurities from the original fraction. A HPLC chromatogram of the results over Amberlyst-15 is shown in Figure 24.

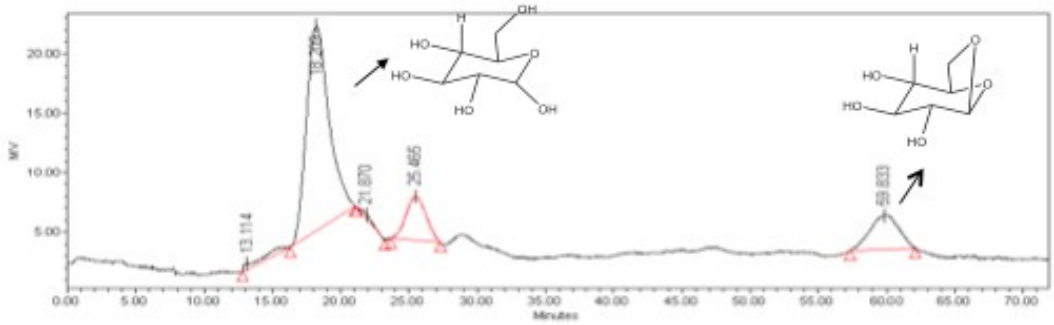

Figure 24. HPLC chromatogram of reaction products after the hydrolysis of soluble carbohydrate fraction with Amberlyst-15

Partial Oxidation of Model Compounds

Due to the 100% selectivity to glucose obtained upon the conversion of levoglucosan, glucose was chosen as the model compound for the subsequent partial oxidation. 5wt% Pd/C was chosen as a promising catalyst for the conversion of glucose to gluconic acid. The following conditions (Table 8) were chosen for the conversion of glucose to gluconic acid over Pd/C.

Table 8. Reaction conditions for conversion of glucose to gluconic acid

Reactor	Glass reactor
Reactant	Glucose
Concentration	0.25 M
Catalyst	5% Pd/Carbon
Temperature	60 ^{o}C
Pressure	Atmospheric pressure
Reaction time	24 hrs
Volume of reactant	10 ml
Amount of catalyst	80 mg
Flow rate of Air	62 ml/min
Medium	Alkaline (NaOH)
pH	9.3

Initial conversion of glucose was attempted with hydrogen peroxide as the oxidant, but these conditions show promising conversion with air as will be shown later. NaOH was shown as the basic stabilizer for the oxidation. Without the presence of NaOH, the acid molecules do not desorb from the catalyst surface and the catalysts do not show measurable activity. Reactions were conducted at a constant pH, so NaOH was constantly added to maintain this pH as acids were formed.

The conversion of glucose over 5% Pd/C under the conditions discussed above were adequate to convert 56% of the glucose with a selectivity of 78% to gluconic acid. The corresponding HPLC chromatograms are shown in Figure 25

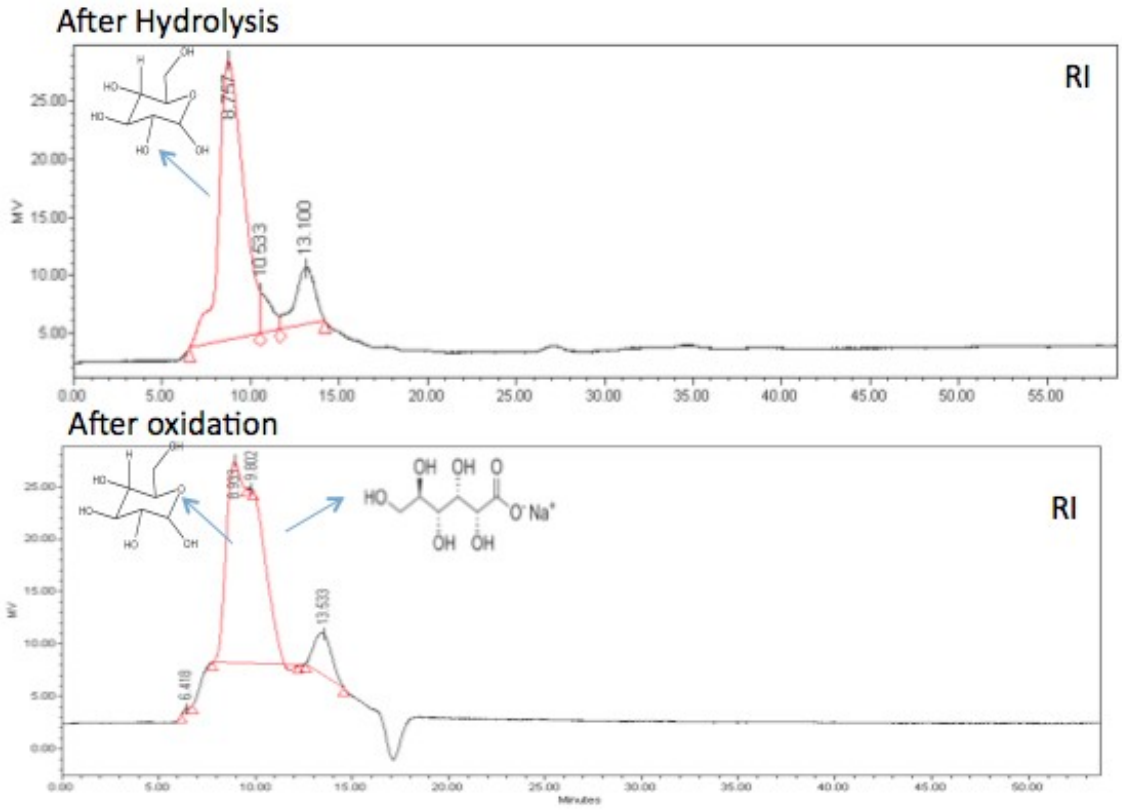

Figure 25. Chromatograms of glucose conversion to gluconic acid over Pd/C

Partial Oxidation of Hydrolyzed Soluble Carbohydrate Fraction to Obtain Sugar Acids

The same catalyst used in the model compound studies was selected for conversion with the real hydrolyzed SF1 and SF2 fractions. The reaction conditions shown in Table 9 were chosen. The pH was still maintained at 9.2, but through the use of a 0.1M carbonate buffer. This simplified the reaction by maintaining a more constant pH.

Table 9. Reaction conditions for conversion of hydrolyzed soluble carbohydrate fractions to sugar acids

Reactor	Glass reactor
Reactant	Hydrolyzed SF1 and SF2
Initial pH of reactant	2.77
Concentration	0.21 M
Catalyst	5% Pd/Carbon
Temperature	40 ^{o}C
Pressure	Atmospheric pressure
Reaction time	6 hrs
Volume of reactant	10 ml
Amount of catalyst	80 mg
Medium	0.1 M Carbonate Buffer (9.2)
Flow rate of Air	65 mL/min

The resulting products can be observed in Figure 26. Results indicate that glucose is converted to gluconic acid under these conditions. Conditions still need to be optimized, but these preliminary results demonstrate promise.

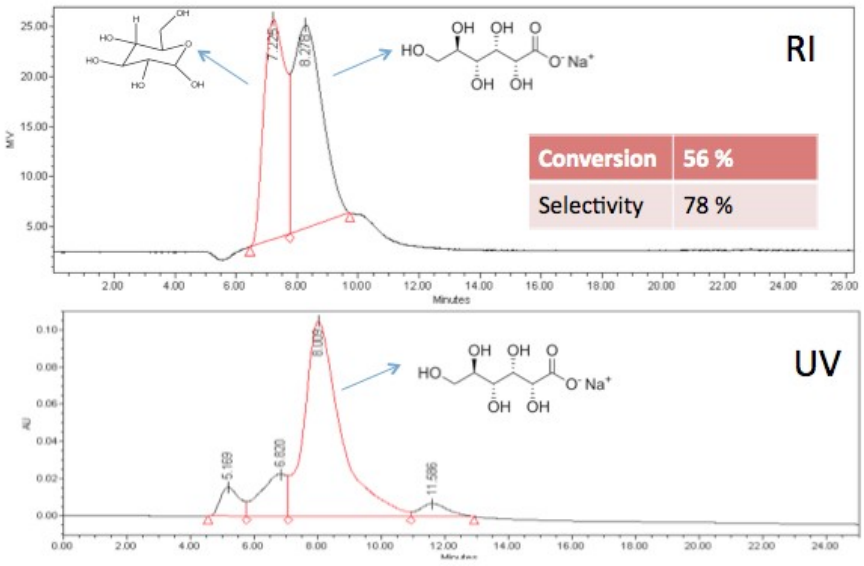

Figure 26. Result of oxidation of hydrolyzed SF1 and SF2 over Pd/C

Upgrading of Sugar Acids

The conversion of sugar acids proceeds through a complicated reaction path, as too much acidity may lead to excessive condensation reactions. The balance between dehydration over acids and the metal function has important implications on the reaction products. The conversion to useful products was not significant in the previous studies conducted at atmospheric pressure. The pressure has been increased to improve the hydrogenation and decrease coke formation. In all cases blank tests were conducted to ensure that reactions with the solvent were negligible.

Three catalysts were chosen, The first is a combination of Pd with a zeolite with a hydrophobized surface. The combination of Pd with zeolite was chosen to both increase the proximity of the metal with the acid sites. The combination of acidity with the metal on the same catalyst reduces the proximity of the two functional groups on the same catalyst. Another very important property of this catalyst is the hydrophobized surface. This significantly improves the stability of the zeolite in hot liquid water, enhancing its prolonged activity. Hydrophized zeolites can also reside at the oil/water interface and produce pickering emulsions. This enhances the rate of mass transfer to the catalyst while forming an oil film over the catalyst to further improve the catalyst stability in hot water.

We have combined this catalyst with Pd/SiO2 to increase to total metal content in the system and change the product distribution. Finally, this is compared with copper chromite, a catalyst that has both acidity and a metal function, while limiting the ability to decarbonylate C=O bonds to produce CO. This reaction can be readily accomplished over many metals, including Pd.

Table 10. Reaction conditions for conversion of sugar acids to aliphatic acids

Parr Reactor	Test with octane as solvent
Reactant	Gluconic acid
Concentration	0.25 M
Catalyst	1% Pd-OTS /HY 30
Temperature	200 ^{o}C
Pressure	1000 psi H_2
Reaction time	24 hrs

Below is a comparison of the products reacted and removed from the aqueous phase after reaction. Products removed from the aqueous phase can either be soluble in the oil phase, or may be solid particulates or coke on the catalyst. In each case, the conversion is significant, but still a great deal of products are present in the aqueous phase.

Table 11. Comparison of carbon content in products reacted and removed from aqueous phase

C wt% in Aqueous phase		
Reaction condition	**Before reaction**	**After reaction**
500mg 1% Pd-OTS /HY 30	2.54 (0.12) *	1.6 (0.09)
500mg 1% Pd-OTS /HY 30 + 150 mg 1% Pd/ SiO2	3.12** (0.11)	1.99(0.11)
500mg 1% Pd-OTS /HY 30, with octane as oil phase	2.54 (0.12)	1.30(0.10)

Note:

* the number in the bracket is the standard deviation over 3 measurements
2.54 C% corresponding to 5ml gluconic acid solution diluted with 45mL H2O.

** 3.12 C% corresponding to 5ml gluconic acid solution diluted with 35mL H2O.

Ketonization of aliphatic acids

Based on detailed kinetics of model compounds as a function of chain length, we can predict the activation energy necessary to convert the C6 aliphatic acids that we aim to produce from levoglucosan. These results are shown in Figure 27.

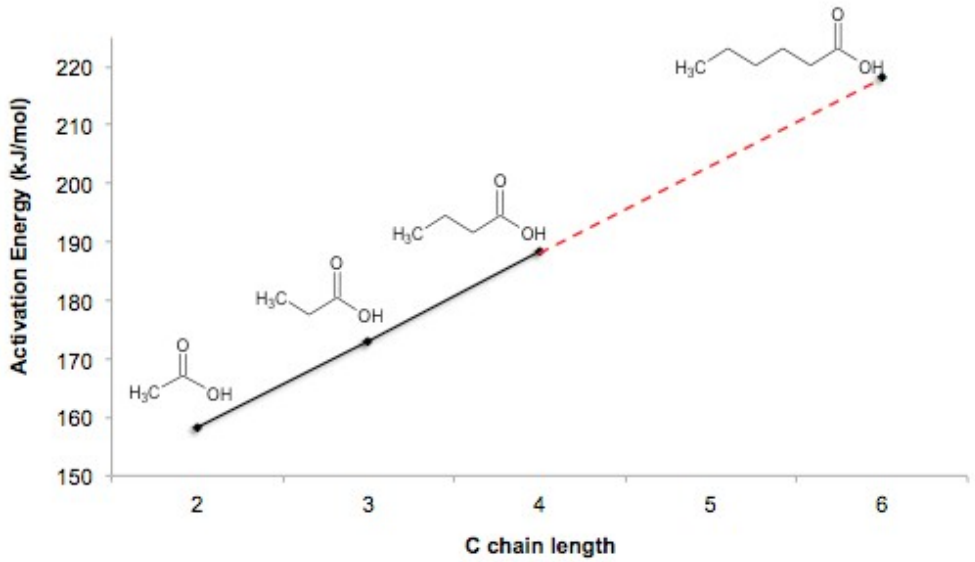

Figure 27. Predicted activation energy required to convert C6 aliphatic acids

These higher activation energies indicate that higher temperatures may be necessary to convert the larger acids. This is indeed what is found by reacting the model compound hexanoic acid, over Ru/TiO_2 supported on C, a catalyst that has demonstrated considerable

promise for the conversion of carboxylic acids to the desirable ketone. This trend is observed upon conversion of hexanoic acid as shown in Figure 28. It is important to note the very low conversions observed in all cases resported here. At higher reaction temperatures, thermal reactions become dominant, producing coke and an array of less desirable products.

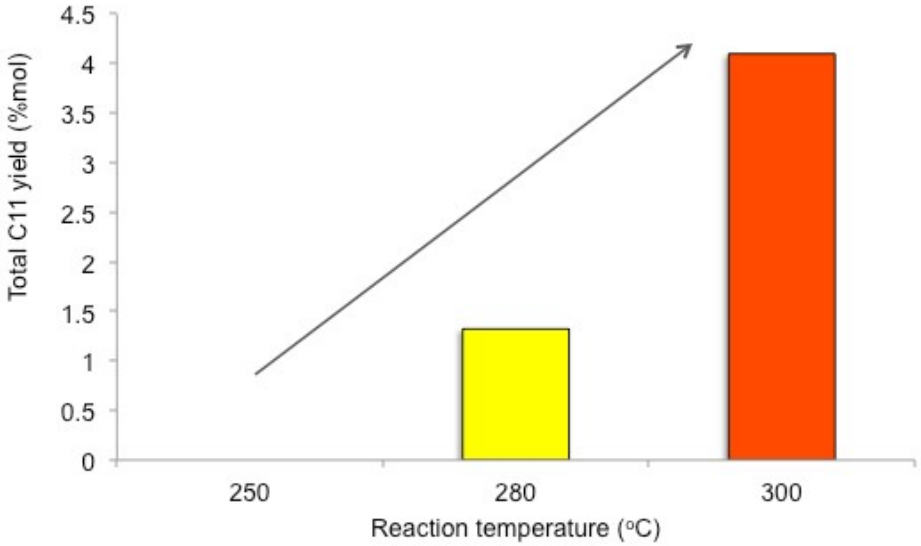

Figure 28. C11 yield as a function of reaction temperature

We have devised two separate strategies to approach this challenge. One is to co-feed an alcohol to form an ester intermediate. This ester will have a higher thermal stability, and will reversibley form lower concentrations of the carboxylic acid that can couple to form the ketone. A schematic of the process as well as yields and the C balance are shown in Figure 29. Both the yield of C11 ketone as well as the C balance are improved upon comparsion with the feeding of the acid without the alcohol at the same temperature, 300°C.

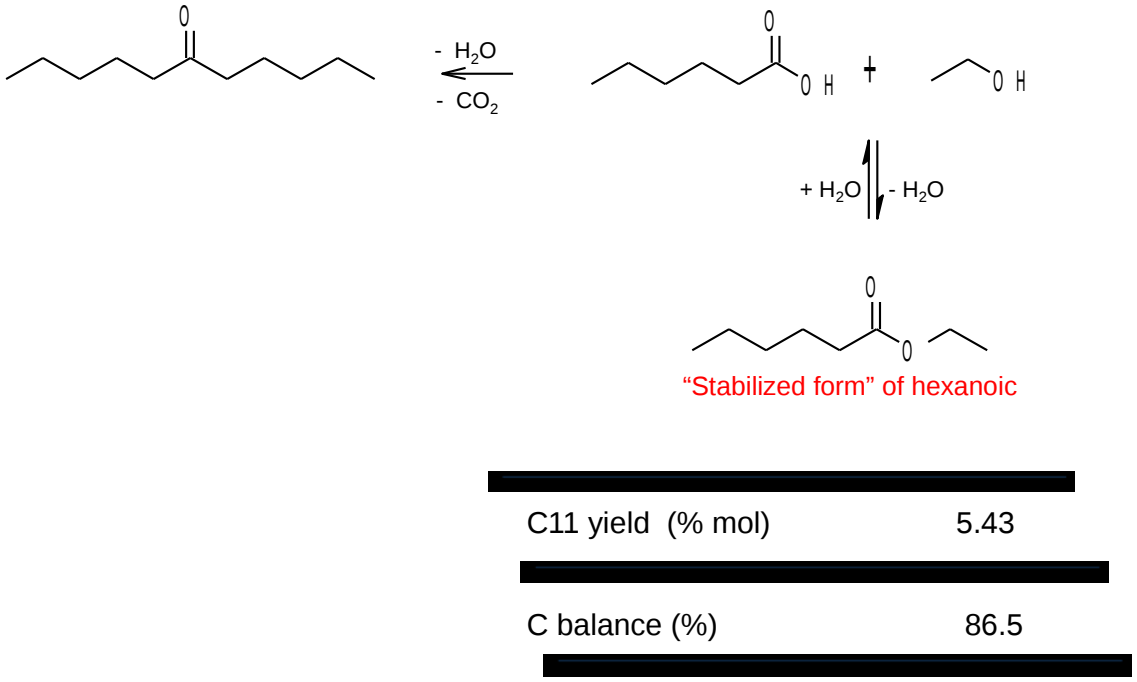

Figure 29. Ketone formation using alcohol co-feed to form ester intermediate

Another option is to take advantage of "cross ketonization" between a light acid with a lower activation energy and conducting the reaction at a lower temperature. Results showing both the conversion in the presence of acetic acid as well as while co-feeding the alcohol, ethanol are shown in Figure 30. In all cases, the yield of products from hexanoic acid are greatly enhanced. In this case, the cross condensation product is amylmethylketone (C7) rather than the larger C11. However, this intermediate will have a more active alpha hydrogen and will be easier to undergo subsequent aldol condensation with, for example, acetone, to produce diesel range products. This is a promising route that could lead to a combined strategy that incorporates the light oxygenate stream with the light acetic acid along with the hexanoic acid produced in this step.

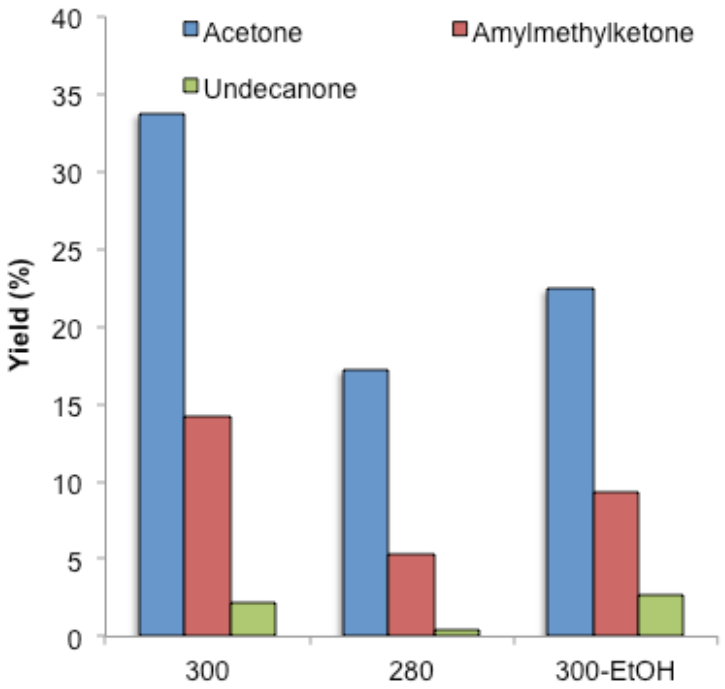

Figure 30. Ketone yield in presence of acetic acid and while co-feeding ethanol

Task 4: Stabilization of Middle Fraction (OU)

Analysis of Middle Fraction

The as-received middle fraction was first filtered through a bed of silica gel to remove all char residues. The pre-filtered sample was then analyzed by GC-MS and GC-FID. The chromatograms are shown in Figure 31. As shown, the SF5 contains light oxygenates including acetaldehyde, acetone, acetic and acetol as expected. However, a significant amount of furanic compounds (primarily furfural) and phenolics were also detected. As discussed below, the presence of furanics has a strong deactivating effect on the catalyst.

The pure feed was first dissolved in acetone and then analyzed by GC-MS, which showed that the middle fraction contains light oxygenates, furfurals, phenolics and nitrogen-containing compounds. In the graphs below we compare the percentage of the areas under the curve for each family of compounds. We can see that the phenolics and furanics are the main components of this fraction.

After filtering, the middle fraction mixture remains as a viscous liquid with a dark brown color. It is impossible to observe any difference between before and after filtering. For further analysis and processing, the middle fraction was diluted in acetone. A silica gel filter helps to remove the char and solid in the middle fraction, which is evident in the more diluted samples. The middle fraction contains furanics, carboxylic acids and phenolics.

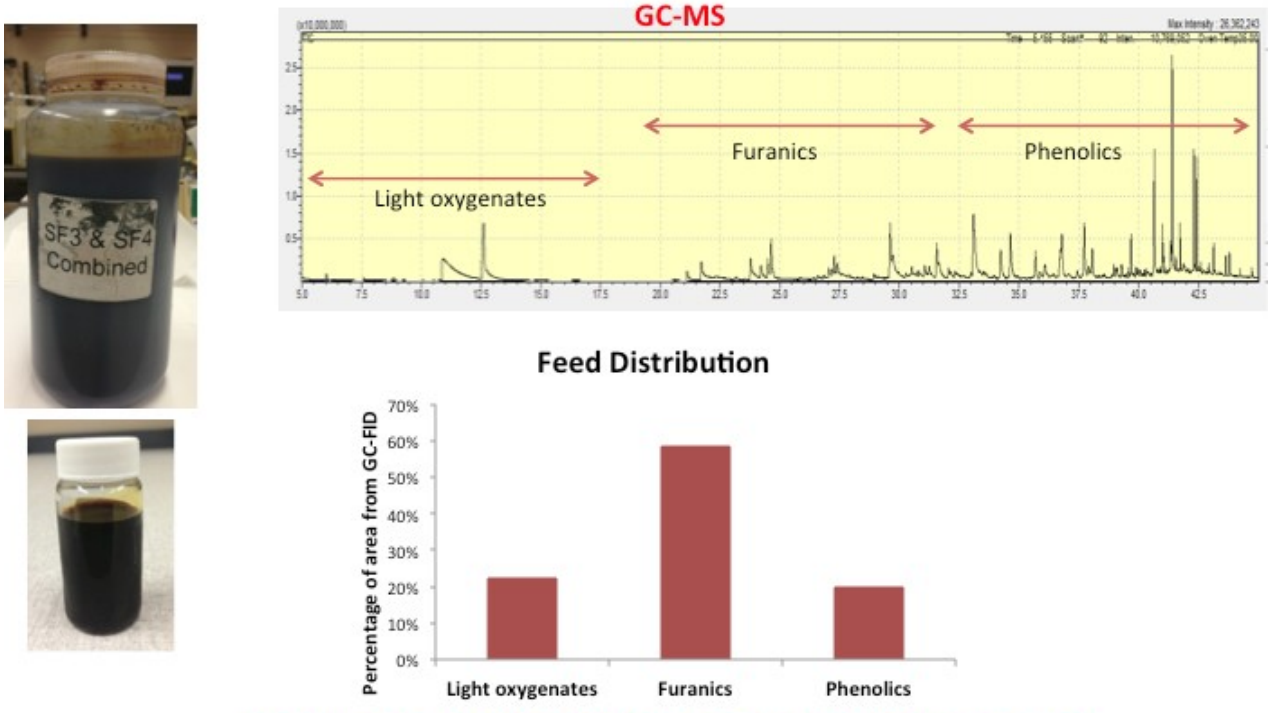

Figure 31. Major species content in middle fraction

Targets and Approach

The targets for the middle fraction were to:

- Eliminate/reduce the amount of oxygen in the middle fraction and create more hydrocarbons
- Alkylate to make longer carbon chain, capture small molecules and transfer them into fuel range compounds
- Maximize the carbon balance before and after the upgrading processes

To achieve these targets, two approaches were used:

- Biphasic reaction (emulsion): After being filtered through silica gel, the middle fraction is fed directly into the reactor.
- Single phase reaction: After being filtered through silica gel, the middle fraction is dissolved in water and decalin. Then execute catalytic reaction with each individual phase.

Liquid Phase Hydrodeoxygenation

In the biphasic reaction, the solvents are water and decalin, in which the ratio of each solvent to middle fraction is 2:1. In order to prevent coke deposition inside the reactor, we use a teflon liner. First, the catalyst is horn sonicated in water for 15 minutes, then add decalin and continue to sonicate for 15 more minutes. At this point, emulsion is formed. Then we add middle fraction after filtering through silica gel to the mixture and batch sonicate for 30 minutes. After that, the whole mixture is put into a batch reactor and the reaction is carried out at the specified conditions.

From Figure 32 below it can be observed that there is a serious problem when attempting to run this reaction with the full mixture. Polymerization becomes a serious impediment for an efficient upgrading. Polymerization is undesirable because it decreases the yield and selectivity of the reaction. As pressure increases from 300 psi to 1000 psi, the problem of polymerization is slightly reduced, but the problem still persists.

It was hypothesized that the residue in the feed that is insoluble in either aqueous or organic phase expedites the polymerization process. If we can remove the residue and work with each phase individually, we can reduce the problem of polymerization

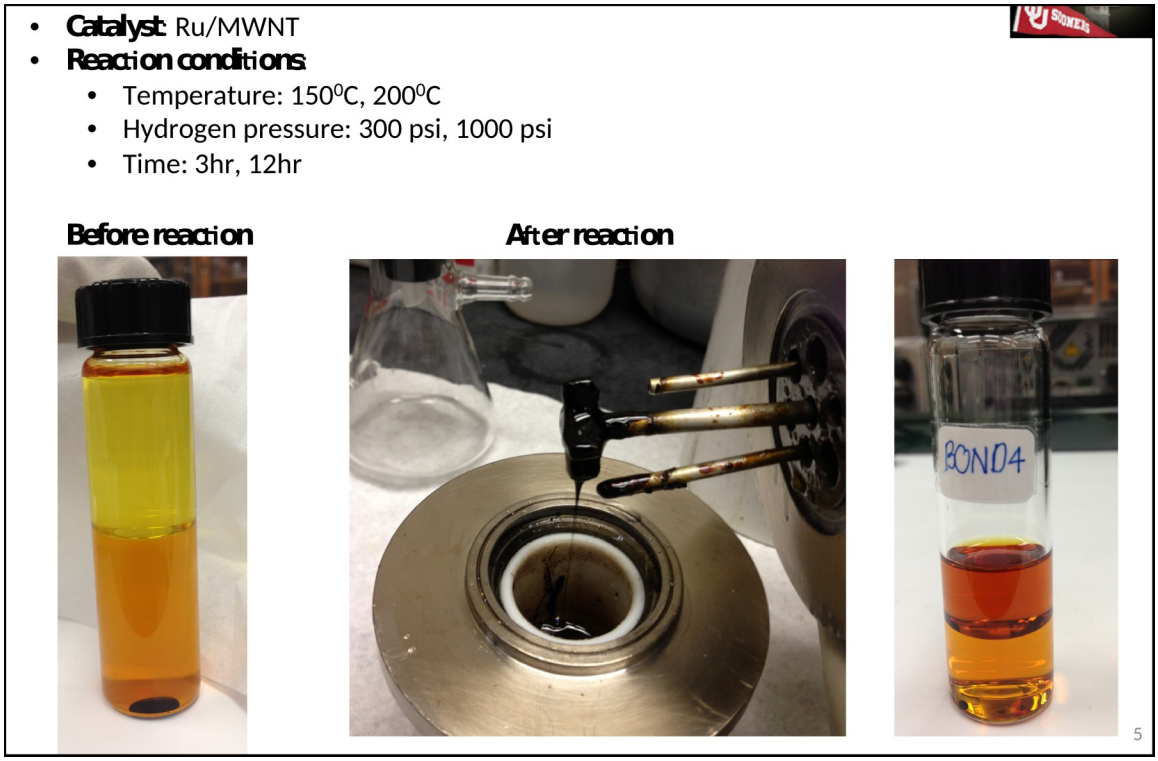

Figure 32. Polymerization of middle fraction during hydrodeoxygenation

In this approach, middle fraction is dissolved in water and decalin solvent. Almost all of the phenolic compounds dissolve in the decalin phase, while almost all of the light oxygenates and furanics dissolve in the aqueous phase. Since we aim to preserve the greatest majority of products after upgrading, the organic and aqueous sub-fractions as the solvent for this heavy fraction, we used the following strategy with this fraction:

a) For the decalin-soluble sub-fraction, we perform hydrodeoxygenation reaction to remove oxygen and create hydrocarbons in the fuel range.
b) For the water-soluble sub-fraction, first we do ketonization to remove the reactive carboxylic acid functional group and increase the chain length of small acids. Then, similarly to the organic phase, we want to carry out hydrodeoxygenation reaction.
c) We have found that the heavy compounds insoluble in water and/or decalin are soluble in tetrahydrofuran (THF). This sub-fraction contains compounds that should be directly hydrodeoxygenated.

For the upgrading of the decalin-soluble part, we added the catalyst (either Pd-Cu/C, Pt-Sn/Al_2O_3) to decalin, reduced it at 300^{0}C in 500 psi H_2 for 3 hours and then injected the feed of the organic phase into the reactor and run the reaction at the specified conditions. The selection of these two catalyst candidates was made on the basis of previous model compound studies. We have observed before that the addition of oxophilic elements (such as Sn or Cu) to the supported Pt catalysts greatly enhanced the deoxygenation and reduced the saturation of the aromatic rings, which would unnecessarily increase the H_2 consumption.

We can clearly see that the reaction mixture is much cleaner than that of the full middle fraction and the polymerization is completely eliminated. As seen in Figure 33, the image on the right shows the change in the color of the solution after the reaction using the two different catalysts.

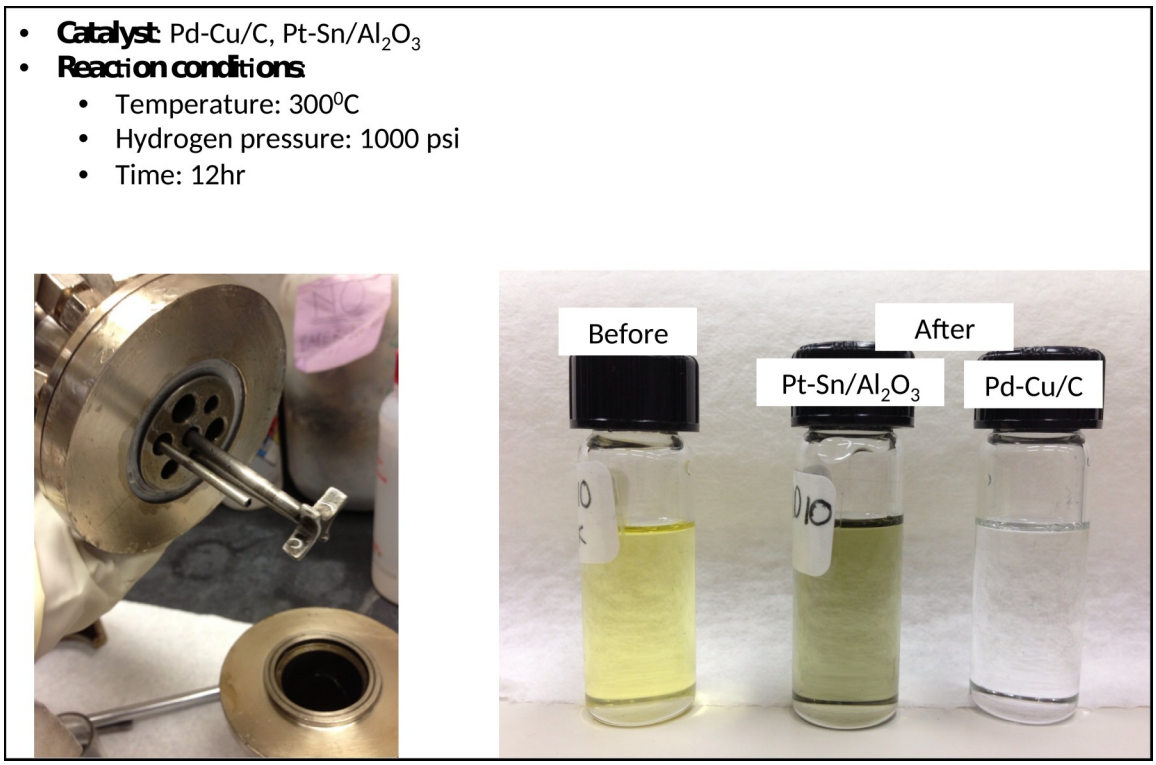

Figure 33. Upgrading of the decalin-soluble portion of the middle fraction

In Figure 34 we summarize the quantitative analysis of the products after reaction of the decalin-soluble sub-fraction. We can clearly see that large amounts of long-chain hydrocarbons are produced, while furanics, light oxygenates and methoxy phenols greatly decrease. We are able to efficiently remove oxygen from the compounds and make more long chain hydrocarbon. The Pt-Sn/Al_2O_3 catalyst showed to be more effective than Pd-Cu/C since it produces more hydrocarbon and less long-chain oxygenates.

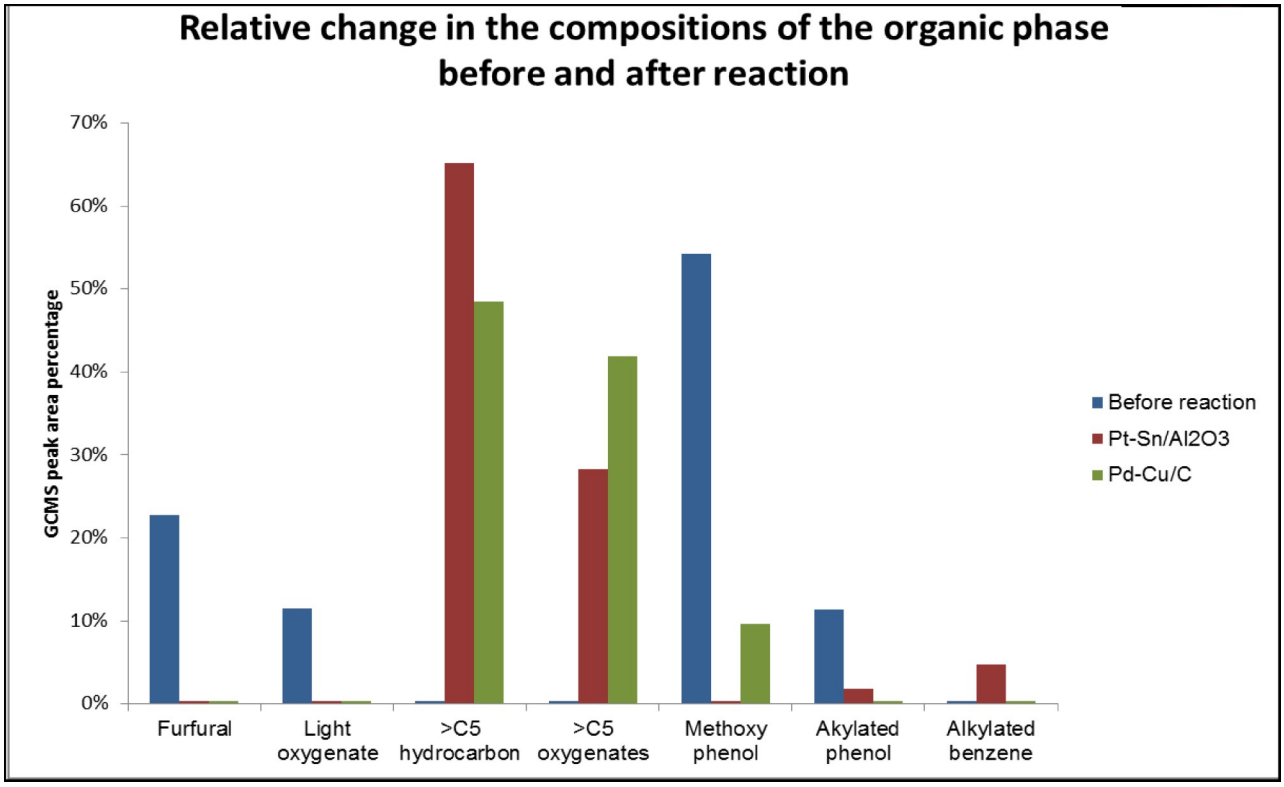

Figure 34. Comparison composition of the decalin-soluble portion of the middle fraction before and after reaction

Further Fractionation of the Middle Fraction

As stated above, in order to have a cleaner feed to the reactor and to prevent the problem of polymerization, it is necessary to remove the heavy compounds from the middle fraction. When the middle fraction is dissolved in decalin and water, there are three separate portions including water-soluble, oil-soluble and heavy compounds portions. The heavy compounds are not dissolvable in either water or oil. The weight distribution of the middle fraction in each portion is reported as above. The oil-soluble portion is minimal compared to the other two portions, while the major one is water-soluble. Therefore, the main focus of the upgrading strategy will be the water-soluble portion and the heavy compounds.

The carbon percentage of the middle fraction and the water-soluble portion are measured with the Elemental Analysis Instrument. It was calculated that 74% and 26% of carbon in the middle fraction is in the water-soluble portion and the heavy compounds, respectively.

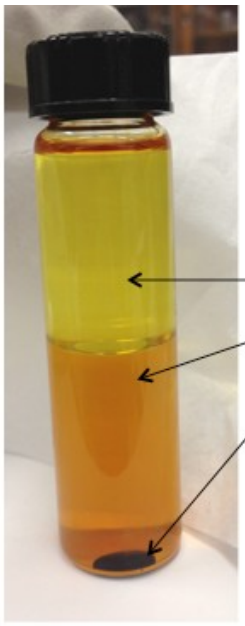

Volume ratio of SF34 : decalin = 1:5
Volume ratio of SF34 : water = 1:5

Weight Distribution
Oil-soluble : 0.5%
Water-soluble : 73%
Heavy compounds : 26.5%

Amount of carbon in water−soluble/
Amount of carbon in the whole SF3&4
=74%

The distribution in the organic phase is minimal compared with two other portions

Figure 35. Separation of the middle fraction into oil-soluble, water-soluble and heavy compounds sub-fractions

Reaction of Sub-Fractions

First, the water-soluble portion is upgraded using ***single phase reaction*** and biphasic reaction. In single phase reaction, two catalysts Pt-Sn/Al_2O_3 and Pd-Cu/C were performed. As shown in Figure 36, polymerization still occurs, but is much less severe than reactions with direct feed of the entire middle fraction. From the product distribution (Figure 37), it shows that furfural was completely removed, the amount of methoxy phenols reduces and the amount of cyclic ketones increases.

Table 12. Experimental procedure for single phase reaction of the water-soluble sub-fraction

Catalyst	**Pt-Sn/Al_2O_3** *(1% Pt, Pt:Sn=1:1) (Lei)*	**Pd-Cu/C** *(5% Pd, Pd:Cu=1:1)*
Solvent	Water	Water
Catalyst reduction conditions	• 100 mg cat. in 7 ml water • 300 rpm, 800 psi, 300^{0}C, 3hrs	• 100 mg cat. in 7 ml water • 300 rpm, 800 psi, 300^{0}C, 3hrs
Reaction conditions	• Feed: 7ml of water-soluble portion of SF3&4 • 300 ^{0}C, 800 psi, 350 rpm, 12 hrs	• Feed: 7ml of water-soluble portion of SF3&4 • 300 ^{0}C, 800 psi, 350 rpm, 12 hrs

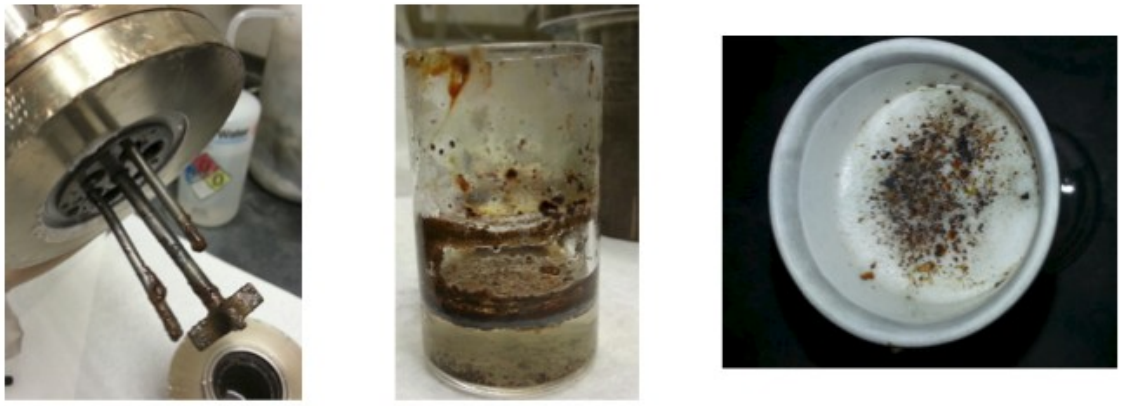

Figure 36. Polymerization after reaction with Pt-Sn/Al_2O_3

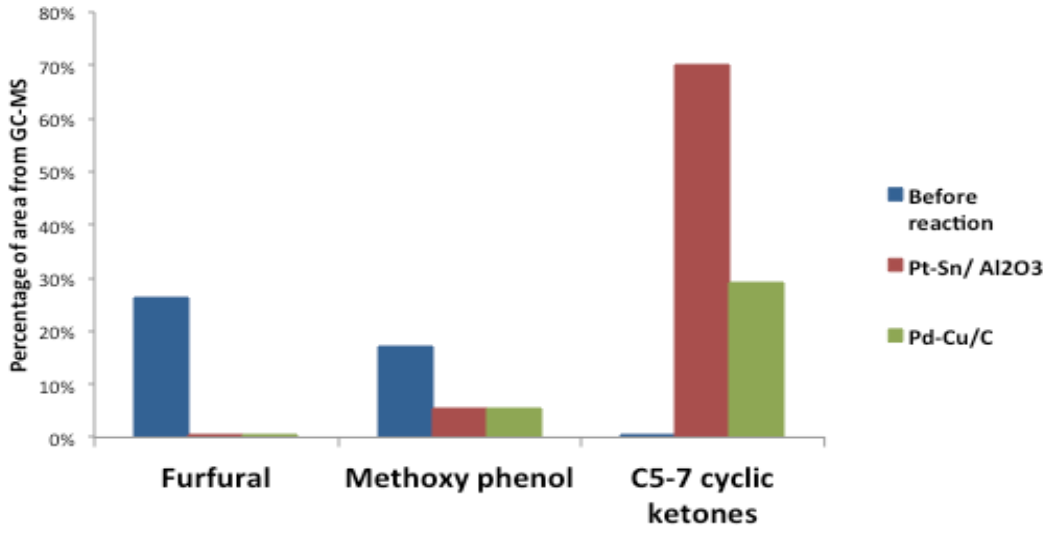

Figure 37. Product distribution before and after reaction of water-soluble sub-fraction with Pt-Sn/Al_2O_3 Pd-Cu/C

Table 13 shows the procedure for ***biphasic reaction*** of water-soluble portion using Pt-Sn/MWNTs.

Table 13. Experimental procedure for single phase reaction of the water-soluble sub-fraction

Catalyst	**Pt-Sn/MWNTs** *(1% Pt, Pt:Sn=1:1)*
Solvents	Water and undecane
Creating Emulsion	• Put catalyst in 4ml water, horn sonicate 15 mins • Put 8ml of undecane, horn sonicate for 15 more mins • Put 4ml of the water-soluble portion, batch sonicate 30 mins • Check the formation of emulsion using optical microscope
Reaction conditions	• 300 ^{0}C, 1000 psi, 350 rpm, 15 hrs

The results for the biphasic (emulsion) runs are summarized in Figure 38. The first graph shows the distribution of the products, in which the percentage of hydrocarbons, alcohols, ketones and lactones are 59%, 14%, 16% and 1%, respectively. The rest 9% is phenolic and nitrogen contained compounds. It shows that the major product after the reaction is hydrocarbon. The second graph shows the distribution of hydrocarbons in the total products. We can see that C6 hydrocarbons is the most abundant, then C5 and C7. The percentage of C4 and C8 are smaller. This is a very promising result that demonstrates the great potential of the biphasic approach.

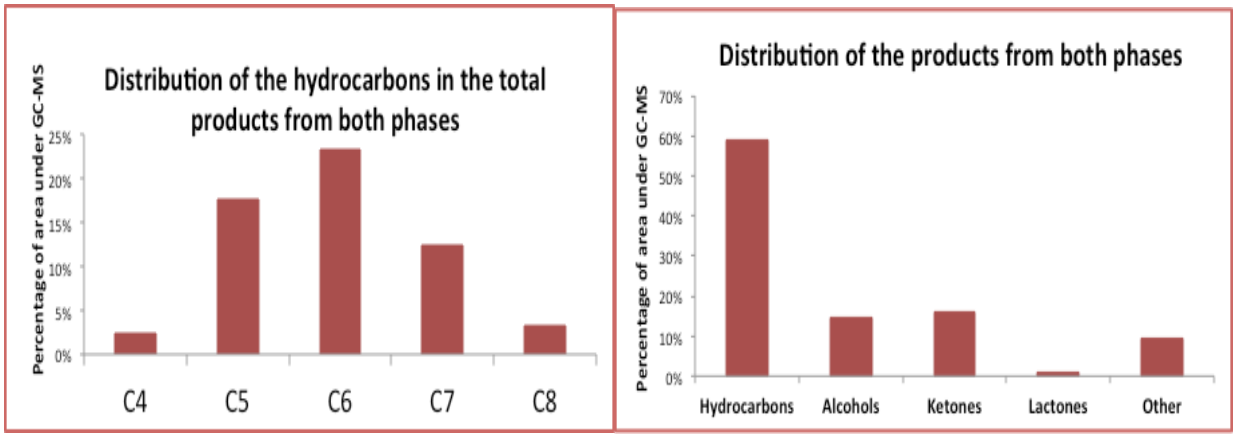

Figure 38. Product distribution from biphasic reactions

As reported earlier, when we dissolve middle fraction in water and decalin with the volumetric ratio 5:5:1 of water:decalin:SF3/4, we receive three different portions: water-soluble, oil-soluble and heavy fraction. However, the process of extracting out the heavy fraction of the middle fraction is usually problematic. The total volume of the other two phases, water and oil solubles, is more than 20 times than the volume of the heavy fraction. Furthermore, the distribution of the middle fraction in the oil fraction is negligible compared to the water soluble and heavy resin. Therefore, the extraction of the heavy fraction was carried out using water only, with the volumetric ratio of 5:1 water: middle fraction. The two catalysts that were tested are Pd-Cu/C and Pt/TiO_2. After reaction, in order to extract any oil-soluble products that are not dissolved in water-GVL mixture, 1 ml of decalin is added to the solution.

Table 14. Experimental procedure for upgrading the heavy sub-fraction using GVL

Solvents	**GVL and water**
Procedure	• 250mg catalyst • 3:1:1=GVL:H2O:Residue
Reaction condition	• Initial pressure of H_2 = 1000 psi, 200^0C • Stirring rate = 500 rpm • Time = 7 hrs

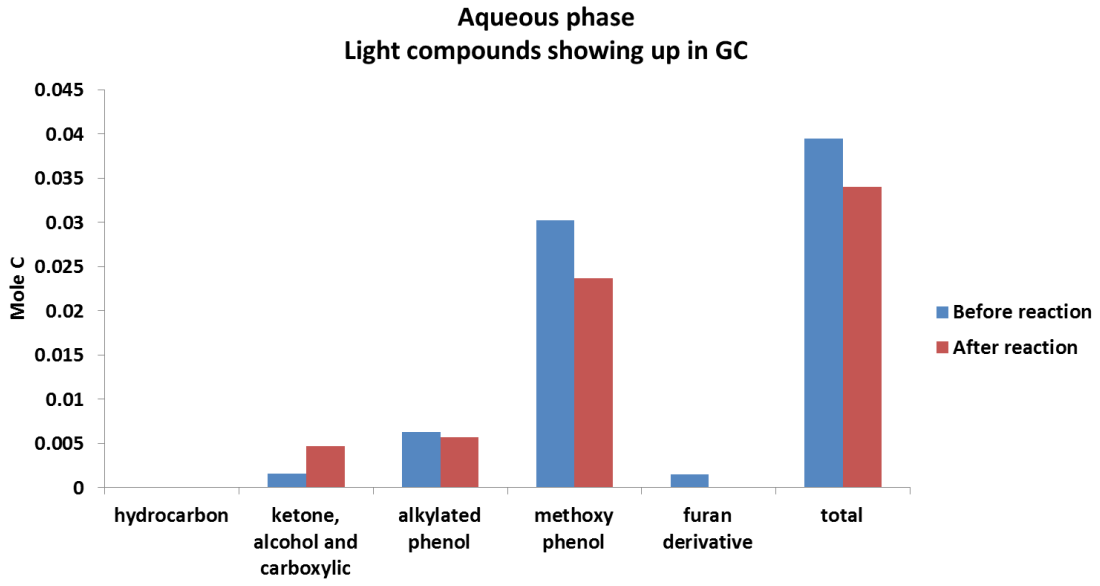

Figure 39. Product distribution from water-soluble sub-fraction before and after reaction with Pd-Cu/C

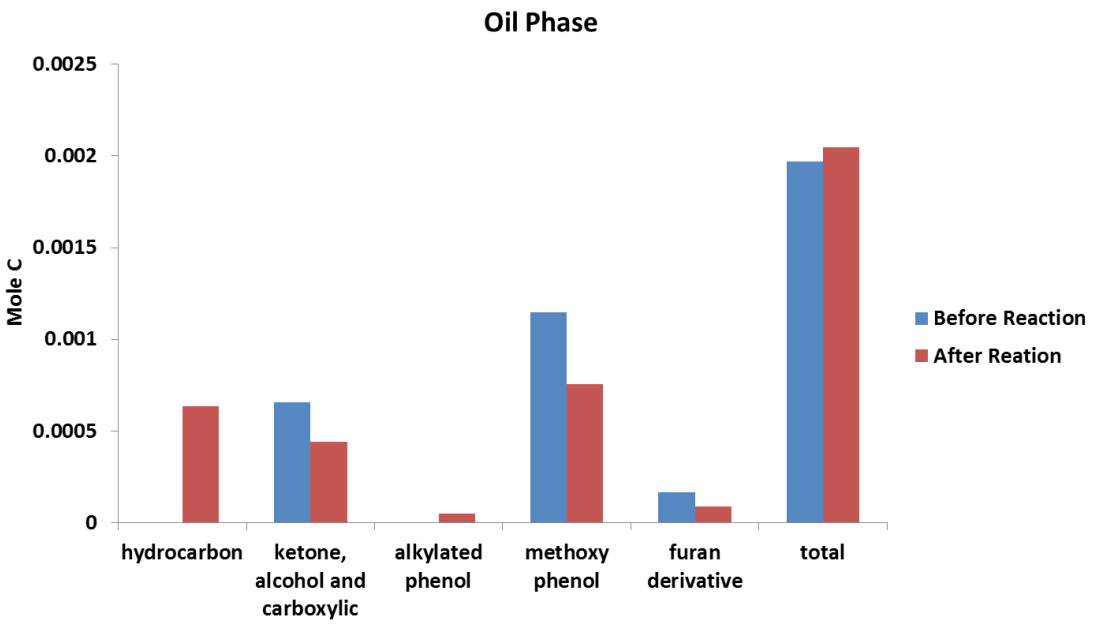

Figure 40. Product distribution from oil-soluble sub-fraction before and after reaction with Pd-Cu/C

The heavy resin composes of big molecules or polymerization products that cannot be detected by GC. As the product analysis shows us, the amount of light products reduces while the amount of heavy products increases. It means we have more polymerization products. The deoxygenated hydrocarbon in the oil phase after reaction is believed to come from the oil-soluble components that were left in the heavy resin when we used only water to extract the heavy resin out of the middle fraction.

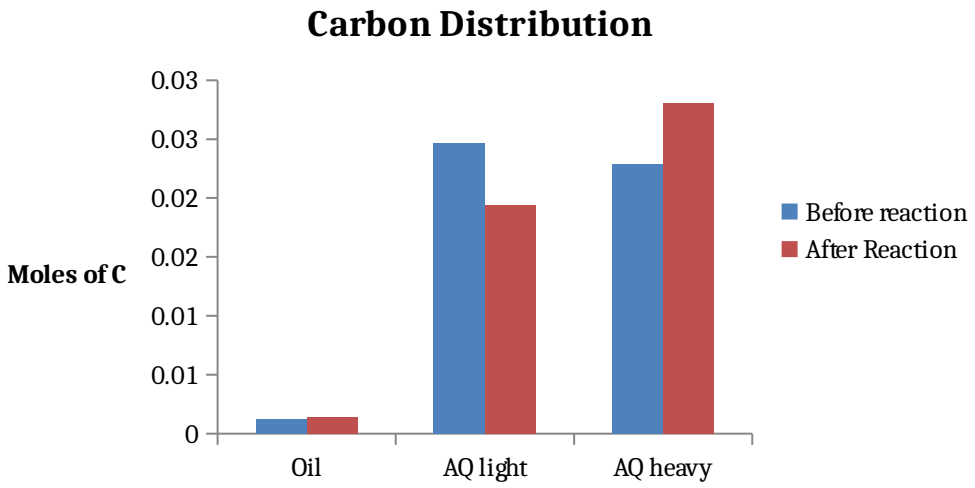

Figure 41. Carbon distribution of sub-fractions before and after reaction with Pt/TiO_2

We obtained the same result with Pt/TiO_2. The amount of heavy products increases while the amount of light products decreases.

Therefore, the upgrading of the heavy fraction is very difficult even with the use of GVL as the solvent. The heavy fraction may deactivate the catalyst or the heavy fraction is too heavy for HDO reaction to be effective. Even with a high ratio of GVL such as 8:1:1 of GVL:water:resin, we cannot obtain any promising result with the heavy fraction. Therefore, no further test with lower amount of GVL was executed.

From the NMR analysis we have found that the functional group of aqueous phase before reaction is in consistent with GC-MS and GC-FID. And after the reaction the peak of the solvent had dominated the spectrum which could cause many errors in identifying the functional group. We would like to conclude that NMR analysis is unnecessary and we can explicitly quantify the feed and the products from GC-MS and GC-FID.

Summary

We have recently demonstrate promise associated with the use of GVL to maintain the middle fraction as a single mixture. To highlight these results, an image of the mixture obtained after dissolving in oil/water is shown in Figure 42 on the left, with the same mixture diluted in GVL shown on the right.

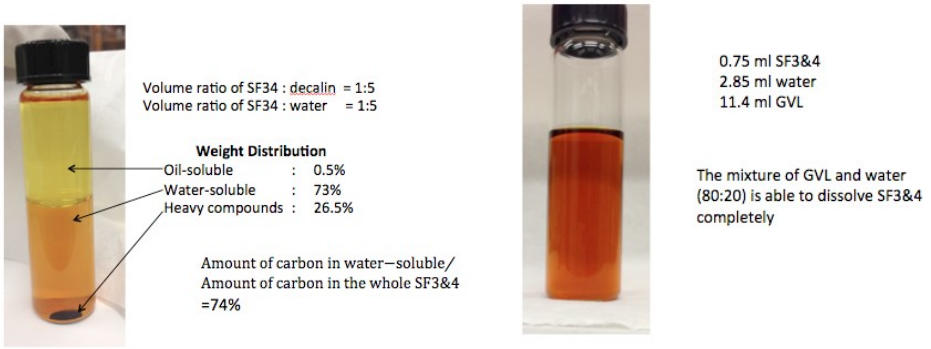

Figure 42. Middle fraction dissolved in decalin/water (left), middle fraction diluted in GVL (right)

By using a PdCu catalyst at 180˚C, we reported promising results as shown in Figure 43.

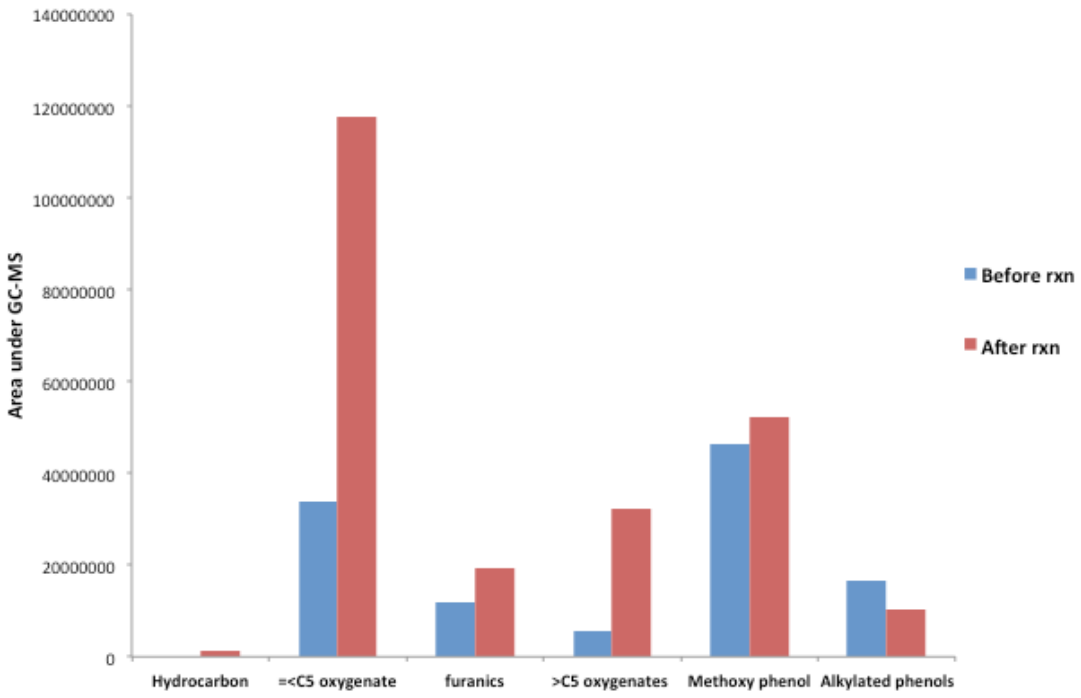

Figure 43. Product distribution before and after reaction of middle fraction using PdCu catalyst at 180 ˚C

Under these reactions, we observed that the GVL conditions did not change throughout the course of the reaction. We wanted to both confirm that hypothesis as well as test the limit by which we could increase the severity while still not converting the more stable GVL. In order to accomplish this, we conducted the experiments shown in Table 15.

Table 15. Experimental plan for reactions of middle fraction using GVL

		$RhReOx/SiO_2$	Rh/SiO_2	PdCu/C	PtSn/MWNT
Catalyst (mg)		100	100	100	100
Reduction	Temp (C)	120	120	290	290
	Pressure H_2 (psi)	200	200	350	500
	Time (hours)	1	1	3	3
Feed		16 wt %	16 wt %	16 wt %	16 wt %
Reaction	Temp (C)	250	180	180	180
	Pressure H_2 (psi)	800	750	750	750
	Time (hours)	4	4	4	4
Conversion		Yes	No	No	No

These results confirm that under a temperature of 180˚C, we do not observe any measurable GVL conversion, although we do observe conversion of the products present in pyrolysis oils. We subsequently increased the severity of this reaction by going to more severe conditions, and testing a broader scope of catalysts.

Table 16. Catalysts and conditions for reactions of middle fraction using GVL under more severe conditions

		PdCu/C	Ru/TiO2	PdOTS/HY	Ru/C
Catalyst (mg)		100	100	100	100
Reduction	Temp (C)	280	250	250	250
	Pressure H_2 (psi)	350	400	400	400
	Time (hours)	3	3	3	3
Feed		16 wt%	16 wt%	15 wt %	16 wt %
Reaction	Temp (C)	250	250	250	250
	Pressure H_2 (psi)	1200	1200	900	1100
	Time (hours)	12	12	12	6 and12

Table 17. Product distribution of reactions of middle fraction with GVL under more severe conditions

Catalyst	2-methyl THF	2-butanol	1,4-Pentanediol	Pentanoic Acid	GVL
PdCu/C	15.3	14.6	0.00	0.00	70.1
Ru/TiO2	1.17	1.38	0.00	3.81	93.6
PdOTS/HY	2.30	0.00	0.00	0.00	97.7
Ru/C	8.39	9.49	3.81	0.00	78.3

It is interesting to note that conversion is rather low for some catalysts (for example the PdOTS/HY) even under the more sever conditions reported here. This implies that while 180˚C does show promise for the conversion of this middle fraction, there is some margin for increasing temperature further to increase reaction rates and minimize the required reactor volume while still using GVL as a solvent.

Task 5: Stabilization of clean phenolic oligomer fraction (PNNL)

The objective of this research was to evaluate the potential production of petroleum refinery feedstocks derived from biomass via fast pyrolysis and product fractionation. In this case fractionation of the bio-oil, and washing of certain fractions resulted in a clean phenolic oligomer product which served as the feedstock for hydroprocessing to produce a more hydrocarbon-like refinery feedstock. To date, the vast majority of research in hydrotreating bio-oil to produce liquid transportation fuels is centered upon stabilizing bio-oils through chemical means, including condensed phase low-temperature hydroprocessing, or vapor phase treatment, such as catalytic pyrolysis . This study was formulated to assess the impact of the bio-oil fractionation and to determine if existing barriers, particularly hydrotreating catalyst lifetime, can be mitigated through the use of fractionation to form a more stable hydroprocessing feedstock.

A woody and herbaceous biomass were selected as the feedstocks for this study. Bio-oils were produced in a fluidized-bed reactor at Iowa State University and the impact of fractionation on oil properties assessed. Pacific Northwest National Laboratory (PNNL) hydrotreated the Clean Phenolic Oligomer (CPO) oil fractions produced at ISU, in a bench-scale, continuous-flow, packed-bed catalytic reactor to validate CPO separation and its impact on subsequent hydroprocessing to hydrocarbon fuels. This collaboration between ISU and PNNL leverages existing expertise to assess the impact of bio-oil fractionation at ISU on the hydrotreating process to produce liquid transportation fuels at PNNL.

The CPO samples produced at ISU were shipped to PNNL. The CPO samples included one from each feedstock, oak wood and a corn stover. The bio-oils were hydroprocessed in the mini-hydrotreater (see **Figure 44**). In fact, the precious metal (non-sulfided) tests were performed in a different, but similar, reactor system than were the sulfided CoMo tests. The hydrotreater was configured as a single pass, co-current, continuous, down-flow reactor. The system can operate at up to 12.4 MPa (1800 psig) with a maximum catalyst temperature 400 ^{o}C. The system consists of a gas and liquid feed system, heated reactor system, and a gas-liquid separation system. The gas feed system consists of a manifold for feeding hydrogen through one mass flow controller and helium through a second mass flow controller. The liquid bio-oil feedstocks are delivered to the pressurized reactor system by two high pressure ISCO syringe pumps. The tubular fixed-bed catalytic hydrotreater was made of 316 stainless steel, 13 mm (1/2”) internal diameter by 64 cm long with 40 ml capacity for single stage heater or 24 + 24

ml capacity for two-stage hydrotreating. The reactor was heated by either a single heating zone heater for single stage hydrotreating or a two heating zone heater for two stage hydrotreating. The liquid feedstock and hydrogen gas entered the top of the catalyst bed and passed downward through the bed, assumed to be in a trickle flow. The temperature of the catalyst beds was monitored by thermocouples in a thermocouple well (5 mm (3/16") tubing). After exiting the catalytic reactor, the liquid products were separated from the gaseous products in one of two pressurized and cooled traps placed in parallel flow downstream of the reactor system. Periodic liquid samples were collected when switching collection vessels and venting/draining the trap. The recovered liquid products were phase-separated, weighed, and sampled for further analysis. The off-gas passed through the back-pressure regulator and was then directed through a DryCal gas meter to measure gas flowrate. Periodic gas samples were analyzed by an online Inficon Micro-GC 3000 4-Channels micro gas chromatograph with molecular sieve, Plot U, Alumina, and Stabilwax columns. Prior to each hydrotreating test, the micro GC was calibrated by using a calibration gas.

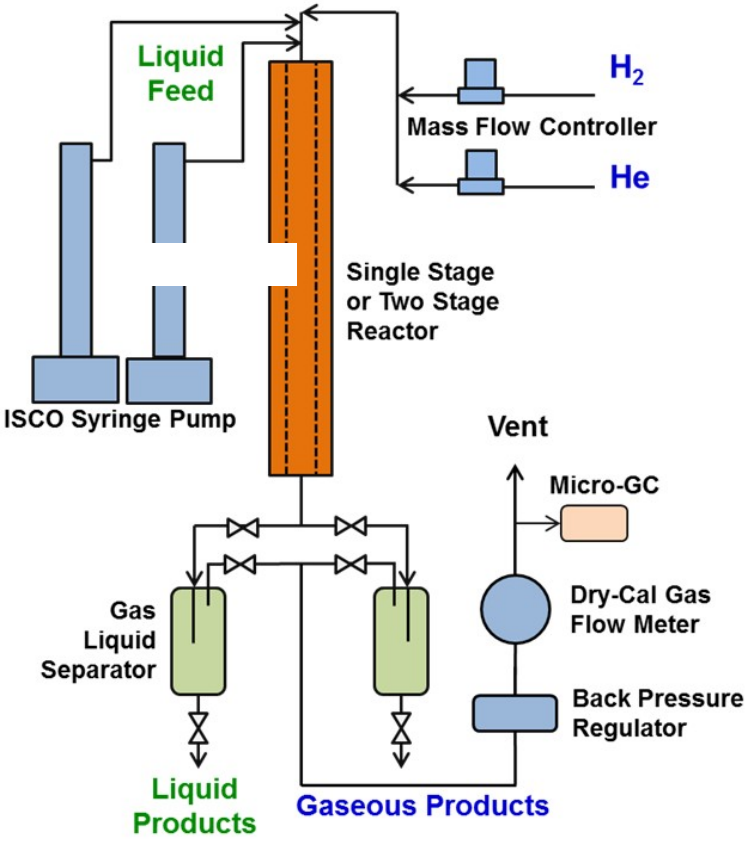

Figure 44. Schematic of the mini-reactor hydrotreater system

Campaigns were performed for each feed over the course of a five-day test, and the products and feed were collected to assess performance for each CPO feed type with the two catalyst systems to compare to the results with unfractionated bio-oil.

The hydroprocessing tests showed good results using a two-stage catalytic hydroprocessing strategy. Equal-sized catalyst beds, a Ru/ C catalyst bed operated at 140 °C and a Pd/C catalyst bed operated at 370 °C, were used with the entire reactor at 12.5 MPa operating pressure. The space velocity in these tests was low. The hydrogen flow was in great excess, as is typical for hydrotreating.

For the CoMo tests, the catalyst bed was sulfided in-situ. The reactor tube containing the catalyst was heated to 150 °C in H_2 flow, heated from 150 °C to 350 °C over 3 h in flow of H_2 and sulfiding agent (35% di-tertiarybutyl-disulfide (DTBDS) in decane). Then heated to 400 °C and held for 5 h with H_2 and sulfiding agent flowing.

For the hydroprocessing tests the flow ratio of H_2/liquid was 1.89 L H_2 (L bio-oil)$^{-1}$. The operating pressure was 12.5 MPa (1780 psi). When using the sulfided catalyst, DTBDS was added to the CPO at an amount equal to 150 ppm S. **Figure 45** shows a schematic of the catalyst beds with a super-imposed temperature profile for the single stage and the two-stage testing modes. The temperatures were measured at the center line of the catalyst bed by a thermocouple which was adjustable within a full length thermowell. The isothermal portions of the catalyst bed are clearly shown and the lengths of the isothermal portions of the catalyst were used to calculate the space velocity.

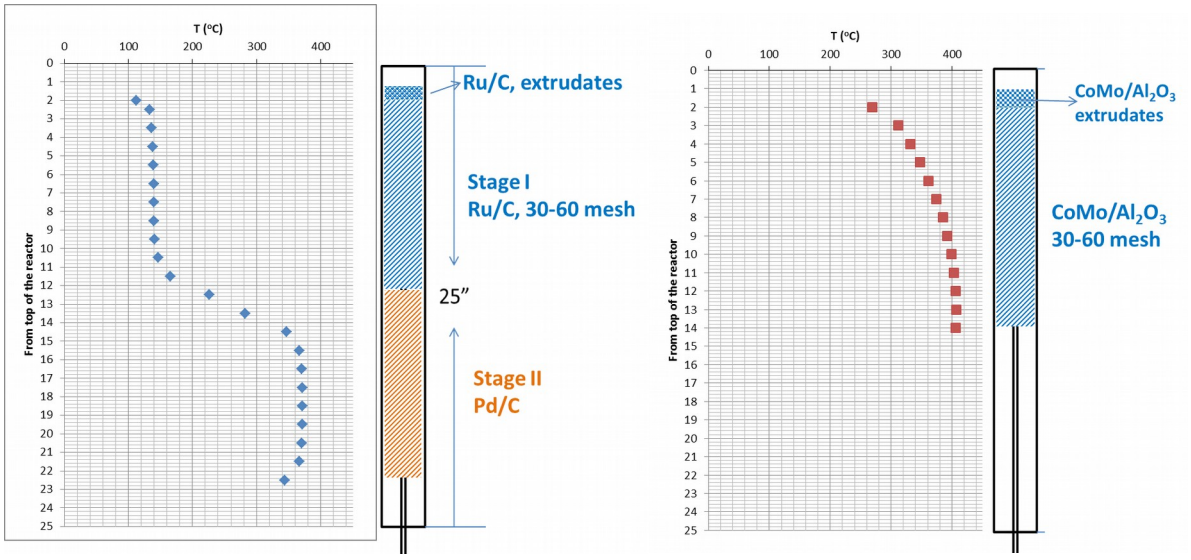

Figure 45. Schematic of the catalyst beds in the mini-hydrotreater reactor

The CPOs and hydrotreated products were characterized at PNNL for elemental analysis including C, H, N, O, S, Total Acid Number (TAN), water content, metals content, and solids. In addition, the products were analyzed by simulated distillation (ASTM D2887) in order to assess the relative amounts of fuel products in the gasoline, diesel, jet fuel, and residual ranges.

Process evaluation was based on mass and elemental balance during the operations of the continuous-flow reactor. In particular, carbon balance was an important indicator of energy

efficiency in the process while high mass balance was an important indicator of the validity of the product recovery. Product samples and process data from various time windows were collected and calculations determined for representative steady-state operation. Elemental analysis (C, H, N, S, O) of the feedstocks and products were measured. The liquid products included both a hydrocarbon phase and an aqueous phase which were separated by gravity after draining from the reactor system. Calculations of the elemental composition of the gases were determined based on gas chromatographic analysis of measured volumes of gas. By these measurements the liquid product yields were determined as well as hydrogen gas consumption. The properties of the hydrocarbon products can be judged against fuel standards. The gas product analysis can be used to determine its value for recycle to the hydroprocessing and/or reforming to more hydrogen gas. The aqueous composition can be used to determine the wastewater treatment requirements.

The used catalyst beds were also analyzed to determine the potential for long-term operation with the specific catalyst and feedstock pair. The recovered catalyst beds were evaluated for catalyst fouling and considered in light of any pressure-drop which might have developed during the test. Time-on-stream until pressure-drop build-up or plugging is an important parameter to determine ling-term operability. The elemental analysis was used to judge both the dilution of the metal components by carbon deposition but also to determine any poisoning of the catalyst by trace components in the CPO.

The initial samples of Clean Phenolic Oligomer (CPO) fraction were received at PNNL from ISU in March and April 2013. A subsequent shipment of a larger product quantity was received in June. These products were sampled and stored for the hydrotreatment tests. Analyses of the samples included density, viscosity, accelerated aging, trace elements by ICP and GCMS analysis for component identification.

The CPO feedstocks were analyzed at PNNL with the results shown in **18**. The wet CPOs were the samples actually analyzed and the reported C, H, O compositions are calculated to a dry basis by subtracting out the amount of oxygen and hydrogen in the measured moisture content. Detailed trace element analysis of the wet bio-oils was performed by ICP as shown in**Error: Reference source not found19**. At PNNL, the CPOs were also measured for percent filterable solids, using ASTM D7579. The TAN (total acid number) was also determined by PNNL. Viscosity and density were determined with the Stabinger apparatus using ASTM D7042.

Table 18. Analysis of CPO feedstocks used for hydroprocessing tests

	C	H	H/C ratio	O	Moisture	N	S	Density	TAN	Viscosity	Solids
Sample name	Wt % dry	Wt% dry	dry basis	Wt% dry	Wt%	Wt% wet	Wt% wet	g/ml @40°C	mg KOH/g	mm^2/s @40°C	Wt% wet
Red oak	67.2	6.08	1.08	26.5	14.5	0.17	0.02	1.20	61	4100	1.37
Corn stover	na	na		na	13.0	na	na	1.18	na	21000	2.75

na = not analyzed, corn stover raw CPO was not analyzed completely by PNNL

Table 19. Trace analysis of CPO feedstocks used for hydroprocessing tests

	Al	Si	K	S	Ca	Mg	P
Red oak	251	205	112	40	<30	<30	<30
Corn stover	271	597	312	334	168	116	82

na = not analyzed, corn stover raw CPO was not analyzed completely by PNNL

Semi-quantitative analysis of the two CPO feedstocks was performed with gas chromatography-mass spectrometry (GC-MS). Using a DB-5 column over a temperature program separation of the CPOs was performed and mass spectrometric analysis undertaken with a Mass Selective Detector. Using the Agilent peak matching program, tentative identifications were applied to the components and their relative quantities determined based on total ion current. The results are shown in **Table 20.** The CPO is aptly named as the vast majority of the volatile components are phenolic in nature. For the most part they are syringol (2,6-methoxy phenol) or guaiacol (2-methoxyphenol) analogs with substituents on the 4 position. There is a significant amount of levoglucosan in both CPOs. Comparison of the relative amounts of components shows that most are common in both CPO, at similar concentrations. However, the corn stover CPO has a large dihydrobenzofuran fraction, as well as ethyl phenol, which were not found in the red oak CPO. On the other hand, the red oak contained a much larger fraction of methyl syringol while the corn stover had a larger fraction of vinyl guaiacol.

Table 20. Components in CPOs based on GC-MS analysis

		Red Oak CPO	Corn Stover CPO
Component	Retention time	Quantity	Quantity
levoglucosan	19.55-76	5.69	1.44
2,3-dihydrobenzofurans	**16.41-48**	**ND**	**4.17**
ethyl phenol	**15.70**	**ND**	**2.76**
syringol	17.96	5.25	2.21
propenyl syringol	21.51	5.21	1.45
methyl syringol	**19.00**	**3.20**	**0.40**
propenyl guaiacol	19.03	2.88	1.27
unknown	20.22	2.62	0.97
syringol formaldehyde	21.19	2.44	ND
2-propenyl syringol	21.05	2.00	0.40
propenyl syringol	20.57	1.96	0.39
syringol ethanone	21.85	1.45	0.32
guaiacol propenal	21.88	1.31	present
vinyl guaiacol	**17.52**	**1.26**	**2.36**
ethyl guaiacol	17.08	1.10	0.66
methoxy catechol	16.94	1.10	ND
syringol propionaldehyde	23.98	1.08	ND
syringol propenal	23.98	1.08	present
corylone (hydroxymethylcyclopentenone)	13.48	0.78	0.66
propenyl guaiacol	18.57	0.67	ND
guaiacol ethanone	19.47	0.65	ND
hexadecanoic acid	23.22	0.64	present
guaiacol formaldehyde (vanillin)	18.55	0.55	bad integration
catechol	16.30	0.51	present
methyl guaiacol	16.00	0.45	present
guaiacol ethanol (homovanillyl alcohol)	19.17	0.43	ND
hydroxy-propenyl guaiacol	21.29	0.42	ND
guaiacol	14.52	0.42	present
2 and 4 methyl phenol (m,p-cresols)	14.42	0.40	present
hydroxy-propenyl guaiacol	20.34	0.24	ND
methyl syringol bis-dimer	29.08	0.18	present

ND = not detected

The CPO products were also analyzed by ^{13}C Nuclear Magnetic Resonance (NMR) spectrometry. In **Table 21** the functional groups determined by NMR for an oak fast pyrolysis bio-oil from our laboratory can be compared with the red oak CPO and the corn stover CPO. Both CPOs contain less non-phenolic type components than the whole bio-oil. The corn stover CPO contains more carbonyl/carboxyl types as well as more carbons, which are not directly bonded with any oxygen. The ratio of aliphatic to aromatic carbons underscores the conclusion that the phenolics are concentrated in the CPO.

Table 21. ^{13}C NMR analysis of bio-oil and CPOs

carbon type	Bio-oil - Oak	CPO - Oak	CPO - Corn Stover
Alkyl (0-52 ppm)	11.32	2.61	22.38
Carbonyl (192-222 ppm)	5.78	0.77	3.66
Carboxyl (170-192 ppm)	6.78	1.56	2.65
Ether, alcohols, sugars (53-96 ppm)	25.91	19.46	4.29
Phenolic (140-170)	12.85	22.51	22.6
Aromatic (96-140 ppm)	37.37	53.09	44.42
Ratio aliphatic/aromatic C	0.74	0.29	0.40

The mini-scale hydrotreaters were built for bio-oil upgrading by catalytic hydroprocessing. Tests with the red oak CPO were completed with either sulfided or non-sulfided catalysts as shown in **Table 22.** For all of the reported tests the products and data were collected over the entire period with individual products and data sets collected in operating windows from 2 to 6 h long. The hydrogen consumption has been calculated and the yield of gas and oil products determined.

In the first experiment using a single temperature stage with a Pd-Re/C catalyst, the test was short-lived and was terminated after only 6 h due to an increase in pressure drop across the reactor. This effect is typical for unfractionated bio-oil and indicates an excessive amount of catalyst fouling leading to blockage of the reactor flow. In this test the examination of the bed following the test indicated that the blockage may have been due to fine particulate buildup in the fixed catalyst bed rather than fouling by cross linking reactions of the highly reactive components in the feedstock. Subsequent tests with precious metal catalyst utilized the two-stage hydroprocessing concept which has been found to alleviate the catalyst fouling difficulty.

Table 22. Summary of hydrotreater tests with red oak CPO

temperature	pressure	LHSV	catalyst	TOS	comment
350 °C	1520 psig	0.5	5%Pd-5%Re	6 h	plug
140 °C / 370 °C	1750 psig	0.2/0.2	7.8%Ru/2.5%Pd	24 h	feed line plugged
140 °C / 370 °C	1750 psig	0.1/0.1	7.8%Ru/2.5%Pd	48 h	catalyst bed clear
400 °C	1510 psig	0.5	3%Co-9%Mo sulfided	5 h	catalyst bed fouled
400 °C	1800 psig	0.2	3%Co-9%Mo sulfided	18 h	catalyst bed fouled

Using two sequential beds of different precious metal catalysts at different temperatures, the pressure drop build-up in the reactor was avoided. The first bed was filled with the more active ruthenium metal on carbon extrudate operated at a lower temperature to avoid methane formation (which would be expected at temperatures of 300 °C or above) but still hydrogenate the more active components in the CPO and thereby stabilize the feedstock for higher temperature hydroprocessing. The second bed was filled with a palladium on granular carbon catalyst, which has been found to be useful for bio-oil hydroprocessing. The first test at higher

space velocity was ended early when a plug occurred in the feed line, apparently due to particulate in the feedstock being caught in the small diameter (1/8”) tubing. The second test at lower space velocity was kept on line for 48 h and terminated as planned when using the minihydrotreater with the larger diameter (1/4”) feed line.

In the case of the use of a sulfided catalyst the typical catalyst bed fouling seen with fast pyrolysis bio-oil was not found after the test was terminated early, based on pressure drop build-up during the test. Instead, fine particulate was found packed in the catalyst bed at two intervals in the heat-up zone of the bed. Use of the lower space velocity in the second test allowed a longer operating window, even somewhat in excess of the allowance for lower feedstock processing rate, but the bed still became blocked. This result suggests that a filtering preliminary step will be required for processing the CPO. The typical catalyst bed following an experimental runs with CPO had evidence of carbonaceous particulate packed “tight” into the catalyst bed, as shown in **Figure 46.** The balance of the catalyst beds were free flowing and easily removed from the reactor tube for analysis.

Mass balances for red oak runs ranged from 87 to 97% for the steady-state windows calculated, with carbon balances somewhat lower, ranging from 80 to 92%. Since the liquid and gaseous products were all measured, the carbon loss can be attributed to experimental error and to deposits on the catalyst particles. The process results for hydrotreating with the two catalyst schemes are shown in **Tables 23 and 24.**

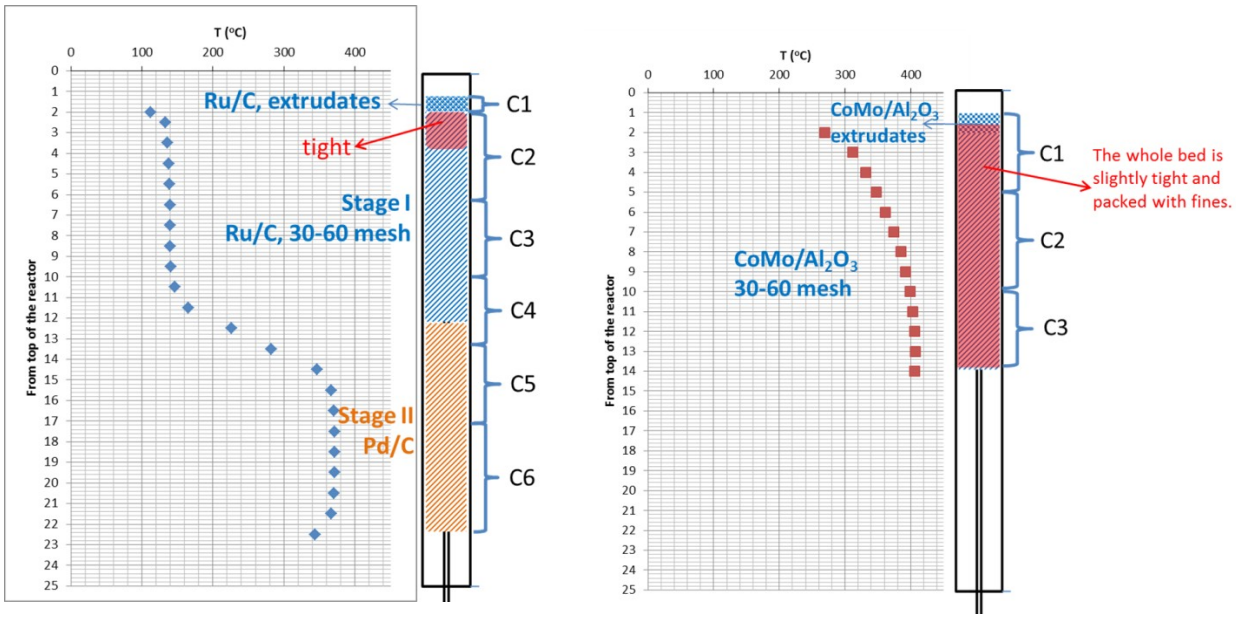

Figure 46. Schematic of the catalyst beds after use with red oak CPO

Table 23. Red oak processing results over time on stream with Ru-Pd catalysts

TOS and	Oil Yield	Carbon	Oil	Gas	Produce	H2	Mass	Carbon

duration		Yield of oil	density	yield	d water yield	consume d	Balance	Balance
	g dry/g dry feed	g C/g C in feed	g/ml	g per g dry feed	g per g dry feed	g H2/g dry feed	%	%
12-18 h[a]	0.585	0.719	0.87	0.074	0.164	0.042	86.9	80.5
24-30 h[b]	0.599	0.748	0.85	0.104	0.217	0.037	94.6	84.8
36-42 h[b]	0.657	0.812	0.88	0.083	0.189	0.039	95.2	90.4

[a] high LHSV 0.2 in each bed (0.1 total)
[b] low LHSV 0.1 in each bed (0.05 total)

Table 24. Red oak processing results over time on stream with CoMoS catalyst

TOS and duration	Oil Yield	Carbon Yield of oil	Oil density	Gas yield	Produce d water yield	H2 consume d	Mass Balance	Carbon Balance
	g dry/g dry feed	g C/g C in feed	g/ml	g per g dry feed	g per g dry feed	g H2/g dry feed	%	%
4-5h a	0.617	0.805	0.835	0.099	0.247	0.046	93.7	90.1
12-18h b	0.614	0.792	0.835	0.113	0.307	0.074	96.8	92.1

a high LHSV 0.5
b low LHSV 0.2

The products from the red oak CPO tests are shown in **Table 25.** These catalytic hydroprocessing experiments resulted in mostly deoxygenated products but required long processing residence times resulting in low processing space velocities. The precious metal catalysts, which were operated at lower space velocity but also lower temperature, resulted in more saturated product oil (higher hydrogen to carbon ratio), but the sulfided CoMo catalyst was more effective in hydrodeoxygenation. The low overall recovery of elements, (C+H+O)<100, in the high LHSV test with the CoMoS catalyst along with the significant amount of dissolved water in the product, suggests that the oxygen content was actually higher than reported by the analysis. Hydrotreating of the nitrogen content was also effective, being reduced below the level of detection. The sulfur level is quite low in the CPO, but its removal to below the level of detection was also determined.

Table 25. Hydrotreater feed/product analyses for red oak CPO tests

	C	H	O	H/C	N	S	moisture	density
feed CPO	71.03	6.42	22.36	1.08	0.17	0.02	14.50	1.18
Pd/Re 2-4 h	83.57	12.60	1.70	1.79	<0.05	<0.005	0.20	0.819
Pd/Re 4-6 h	83.10	11.75	3.05	1.68	<0.05	<0.005	0.20	0.878
Ru/Pd hi LHSV 12-18 h	81.12	12.11	5.11	1.77	<0.05	<0.005	0.22	0.870
Ru/Pd lo LHSV 24-30 h	82.09	12.40	3.43	1.80	<0.05	<0.005	0.08	0.846
Ru/Pd lo LHSV 36-42 h	81.38	11.73	4.84	1.71	0.045	0.013	0.23	0.880
CoMoS hi LHSV 4-5 h	79.86	10.78	0.40	1.60	<0.05	<0.005	0.20	0.835
CoMoS lo LHSV 6-12 h	79.01	12.55	1.90	1.89	<0.05	<0.02	<0.01	0.792
CoMoS lo LHSV 12-18 h	82.26	12.00	1.85	1.73	<0.05	<0.02	<0.01	0.835

^{13}C NMR analysis of the products also shows dramatic changes in carbon types, as seen in **Table 26.** There are very few oxygenates left. The Ru/Pd two-stage catalyst bed was most active for saturating the hydrocarbon products. The shift in the entries in the two last columns shows the catalyst deactivation as the test progressed.

Table 26. ^{13}C NMR analysis of red oak CPO hydrotreatment products

carbon type	CoMoS hi	PdRe	Ru/Pd hi	Ru/Pd lo	Ru/Pd lo
Alkyl (0-52 ppm)	68.03	80.38	88.49	89.91	88.43
Carbonyl (192-222 ppm)	0	0.28	0.59	0	0.82
Carboxyl (170-192 ppm)	0.39	0	1.16	0.48	0.90
Ether, alcohols, sugars (53-96 ppm)	0	1.43	1.29	1.22	0.28
Phenolic (140-170)	3.45	2.61	0.98	1.09	2.57
Aromatic (96-140 ppm)	28.14	15.30	7.50	7.30	7.00
Ratio aliphatic/aromatic C	2.15	4.49	10.44	10.72	9.24

Two of the hydrotreated CPO products from red oak were also analyzed by gas chromatography simulated distillation (SimDist ASTM D2887). This method is standardized for analysis of diesel fuels, so its application to these products, which are more comparable to sweet crude, shows the important difference in the low temperature distillate range. As shown in **Figure 47,** there was a significant portion of the hydrotreated products which falls in the gasoline range. There was a small tail in each product which fell into the distillation range of heavy oil, but not much more than was found in the diesel standard fuel.

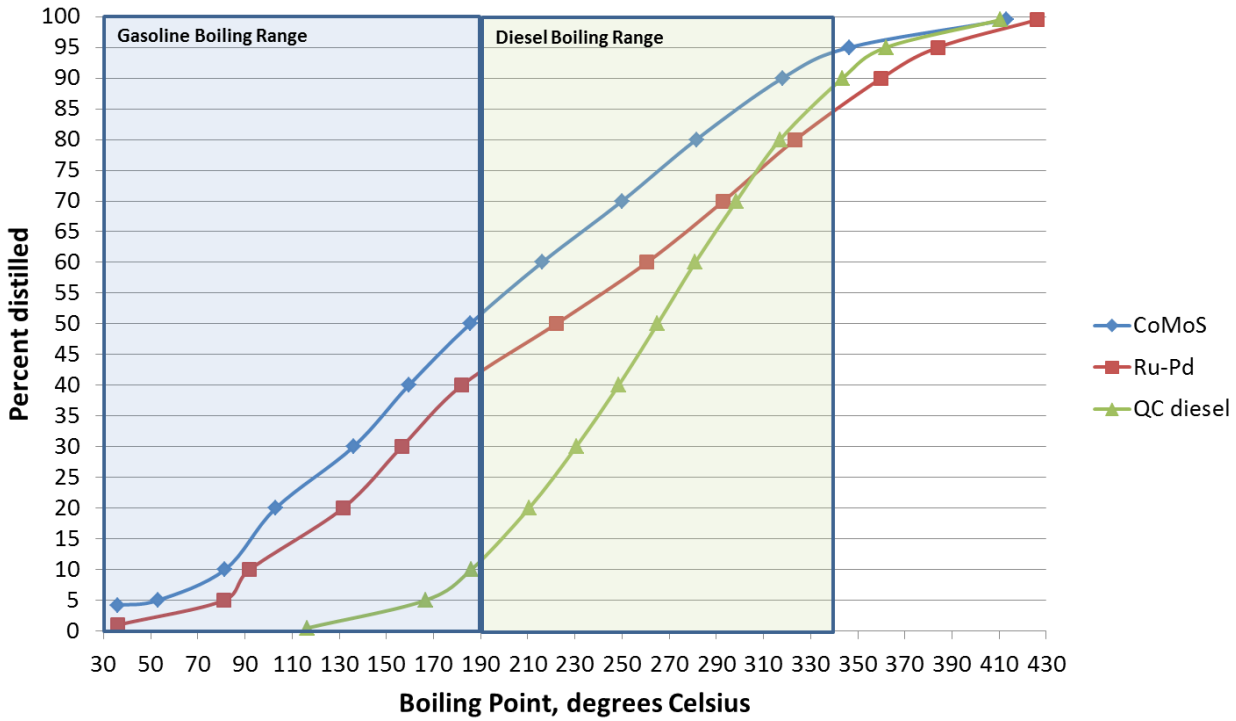

Figure 47. SimDist of hydrotreated CPO

The product gas composition showed some interesting variations throughout these tests. In **Table 27** there are gas products for each test, demonstrating the differences for catalyst and space velocity. The composition is presented on a hydrogen-free basis and shows only the product gases. For these tests there was a large excess of hydrogen, as is typical for hydrotreating, amounting to about 95 vol % of the process off-gas. The PdRe catalyst resulted in a much higher methane product while the CoMoS catalyst also produced more methane, as well as the other hydrocarbons. CO production is associated with the use of the Ru-Pd catalyst system. The product gas would likely be recycled through a membrane recovery system for hydrogen, followed by processing through a steam reformer to produce more hydrogen.

Table 27. Product gas composition in CPO hydroprocessing, volume percent (H_2-free basis)

TOS	CH_4	C_2H_6	C_3H_8	C_4H_{10}	C_5H_{12}	CO	CO_2
PdRe							
4-6 h[a]	71.3	5.5	5.6	0.7	0	0	16.9
Ru-Pd							
12-18 h hi[c]	23.0	4.4	5.4	0	0	19.7	47.6
24-30 h lo[d]	17.9	3.4	5.0	2.4	1.0	11.8	58.6
CoMoS							
4-6 h hi[a]	52.0	8.0	11.0	2.8	0.4	0	25.9
12-18 h lo[b]	53.6	12.6	23.4	3.8	2.2	0	4.4

[a] high LHSV 0.5
[b] low LHSV 0.2
[c] high LHSV 0.2/0.2
[d] low LHSV 0.1/0.1

The variation in the mineral content in the CPOs and the fate of the minerals in the hydroprocessing tests were determined. In the case of the red oak CPO, the mineral content is primarily Al and Si with lesser amount K and S (see Error: Reference source not found2). Analysis of the catalyst bed fractions after the tests (see **Table 28**) shows that mineral deposition is noticeable for either catalyst system. In the test with Ru-Pd two stage bed, the amount of K, as well as Ca, Fe, and Na, was actually lower in the front-end catalyst bed of Ru/C after use, suggesting that those elements are transported from the bed. In the second bed composed of the Pd/C catalyst, those four elements are also reduced from starting catalyst levels, suggesting that they were flushed from the second bed as well. Significant deposits of Si and Al from the CPO are found in the second portion of the Ru/C catalyst bed, which correlates with the portion of "tight" catalyst. Further in the reactor, they are reduced in the Pd/C catalyst bed from the levels measured in the fresh Pd/C, perhaps suggesting their higher solubility at higher temperature. There are no signs of the other metals from the reactor walls (Ni, Cr, Mo), apparently suggesting that corrosion of the reactor walls is not significant. The ruthenium analysis reports a lower level in the used catalysts. Carbon deposition in the pores of the catalyst has been determined to be the agent diluting the ruthenium concentration rather than actual leaching of the metal from the support. This effect was confirmed previously with the CoMo catalyst wherein the carbon deposition was quantified by direct elemental analysis. [Ell14] In the catalyst bed of sulfided CoMo on Al_2O_3 the Ca is only reduced (at levels similar to Co, Mo, Al) by the dilution of the catalyst with carbon particulate, while the K, Fe, and Na are actually deposited onto the catalyst in the front end of the bed. Similar deposition of Si is also evident. The other catalyst components Al, P, and W show evidence of leaching from the catalyst as their relative amounts are less than the diluted Co and Mo major catalyst components.

Table 28. Catalyst analyses for red oak CPO hydroprocessing

	Ru/C			Pd/C			$CoMo/Al_2O_3$			
	fresh	C2*	C3*	C5*	C6*	fresh	fresh	C1*	C2*	C3*
Al	695	1145	786	630	522	1040	386000	283900	314100	331450
Ca	417	262	157	192	367	484	987	740	842	931
Co	NA	NA	NA	NA	NA	NA	33430	26560	28940	30400
Fe	199	110	172	368	352	659	75	853	270	202
K	443	238	190	210	708	1197	73	592	96	88
Mg	281	150	149	187	355	463	588	438	470	500
Na	74	<35	<35	<35	727	1363	254	332	238	236
Ni	<35	<35	<35	<35	<35	<35	495	405	424	499
P	<35	<35	<35	45	39	82	11940	7728	8276	8764
Mo	<35	<35	<35	<35	<35	<35	68465	55030	60445	63065
Si	1026	2408	1070	1124	764	1361	1504	2179	2238	1764
S	3145	3060	2054	247	94	76	1036	34585	46470	47910
Ru	51970	40715	45560	83	<35	<40	<45	<45	<45	<45
Pd	<40	<35	<35	3380	3936	5100	<45	<45	<45	<45

NA = not analyzed

* numbering indicated in Figure 3

Sulfidation of the precious metal catalysts was noted. The highest sulfur loading of the Ru catalyst is consistent with a 12% sulfidation as RuS_2. A typical level, based on literature

reports is 40% Ru sulfidation in a hydrothermal environment.[Dre01] The sulfur loading of the Pd catalyst is much less by an order of magnitude. These results suggest that sulfidation of the Ru catalyst may be a significant long-term operational problem, while Pd may be more resistant in this operating environment. Also, sulfidation of the CoMo catalyst was verified wherein the sulfur content was equivalent to molar ratio equivalent to the CoMo loading ranged from 1.1 to 1.3 over the catalyst bed. The ratio of S to metals in the CoMo catalyst suggested that the metals were 70 to 83% of fully sulfided.

In the first test attempted with the corn stover CPO fraction there was plugging of the catalyst bed at a very early stage of the test. No liquid products were recovered from the test. Examination of the catalyst bed after the test suggested that the bed fouling might be a combination of polymerization and char particle capture in the fixed bed of catalyst. The analysis of the corn stover CPO by ISU showed that the red oak CPO had a lower level of methanol insoluble solids, 1 to 2 wt%, while the corn stover CPO had 4 to 6% of methanol insoluble solids. This particulate material is not expected to break down in the hydrotreating and would likely be trapped in the fixed bed of catalyst.

An attempt to clear the CPO of this particulate material was undertaken. A direct filtration (25 μm) attempt was wholly unsatisfactory. Moderate preheating of the CPO (65°C) to reduce viscosity still resulted in excessively long filtration times, which were further complicated by solidification of the material in the filter apparatus (~40°C). Subsequently, the corn stover CPO was diluted with solvent (10% iso-propanol) which greatly facilitated the filtration. However, removal of the solvent after the filtration was not easily accomplished, so the diluted CPO was tested as the feedstock for hydrotreating.

The mini-scale hydrotreater used was a trickle-bed reactor with nominally 50 mL reactor volume and in which nominally two 24 mL fixed-catalyst beds were tested. The second test with filtered, diluted Corn stover CPO used precious metal catalysts, Ru/C at 140°C and Pd/C at 370°C. The test was successfully terminated after the planned 48 h on line without measureable increase in pressure drop (no plugging). Process data is shown in **Table 29**. The calculated hydrogen consumption was found to be higher than for the Red Oak CPO feedstock as was the yield of gas product. A very large amount of propane gas was produced, presumably from the iso-propanol solvent, in stark contrast to the Red Oak tests. Mass balances ranged from 92 to 95%, similar to the red Oak while the carbon balance was slightly lower at 80 to 83%. Analysis of the liquid products (see **Table 30)** and product density measurement show that a high level of saturation of the CPO was accomplished with deoxygenation ranging from 80 to 90%.

Table 29. Dilute, Filtered Corn Stover CPO processing results with Ru-Pd catalysts

TOS and duration	Oil Yield	Carbon Yield of oil	Oil density	Gas yield	Produced water yield	H2 consumed	Mass Balance	Carbon Balance
	g dry/g dry feed	g C/g C in feed	g/ml	g per g dry feed	g per g dry feed	g H2/g dry feed	%	%
24-30 h	0.533	0.632	0.82	0.128	0.221	0.045	91.8	80.0
36-42 h	0.580	0.679	0.86	0.111	0.215	0.040	94.6	82.7

Table 30. Hydrotreater feed/product analyses, dry basis) for corn stover, diluted and filtered CPO

	C	H	O	H/C	N	S	moisture	density	TAN
feed CPO*	70.91	7.44	20.59	1.17	1.48	0.04	10.97	1.15	57
24-30 h	84.07	13.89	1.98	1.96	0.070	<0.04	0.00	0.825	0.6
36-42 h	83.03	13.07	3.38	1.87	0.530	<0.04	0.38	0.857	4.9

* corn stover CPO, diluted with 10 wt% isopropanol and filtered with a 25 micrometer sieve

The red oak CPO performed well for up to 48 h when using certain catalyst configurations but was still susceptible to catalyst bed fouling and pluggage in other cases. Use of the minihydrotreater with the larger diameter feed line (1/4" versus 1/8") facilitated operation by avoiding feed line blockage by particulate. However, the unfiltered corn stover CPO had sufficient filterable solids, which resulted in catalyst bed blockage in either system. Filtering of the solids from the corn stover CPO after dilution of 10 wt% isopropanol resulted in a similar smooth operation.

The products from the tests with different catalysts and CPO feedstock were similar. The light oil phase product was sufficiently hydrotreated so that nitrogen and sulfur were at or below the level of detection, while the residual oxygen content was low, <5%. The density of the products varied from 0.79 g/mL up to 0.88 g/mL over the period of the longer tests which correlated with a change of the hydrogen to carbon atomic ratio from 1.9 down to 1.7, suggesting some loss of catalyst activity through the test.

Task 6: Evaluation of the suitability of stabilized fractions for insertion within a refinery

Soluble Carbohydrate Fraction

After upgrading, the oil soluble compounds produced from this stream have similar concentrations of oxygen to those of oils and fats. Oils and fats are capable of conversion to diesel fuel in commercial hydrotreaters. However, even at 10-12% oxygen concentration, this would require some dilution with a hydrocarbon stream. These streams could be blended in roughly 10-20% by volume in an industrial distillate hydrotreater. Another issue with oxygenates in hydrotreaters is fouling of the heat exchangers. This will need to be tested with accelerated aging tests to determine the thermal stability to ensure that these streams will be compatible. Typical thermal aging tests used with pyrolysis oils may be overkill for these purposes. A test that would be more applicable to a heat exchanger and furnace residence may need to be designed to not over-estimate the potential for fouling in heat exchangers.

The lighter oxygenates boiling in the gasoline range are candidates for additional condensation to the diesel fuel range prior to refinery insertion. This would increase the value of the stream. Alternatively, the lighter components boiling in the gasoline range will mainly hydrogenate to hexanes and some pentanes. These could be inserted in a naphtha hydrotreater when blended in low amounts <10%. The product from this step could be blended into the gasoline pool. Alternatively, it could be separated and sent to a C5/C6 isomerization to improve the octane number prior to blending in the gasoline pool.

Because roughly 50% of this stream is lost in the filtration process, upstream optimization to increase the yield of levoglucosan while decreasing the content of solid particulates, humins, and other sugar derived species would have an immediate positive impact on the possible yield of valuable products obtainable from this stream.

Middle Fraction

The gasoline-extractable portion of these products should be higher than the decalin-soluble portion. If they are oil soluble, these could go to a naphtha hydrotreater as discussed above. The aqueous soluble fraction will not be a good blendstock for a hydrotreater. Although refinery insertion may not be a good option for these compounds, hydrogenating to monofunctional alcohols could then be used directly as a blendstcock.

An upstream modification of this fraction that reduces the amount of furanics may help improve the stabilization of this significant part of the bio-oil. A subfraction rich in furanics could be independently refined working at lower concentrations and higher hydrogen pressures.

Light Oxygenate Fraction

After upgrading over the TiO_2 based catalyst, this stream could be lightly hydrogenated to create monofunctional alcohols for direct blending with the gasoline and diesel pools. Condensation products are more amenable for insertion into the diesel pool while the lighter monofunctional alcohols could be blended into the gasoline pool. More severe hydrogenation (via blending in a naphtha hydrotreater) to make hydrocarbons is also possible. The water must be removed prior to this step.

If the light acids from this stream are instead converted with the larger acids produced from the

soluble carbohydrates to make larger ketones, these could undergo condensation and subsequent HDO in a diesel hydrotreater to produce diesel or mildly hydrogenated in a standalone unit to produce monofunctional alcohols for direct blending in diesel. Similar requirements to those outlined for the oil soluble diesel range products obtained from the soluble carbohydrates apply for hydrotreating in a commercial unit.

The removal of furanic and phenolic species from this stream would be highly advantageous. This would limit the degree of pre-filtration necessary to achieve conversion to useful products without deactivation of the catalyst that targets hydrogenation.

Summary

The soluble carbohydrate stream product of gluconic acid alone may hold promise for refinery upgrading via a modified hydrotreating unit, but prior to a ketonization step the benefit may not be great. These sugars would not be miscible in oil, so while hydrotreating of sugars can occur, the main product produced is n-hexane, which is a liquid phase hydrocarbon, but the high vapor pressure and low octane number make it a low value hydrocarbon. The acid group would significantly increase the TAN number, making the requirement of either more costly grades of steel or significant dilution. If the acids decarbonylate directly and do not form larger C-C bonds in the reactor, the value would not be great for refinery insertion in a hydrotreater. A more appealing route would be to use the gluconic acid as a renewable co-monomer for a polymerization process if such facilities are available near the refinery. If the hydrotreating/ketonization route is alternatively chosen, the resulting ketones could be co-processed in a diesel hydrotreater assuming the amount of heavier products with molecular weights greater than 500 are less than 100ppm.

The middle fraction stream products could potentially be incorporated into a hydroprocessing unit. Because the aqueous phase has a fraction of compounds with molecular weights greater than the boiling range of gasosline/diesel, it is anticipated that because these are highly oxygenated compounds, a standard hydroprocessing may not be very effective and a dedicated unit may be necessary. A more appropriate conversion route may be to increase the severity of hydrotreating in the initial upgrading step, as the measurable products produced in this phase are monofunctional oxygenates which may have the potential for coprocessing. Alternatively, the heavy compounds present in this partially upgraded stream may undergo filtration or adsorption with activated carbon in an attempt to remove these compounds from the stream. The products that partition to the oil phase carry much more promise for refinery insertion via hydroprocessing as they contain oil soluble compounds that can be diluted in an existing refinery stream and the compounds are either hydrocarbons or monofunctional oxygenates.

The fact that the CPO stream has already undergone severe hydrotreating may allow for refinery insertion via a hydrotreater. What is not known is the degree of hydrogenation of the aromatic ring under these conditions. This reaction produces a gasoline range product with lower octane number with higher hydrogen consumption requirements. One option may conceivably be to insert this stream in a naphtha hydrotreater followed by a reformer to recover the hydrogen. Alternatively, depending on the degree of ring hydrogenation, the introduction into an FCC unit may be feasible, but the targeted reaction would be for these hydrogenated cyclic alcohols to undergo dehydration and undergo hydride transfer where the remaining hydrogen in the molecules are transferred to olefins and other coke precursors. While this insertion may be feasible, it is anticipated that a great portion of the carbon in this stream would end up as lighter gases such as propylene and isobutylene, while any phenolic species would directly form coke. Hydrotreating as the first insertion point appears to be the more appealing option. It is important

to note that the solids content discussed in this report is assumed to all be deposited on the guard bed in the pretreatment reactor, as the levels of solids in the CPO stream are too high for direct insertion in the refinery.

The products in the upgraded CPO stream have low sulfur and nitrogen content. However, the sulfur and nitrogen analyses are not sensitive enough if the product sulfur levels are in the low ppm range required to meet current fuel specifications. On the other hand the oxygen levels of 2 to 3.4 % are low enough to be consider directly blending these product into fuel if other fuels specifications such as gum formation and storage stability are met.

Fractionating the product into gasoline (C5-400 F, diesel (400-650 f), gasoil (650-950 F) and residue (950 F+) and analyzing these fractions for heteroatom content, ignition properties such as Octane and Cetane, and processing properties such as aromaticity, carbon residues and asphaltenes would provide sufficient insight to determine what refinery processing units such as hydrotreating versus catalytic cracking versus hydrocracking would be best for further processing of these products. For example the aliphatic nature of the product (90%) suggest that for the heavier fraction catalytic cracking would product high conversions to gasoline. On the other hand the diesel fraction may need only simple hydrotreating for deoxygenation while the gasoline fraction may require reforming to increase octane values.

Task 7: Technoeconomic analysis of system for producing stabilized fractions of bio-oil from biomass for insertion within a refinery (ISU)

Overview of project activities

The techno-economic analysis (TEA) activities consisted of developing a commercial-scale chemical process design, estimating facility capital and operating costs, and a sensitivity analysis of key process parameters.

The conversion of biomass into stable bio-oil and their subsequent upgrading to gasoline and diesel was modeled in Aspen Plus v8.3. The model incorporates experimental data gathered by collaborators in this project. Experimental data informed the fast pyrolysis, bio-oil recovery, and bio-oil stabilization sections of the model.

Equipment cost estimates employ publically available data and Aspen Process Economic Analyzer (APEA). In particular, recent reports by PNNL and NREL provide estimates for similar stabilization reactors. Installation factors are based on Peters and Timmerhaus cost factors for chemical conversion facilities.[Pet03] Operating costs are based on similar price assumptions as those found in national lab reports. Recent (<5 years) market price data was considered for materials unique to this process. The capital and operating costs support a 30-year discounted cash flow rate of return (DCFROR) analysis to estimate the minimum fuel-selling price (MFSP) required to achieve a 10% internal rate of return.

The sensitivity analysis identifies and evaluates several key processing parameters in terms of their impact on the MFSP. These parameters include overall fuel yield and financial assumptions. The input parameters were varied by ±20% to estimate their impact on the MFSP.

Process overview

The overall process is illustrated in Figure 48. As shown, the process consists of five primary processing sections: biomass conversion, bio-oil fractionation, bio-oil stabilization, hydrogen generation, and bio-oil upgrading. The process converts raw biomass (red oak) into a blend of gasoline and diesel type hydrocarbons. The experimental data gathered from this project pertains to the conversion, fractionation, and stabilization steps. Although the process model includes upgrading, it is envisioned that the final step will take place at an existing refinery.

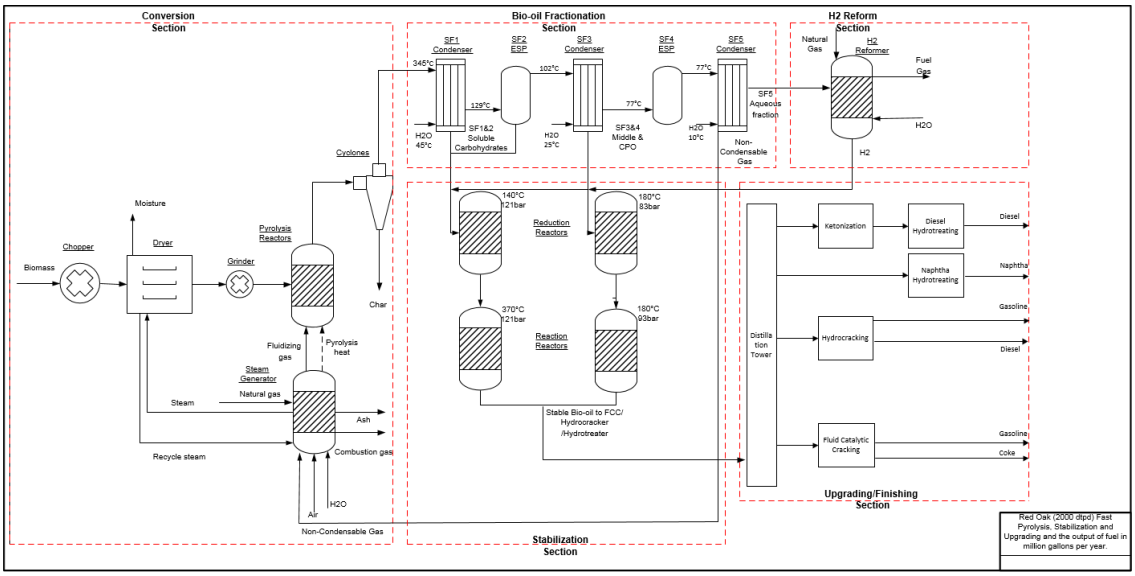

Figure 48. Simplified biomass fast pyrolysis and bio-oil stabilization process flow diagram

The process model incorporates new model compounds as defined in the 2013 PNNL/NREL/INL fast pyrolysis and hydrotreating bio-oil pathway report[Jon14]. The yields for different compounds are based on experimental data gathered at ISU and reported by Rover et al.[Rov14]. Figure shows the yield of bio-oil compound groups for varying pyrolysis temperatures.

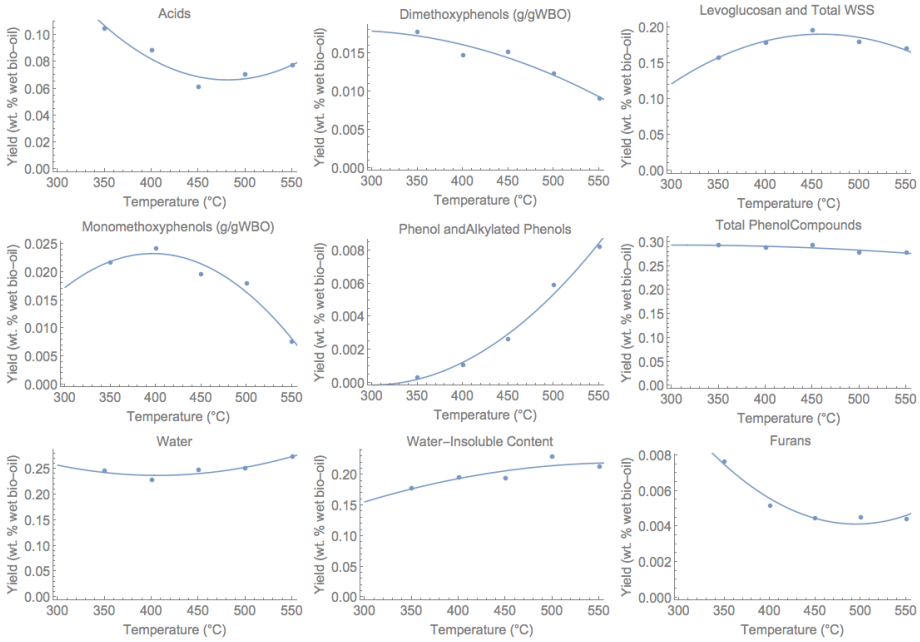

Figure 49. Red oak fast pyrolysis yields of bio-oil compound groups by reaction temperature [3]

A novel fractionation system consisting of a series of condensers, and electrostatic precipitators was designed to recover bio-oil from the pyrolysis reactor into five stage fractions (light oxygenates, soluble carbohydrates, middle fraction, and clean phenolic oligomers denoted as SF1&2, SF3, SF4, and SF5 in Figure 3), which have distinctive characteristics. The basic principles of the fractionation system are described by Pollard et al.[Pol12] Figure 50 shows the simplified flow diagram of the bio-oil recovery section.

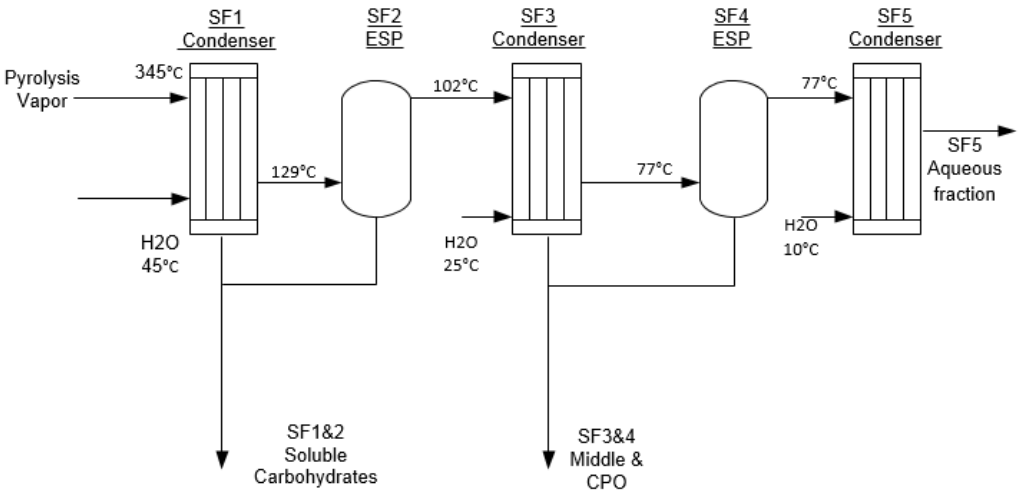

Figure 50. Bio-oil recovery section of stabilization system

Figure 51 below shows the simulated mass flow rates of stage fractions products grouped by carbon chain length. Overall stage fraction rates are based on Rover's experimental data, and the carbon distribution is estimated with Aspen Plus™.[Rov14] Heavier hydrocarbons are primarily recovered in SF1 and SF2, whereas moisture is predominantly found in SF5.

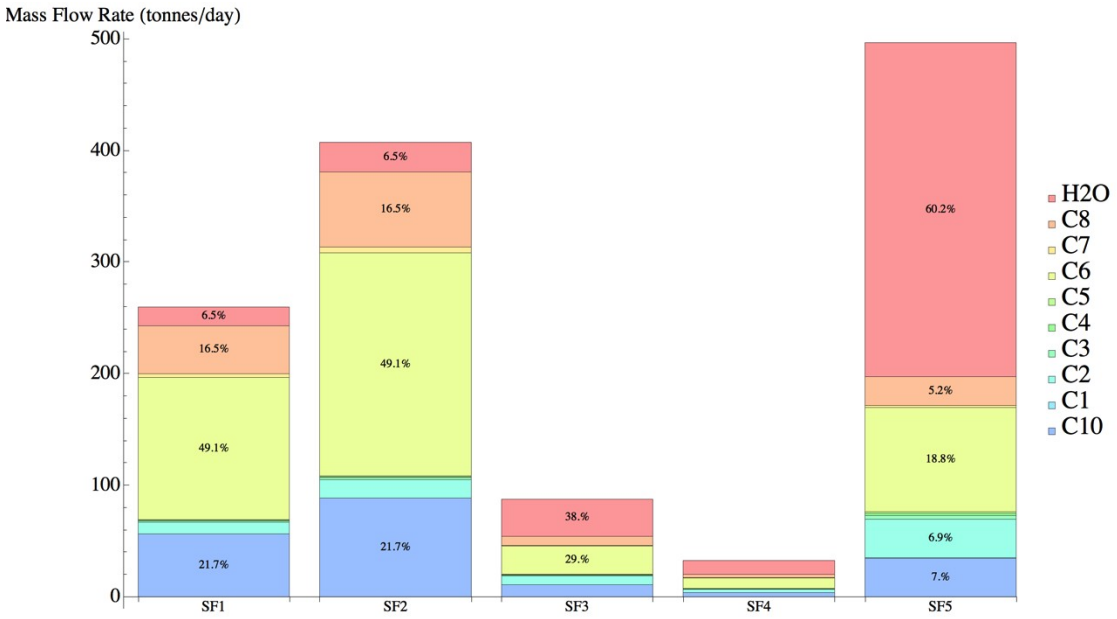

Figure 51. Simulated mass flow rates (tonnes/day) of stage fraction (SF1-5) products grouped by carbon chain length (C1-10) and water. Results based on a 2000 dry metric tonne per day biomass input.

The recovered stage fractions were upgraded in the stabilization unit. The stabilization unit employs operating conditions and experimental data gathered from this project. Stabilization of SF1&2 and SF3&4 takes place in 2-step reduction/reaction reactors under hydrogen-rich conditions. SF5 was reformed with merchant natural gas and fuel gas to produce hydrogen for the upgrading processes. The stabilization system is described in Figure 52.

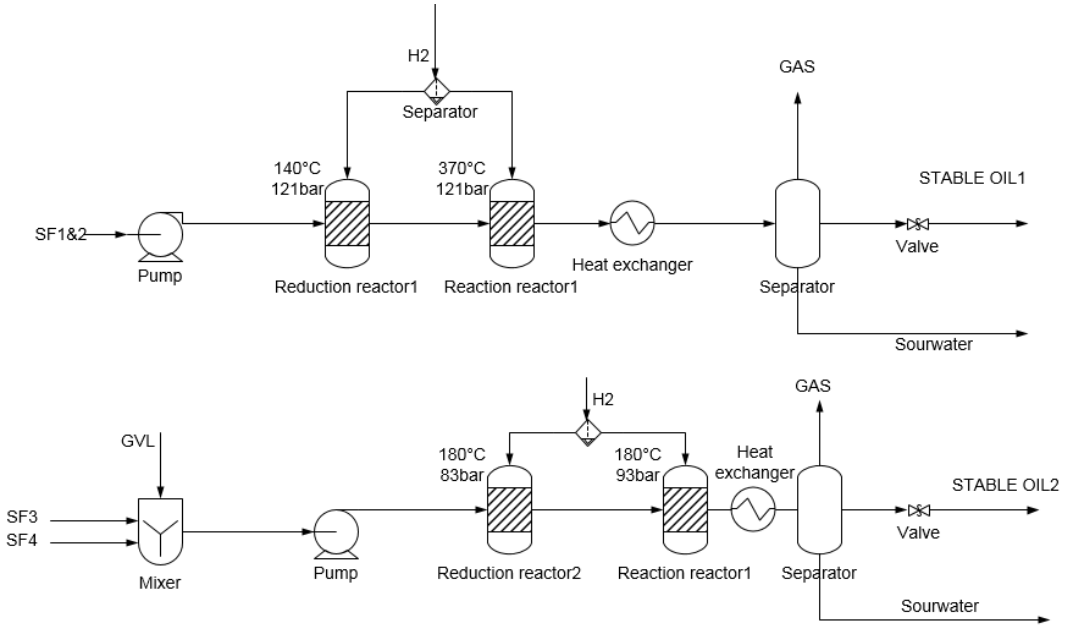

Figure 12. Bio-oil stage fraction 1-4 stabilization section with reactor temperature and pressure properties. Stabilization units include 2-step reduction/reaction reactors.

Figure 53 shows the final design for upgrading stable oil into gasoline and diesel via several distillation steps and a hydrocracking process. The first step involves a de-butanizer where the off-gas is removed and recycled to the reforming section (not shown). The second step occurs in the naphtha splitter where the gasoline-range products are recovered. Heavier compounds flow into the diesel splitter where a portion of the diesel is recovered. The other portion is recovered after a final hydrocracking and distillation step that yields additional gasoline product. Hydrocracking employs hydrogen from natural gas and process off-gas reforming.

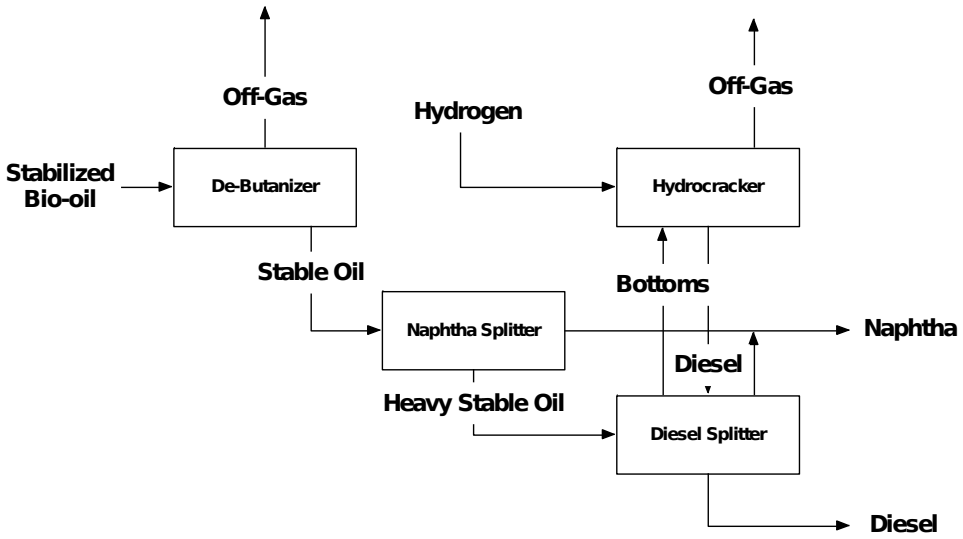

Figure 53. Hydroprocessing and product separation from upgraded stable oils

Techno-economic analysis has been developed to analyze the costs of producing renewable transportation fuels from stabilization bio-oil stage fractions process. The TEA evaluates the incremental cost of the stabilization units and the overall MFSP of the finished products. lists the process material and utility prices employed in this study.

The feedstock cost of $75/ton is based on plant-gate, wet feedstock and does not include drying or grinding costs. Hydrogen, natural gas, catalyst, chemical, and utility prices are based on previous reports and market data[Thi14], [Bro12].

Table 31. Process material and utility prices

Raw Materials	Price	Units
Red Oak	75.0	$/short ton
Hydrogen (merchant)	1.5	$/kg
Natural gas	5.10	$/kscf
Pyrolysis catalyst	5.0	$/lb
Hydrotreating catalyst	15.5	$/lb
Hydrocracking catalyst	15.5	$/lb
Hydrogen plant catalysts	3.6	¢/kscf H_2
Boiler chemicals	1.4	$/lb
Cooling tower chemicals	1.00	$/lb
GVL	0.85	$/kg
Waste Disposal		
Sand & ash	0.01	$/lb
WWT	0.09	$/kg COD
By-product credits:		
Char	20	$/tonne
Utilities		
Cooling Tower makeup	100.80	¢/1000 gal
Boiling Feed Water makeup	100.80	¢/1000 gal
Hydrogen Plant Process Water	100.80	¢/1000 gal
Electricity	6.16	¢/kwh

Table 32 summarized yields of gasoline and diesel, accounting for 40.9 and 41.7 gallons/dry short ton biomass respectively. The total liquid fuel output capacity is 54.3 million gallons of gasoline equivalent per year. The process employs 2.16 kg of natural gas and 0.04 kg of GVL per gallon of liquid product. The facility imports 3.78 kWh of electricity. The by-product from this process is biochar valued based on its energy content at $20/tonne. Additional by-products including various chemicals remain under consideration.

Table 32. Bio-oil Stage Fraction Stabilization Process Engineering Analysis

Process Result	**Value**
Gasoline production at operating capacity (MM gal/yr)	26.9
Gasoline product yield (gallons/dry short ton biomass)	40.9
Diesel production at operating capacity (MM gal/yr)	27.4
Diesel product yield (gallons/dry short ton biomass)	41.7
Natural gas input (kg/gallon of product)	2.16
GVL input (kg/gallon of product)	0.04
Electricity input (kWh)	3.78
Internal Rate of Return (after tax)	10%
Equity Percent of Total Investment	40%

The total investment cost is illustrated in Figure 54. It consists of project contingency, indirect cost and installed equipment cost of $48.5 million, $116.6 million and $466.4 million, respectively. The estimated total investment cost is $631.5 million. The installed equipment costs for different areas are shown in the stacked bar chart (Figure 55). The installed equipment costs for the stabilization area and pretreatment and pyrolysis area are the largest portion of the total installed equipment cost, accounting for approximately 38% of the total, or $ 178 million.

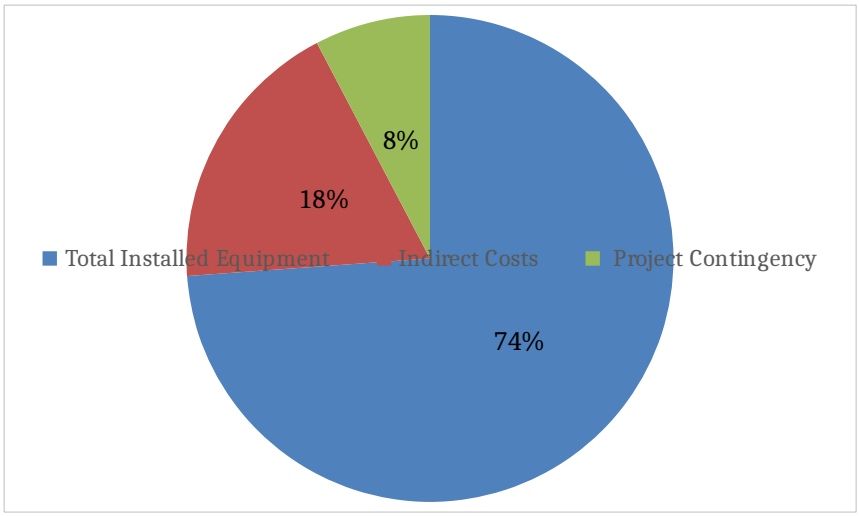

Figure 54. Total investment cost categories for bio-oil stabilization

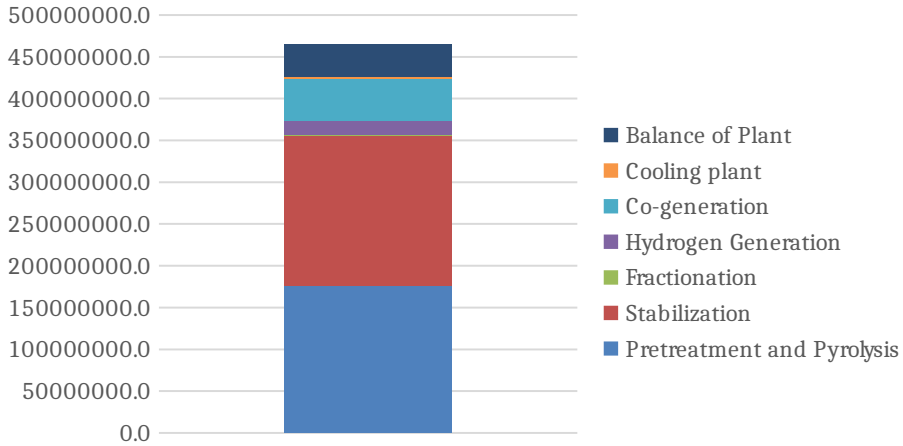

Figure 55. Installed equipment cost components for bio-oil stabilization

Total annual facility operating costs were illustrated in Figure 56 as $ 201.2 million including financing costs. Feedstock costs are the major contributor to the annual operating costs ($49.3 million) followed by fixed costs ($28.3 million), capital depreciation ($18.7 million), electricity and other utilities ($16.3 million). Natural gas cost takes the smallest percentage of the total annual facility operating costs ($ 0.2 million). Catalyst & chemicals ($4.3 million) includes catalyst for pyrolysis, hydrotreating, hydrocracking, hydrogen generation, boiler chemicals, cooling tower chemicals and GVL.

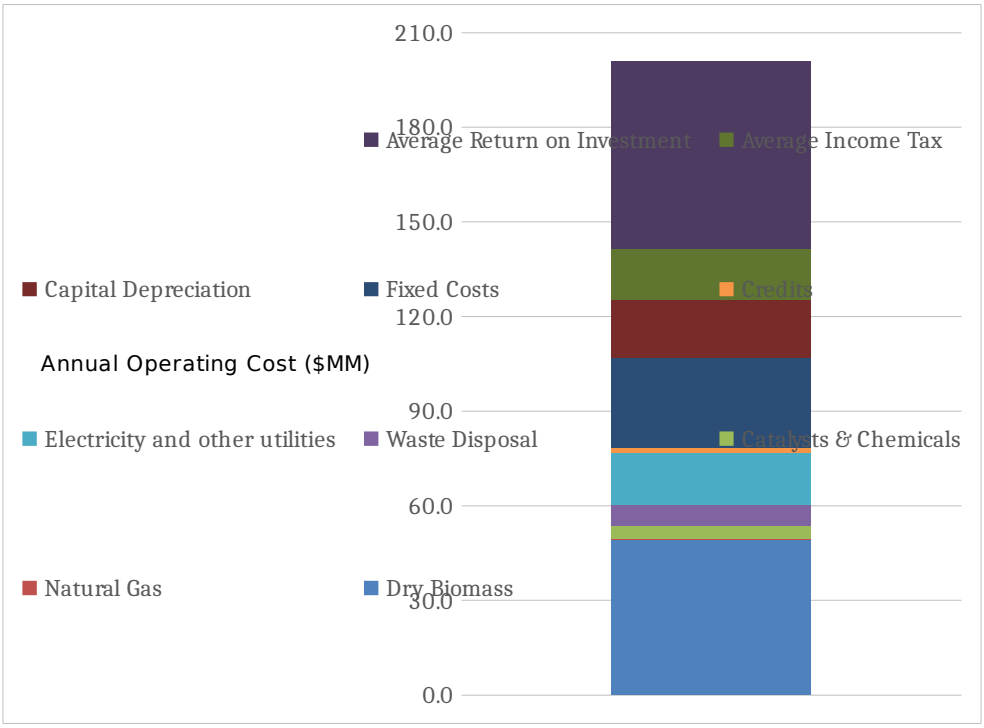

Figure 56. Annual operating costs for bio-oil stabilization

A sensitivity analysis was conducted by ±20% variations in parameters that could have significant impact on the minimum fuel-selling price (MFSP). As shown in Figure 57, diesel yield and gasoline yield have the biggest impact on MFSP. Increases of diesel yield from 33.37 to 50.05 gal/MT and gasoline yield from 32.70 to 49.04 gal/MT decrease MFSP from $4.25 to $3.46/gal and from $4.21 to $3.47/gal respectively. When fixed capital investment decreases from $ 672.72 million to $ 448.48 million, MFSP decreases from $4.04 to $3.48/gal. A ±20% range of internal rate of return results in a MFSP range of $3.54 to $4.02/gal. MFSP increases from $3.61 to $3.95/gal with the feedstock cost increases of $60 to $90/ton. Hydrotreating catalyst price and hydrocracking catalyst price have very small impact on the MFSP. This is based in part on the assumption that the catalysts have matured enough to minimize coking.

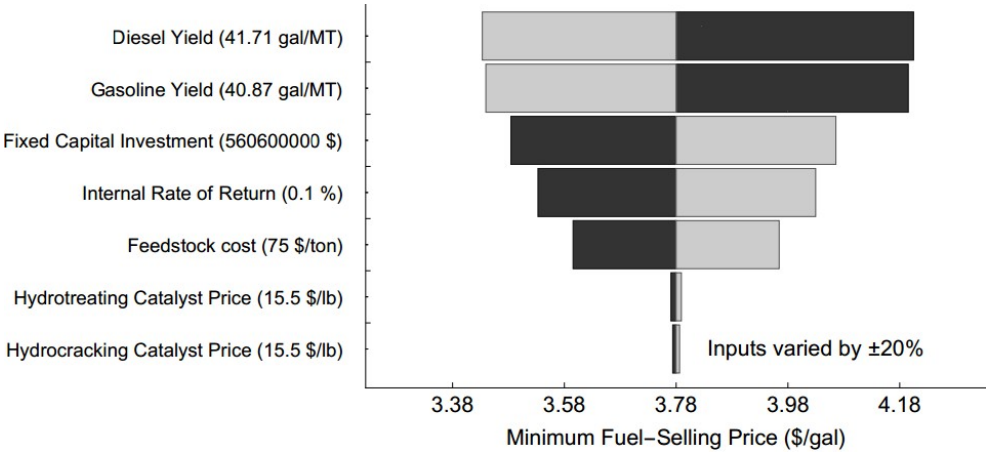

Figure 57. Minimum fuel-selling price sensitivity analysis to key techno-economic parameters. Parameter values were varied by ±20%.

6. Identify products developed under the award and technology transfer activities, such as:

a. Publications (list journal name, volume, issue), conference papers, or other public releases of results. If not provided previously, attach or send copies of any public releases to the DOE Project Officer identified in Block 11 of the Notice of Financial Assistance Award.

- Elliott, D.C., Wang, H., Rover, M.R., Whitmer, L.E., Smith, R.G., Brown, R.C. (2014) Hydrocarbon liquid production via catalytic hydroprocessing of phenolic oligomers fractionated from fast pyrolysis bio-oil. Manuscript in Progress.

- Li, W., Wright, M.M., Brown, R.C. (2013) Stabilization of bio-oil fractions for insertion into petroleum refineries. Poster presentation, International Conference on Thermochemical Conversion of Biomass, September 3-6, 2013, Chicago, IL.

- Santhanaraj, D., Rover, M. R., Resasco, D. E., Brown, R. C. and Crossley, S. (2014), Gluconic Acid from Biomass Fast Pyrolysis Oils: Specialty Chemicals from the Thermochemical Conversion of Biomass. ChemSusChem. doi: 10.1002/cssc.201402431

7. For projects involving computer modeling, provide the following information with the final report:

a. Model description, key assumptions, version, source and intended use;

The motivation of this project is to improve the stability of bio-oil. Recovery of bio-oil into different stage fractions followed by separate upgrading methods was employed for stabilizing bio-oil stage fractions. The stabilized bio-oil stage fractions have improved chemical properties for insertion into petroleum refineries.

This study employed 2000 Metric Tons per day (MT/day) of red oak biomass with 30% moisture, 0.3wt% ash and nominal size of 1mm. Red oak was chopped and dried for improved feeding into the pyrolysis reactor. In the fluidized bed reactor, red oak was decomposed for over a short residence time of 0.5-2s, in the absence of oxygen under a condition of 500 °C and 1 bar. Non-condensable gases from fast pyrolysis yields were used to fluidize the pyrolysis reactor. The solid yield, char, was separated by cyclones while pyrolysis oil was recovered into different stage fractions with distinctive physical and chemical characteristics. The recovery unit consists of a series of condensers and electrostatic precipitators designed to recover bio-oil from the pyrolysis reactor into five stage fractions (SF1-5: light oxygenates, soluble carbohydrates, middle fraction, and clean phenolic oligomers). A two-stage upgrading unit consisting of four reactors was designed to upgrade heavy fraction bio-oils (SF1&2) and middle fraction bio-oils (SF3&4) separately. The first two reduction reactors in the stabilization system were designed to crack complex molecules into simpler molecules, while the second two reaction reactors were used for hydrodeoxygenation reactions. A final upgrading process

and several distillation steps were designed to upgrade stable oils into gasoline and diesel products. Hydrotreating, hydrocracking and fluid catalytic cracking are three upgrading options for output streams from the distillation tower. Only hydrocracking was simulated in the Aspen Plus™ model. Hydroprocessing employed hydrogen generated by SF5, off-gas and natural gas reforming. A heat recovery and steam generator system was designed to provide heat for the dryer, pyrolysis reactor, and other heat sinks in the process.

b. Performance criteria for the model related to the intended use;

Table A-1 below describes the key process metrics for stabilization process. The key performance criteria for this model are the overall yield of gasoline- and diesel-blend stock fuels and MFSP. The overall yield is calculated as 82 gal/ton of biomass, and the MFSP is estimated at $3.77/gal of liquid product.

Table A-1. Key Process Metrics for Stabilization process

Fast Pyrolysis Intermediate	
Gas Species – CO, CO_2, C_1-C_4 (kg/BDMT)	195
Pyrolysis oil (kg/BDMT)	653
Water (kg/BDMT)	165
Char (kg/BDMT)	152
Vapor Upgrading Product	
Hydrogen Utilized (wt %)	7.4
Gas (wt. % of dry biomass)	11
Aqueous Phase (wt. % of dry biomass)	25.3
Organic Phase (wt. % of dry biomass)	20.74
H/C molar ratio	*1.73*
Oxygen (wt. % in organic phase)	*2*
Carbon efficiency (%)	*55*
Final Fuel Blendstock	
Yield (%, w/w dry biomass)	25.5
Overall Carbon Efficiency (% of C in biomass)	45.32
Overall Carbon Efficiency (% of C in biomass + NG)	30.66
Total Product (gal/dry US ton)	82.6
Gasoline Range Product (gallons/dry US ton)	40.9
Diesel Range Product (gallons/dry US ton)	41.7
Oxygen Content in Cumulative Product (wt. %)	0.5
Minimum Fuel Selling Price ($/gal)	3.77
Natural Gas and Electricity	
Natural Gas Energy Input (% of biomass, LHV basis)	85.94
Natural Gas Cost Contribution (¢/gal)	0.3

Surplus Electricity Credit (¢/gal)	29.82
Fuel Blendstock Production Efficiencies (various bases)	
Biomass Feedstock (%, LHV basis)	57.19
Biomass + Natural Gas (%, LHV basis)	30.76
Biomass + Natural Gas + Electricity (%, LHV basis, all electrical energy converted to heat)	32.09

c. Test results to demonstrate the model performance criteria were met (e.g., code verification/validation, sensitivity analyses, history matching with lab or field data, as appropriate);

The process model was developed in Aspen Plus v8.3 and includes a complete mass and energy balance of the process. Sensitivity analyses were conducted in Microsoft Excel to assess the impact of key assumptions on the process profitability. Operating conditions and process yields were matched to experimental data where applicable.

d. Theory behind the model, expressed in non-mathematical terms;

e. Mathematics to be used, including formulas and calculation methods;

f. Whether or not the theory and mathematical algorithms were peer reviewed,

and, if so, include a summary of theoretical strengths and weaknesses;

g. Hardware requirements; and

h. Documentation (e.g., users guide, model code).

8. Ensure the report does not contain any Protected PII. Protected PII is defined as an individual's first name or first initial and last name in combination with any one or more of types of information, including, but not limited to, social security number, passport number, credit card numbers, clearances, bank numbers, biometrics, date and place of birth, mother's maiden name, criminal, medical and financial records, educational transcripts, etc.

References

Brown, T., Zhang, Y., Hu, G., Brown, R. "Techno-economic analysis of biobased chemicals production via integrated catalytic processing." *Biofuels, Bioproducts, and Biorefining*, 2012: 6(1):73-87.

Dreher, M., Johnson, B., Peterson, A., et al. "Catalysis in supercritical water: Pathway of the methanation reaction and sulfur poisoining over a Ru/C catalyst during the reforming of biomolecules." *Journal of Catalysis*, 2013, 301: 38-45.

Elliott, D.C., Wang, H., French, R., Deutch, S., Iisa, K. "Hydrocarbon liquid production from biomass via hot-vapor filtered fast pyrolysis and catalytic hydroprocessing of the bio-oil." *Energy & Fuels*, 2014: Submitted.

Jones, S., Meyer, P., Snowden-Swan, L., Padmaperuma, A. Tan, E., Dutta, A. "Process design for economics for the conversion of lignocellulosic biomass to hydrocarbon fuels: Fast pyrolysis and hydrotreating bio-oil pathway." Richland, WA, 2014.

Peters, M., Timmerhaus, K., West, R. *Plant design and economics for chemical engineers.* New York, NY: McGraw-Hill, 2003.

Pham, T., Dachuan, S., Sooknoi, T., Resasco, D. "Aqueous Phase Ketonization of Acetic Acid over Ru/TiO2/Carbon Catalysts." *Journal of Catalysis 295*, 2012: 169-178.

Pollard, AS, Rover, MR, Brown, RC. "Characterization of bio-oil recovered as stage fractions with unique chemical and physical properties." *Journal of Analytical and Applied Pyrolysis*, 2012: 93:129-138.

Rover, MR, Johnston, PA, Whitmer, LE, Smith, RG, Brown, RC. "The effect of pyrolysis temperature on recovery of bio-oil as distinctive stage fractions." *Journal of Analytical and Applied Pyrolysis*, 2014: 105:262-268.

Thilakaratne, R., Brown, T., Li, Y., Hu, G., Brown, R. "Mild catalytic pyrolysis of biomass for production of transportation fuels: A techno-economic analysis." *Green Chemistry*, 2014: 16(2): 627-636.